CHALMERS
UNIVERSITY OF TECHNOLOGY

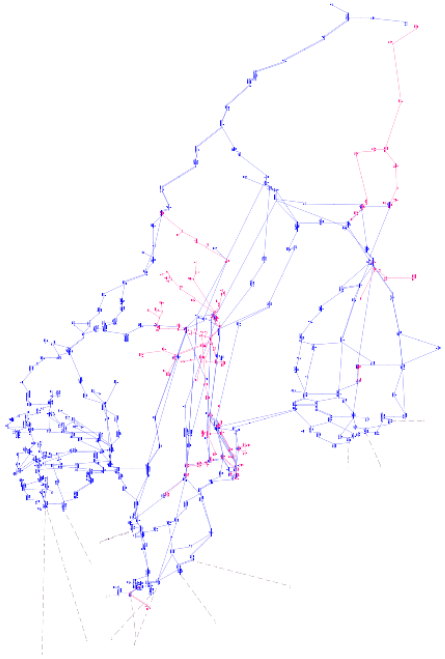

Nordic Power System Model Based on Open-Source Data

Model Verification and Power Flow Analyses with Future Generation and Load Scenarios

Master's thesis in Sustainable Electric Power Engineering and Electromobility

Matilda Arvidsson & Arvid Klang

DEPARTMENT OF ELECTRICAL ENGINEERING

CHALMERS UNIVERSITY OF TECHNOLOGY
Gothenburg, Sweden 2023
www.chalmers.se

Master's thesis 2023

Nordic Power System Model Based on Open-Source Data

Model Verification and Power Flow Analyses with Future Generation and Load Scenarios

Matilda Arvidsson & Arvid Klang

CHALMERS
UNIVERSITY OF TECHNOLOGY

Department of Electrical Engineering
Division of Electric Power Engineering
Chalmers University of Technology
Gothenburg, Sweden 2023

Nordic Power System Model Based on Open-Source Data
Model Verification and Power Flow Analyses with Future Generation and Load Scenarios
Matilda Arvidsson & Arvid Klang

Supervisor: Arvid Björemark, Engineer, Power System Planning Nordics, DNV
Examiner: Peiyuan Chen, Associate Professor, Electrical Power Engineering

Master's Thesis 2023
Department of Electrical Engineering
Division of Electric Power Engineering
Chalmers University of Technology
SE-412 96 Gothenburg
Telephone +46 31 772 1000

Cover: The PSS/E .sld file of the 2045 grid model.

Typeset in LaTeX
Printed by TeknologTryck
Gothenburg, Sweden 2023

Abstract

The Nordic power grid is undergoing a significant transformation in response to ambitious climate goals. Recognizing the urgency of addressing climate change, renewable energy sources are being integrated into the Nordic generation mix rapidly. Furthermore, the electrification of the transport sectors and heavy industry is being prioritized as a key strategy to achieve these goals. To facilitate these changes, the Nordic grid needs to adapt accordingly.

In this thesis, a model of the 2020 power system has been developed and verified based on open-source information. Using the information available through the 10-year development plans by the Transmission System Operators (TSOs), this model was also further developed to represent the power system in 2045. In addition, three different load and generation scenarios for 2045, based on projections published by the TSOs, are developed and presented.

The compatibility between different generation and load scenarios in high and low wind cases and the planned grid reinforcements are investigated through simulations in PSS/E. Regarding the thermal limitations of the lines in the grid, with the ability to shift loads from low to high generation cases, the grid and the different scenarios were generally compatible after adding some limited reinforcements. However, as this thesis solely concentrates on identifying violations concerning thermal limits within the Nordic power grid in static conditions, further studies are needed to determine whether the established compatibility endures when voltage, frequency, and rotor angle stability in dynamic simulations are considered.

With the introduction of large loads at new locations, a shift in power flow was observed. The previously seen north-to-south flow in the Nordics is less prevalent in all 2045 cases. Moreover, with these Gigawatt-sized loads, an increased need for more injected reactive power in proximity to them was observed. Furthermore, suitable locations for new large loads have been investigated and presented.

Keywords: Nordic synchronous system, future power system scenarios, renewable power, grid model, open source, PSS/E

Acknowledgements

We want to thank DNV and the Power Systems Planning team for granting us the opportunity to conduct our Master's Thesis in collaboration with them. In particular, we would like to thank our supervisor at DNV, Arvid Björemark, for his continuous support and feedback throughout the process of writing this report. We would also like to extend our gratitude to the Gothenburg Power System Planning team members, namely Lucas, Johan, Andreas, Reza, and Ingrid, for their warm welcome, constructive feedback, and enjoyable coffee breaks with us. Furthermore, we would like to acknowledge our supervisor and examiner, Peiyuan Chen, who has been a great support in answering our questions and guiding us through the process of writing this report.

Matilda Arvidsson & Arvid Klang, Gothenburg, June 2023

Contents

List of Figures

List of Tables

1
Introduction

1.1 Background

The Nordic power grid is in the early stages of an extensive transformation. Ambitious climate goals have been set [1], and electrification powered by renewable energy is presented as one of the essential tools to reach these goals. According to the Swedish Transmission Operator (TSO) Svenska kraftnät (Svk), some scenarios indicate that the total electrical energy consumption in 2045 could be twice the one of today due to the electrification strategy presented by the Swedish government [2]. The TSOs in the other Nordic countries, Statnett in Norway [3], Fingrid in Finland [4], and Energinet in Denmark [5] also predicts a significant increase in the electrical energy demand in the future.

The electrification strategy of the Nordic countries, primarily for the industry and transport sector, indicates increased requests to connect large loads and renewable production facilities to either the transmission or distribution grid. Therefore, a working model of the Nordic power system would be very beneficial for independent parties to perform viable pre-studies for grid connections. However, for security reasons, the TSO's cannot share their information, thus this model is based on open sources.

Expanding this model to simulate the 2045 grid will provide valuable insights into how the grid conditions may change. Moreover, it enables exploration of the impact of various scenarios on power flow under different weather conditions.

1.2 Purpose

This thesis aims to develop and verify a model of the Nordic transmission grid in PSS/E using only open-source data for power flow analysis and grid flow studies. The model will represent the 2020 grid and be verified for that. It will then be further developed to replicate at least the 2030, but to the best ability given the available information, the grid in 2045.

The model will be used to perform steady-state analyses of different production and load scenarios in 2045 to identify possible congestion and evaluate how the need for reactive power changes in the future and between the different cases. Furthermore, the impact of the placements of new loads and generation will also be evaluated

through a sensitivity analysis in PSS/E. In the end, the aim is to assess the need for further reinforcements in the grid and suggest ideal placements for large loads and generation units.

1.3 Problem Description

The first step of the project is to develop and verify a model of the Nordic transmission grid (220, 300, and 400 kV levels) as it was in 2020, with interconnectors to other countries in the power system simulation software PSS/E. The reason why it is the 2020 grid that is being modeled is due to the availability of the data used to run the model. A method to validate the model will be developed, and the reliability along with the possible limitations of the model will be discussed.

Next, the model will be developed into a projection of what the transmission grid is expected to look like in 2045. Upon this, different load and generation scenarios for 2045 will be run. The development of the future grid and generation and load scenarios will be based on the Nordic TSO's own predictions presented in their grid plans and long-term market analyses.

Contingency and sensitivity analyses for different scenarios will be run on both models. The contingency analyses will be used to evaluate if there are any bottlenecks in the current and future grid. The sensitivity analysis will be used to determine suitable load and generation locations. The need for reactive compensation will also be compared between the cases and scenarios.

The analysis of how the future grid is able to deal with 2045 production and consumption estimates will be performed to provide insights into potential grid deficits concerning capacity and redundancy. In addition, the possibility of mitigating structural grid bottlenecks by re-locating generation sources will be investigated. Flexibility will be discussed as a possible solution to grid capacity and congestion issues, and some assumptions regarding load characteristics will be considered when setting up the future cases.

The results will first be used to conclude how well-balanced the grid expansion plans are compared to the load and generation estimates. Secondly, the results of the grid's performance for the different scenarios will be evaluated. Conclusions will be drawn regarding how well prepared the Nordic grid is for these, and suggestions for changes that would enhance the grid's performance will be presented. Lastly, the aim is to conclude suitable placements of loads and generation and discuss the need for reactive compensation for the different scenarios.

1.4 Scope

This report will not investigate dynamic performance, like changes in inertia, voltage stability, or rotor angle stability. Parameter choices for lines will only depend

on voltage level, and a general ambient temperature will be chosen for the Nordic region. No adaptations are made with regard to different temperatures at different places. The grid model is only run at 220 kV, 300 kV, and 400 kV. Sometimes, the grid is run at higher voltage levels, but this is not implemented in this model.

When expanding the 2020 grid model, the future scenarios include planned improvements to the grid published in the 10-year development plans by the TSOs. These present some of the planned transmission grid development between 2030 to 2045, but not all grid developments are planned yet, which means that the future grid model might not fully represent what it would look like in 2045. However, the plans that go beyond 2030 are included in the model.

The models will not consider changes in grid management and the electricity market but only physical changes to the grid. Flexibility on the production and demand side will likely be necessary in the future and is modeled to some extent in future scenarios. However, the feasibility of the implemented flexibility measures will not be investigated. In future scenario models, only well-documented larger loads, such as new industries, will be added manually.

There is no possibility to include all different weather conditions in the future grid, and the report is therefor mainly focused on investigating the impact of high and low wind scenarios, not changes in generation from solar. The report will not perform any studies on optimal power flow solutions, or investigate economical incentives to move loads or generation for the benefit of the grid performance. Furthermore, the report will not consider the cost of the added reinforcements to the 2045 grid, or investigate the utilization of these lines.

2

Nordic power grid and its transfer capacity

2.1 The Nordic Synchronous Power Grid

The Nordic synchronized grid includes the electricity grids in Sweden, Norway, Finland, and eastern Denmark. Sweden is divided into four bidding zones, SE1-4, Norway into five bidding zones, NO1-5, Finland is one bidding zone, FI, and Denmark is divided into two bidding zones, DK1-2, but only DK2 is synchronized with the Nordic grid. In each country, interconnectors connect the Nordics to its neighboring grids through HVDC connections. Depending on the power balance, power flows in or out through these interconnectors. AC electric energy can not be stored in its own form, thus, it needs to be consumed at the exact moment it is produced; otherwise, the frequency will deviate from the nominal 50 Hz it is supposed to be. The TSOs are responsible for keeping the balance in the grid at all times. The Nordic synchronous system is, to a great extent, characterized by the long and narrow shape with generation surplus in the north and deficit in the south, resulting in a need to transfer large amounts of power through long distances.

2.1.1 Bidding Zones

Power flows from production to consumption through the grid. How much power that can flow is determined by the grid's capacity. Limitations exists everywhere, but some lines limit the transfer capacity as they are the limiting component. These are called bottlenecks and are often where the borders of the bidding zones in the Nordic grid are. When the capacity limit is reached, price differences between the bidding zones arise. In Figure 2.1, the borders of the different bidding zones in are shown, along with the available transfer capacity between the bidding zones. The interconnections to neighboring countries/bidding zones are displayed in orange. What determines the transfer capacity displayed is further elaborated on in Section 2.2.

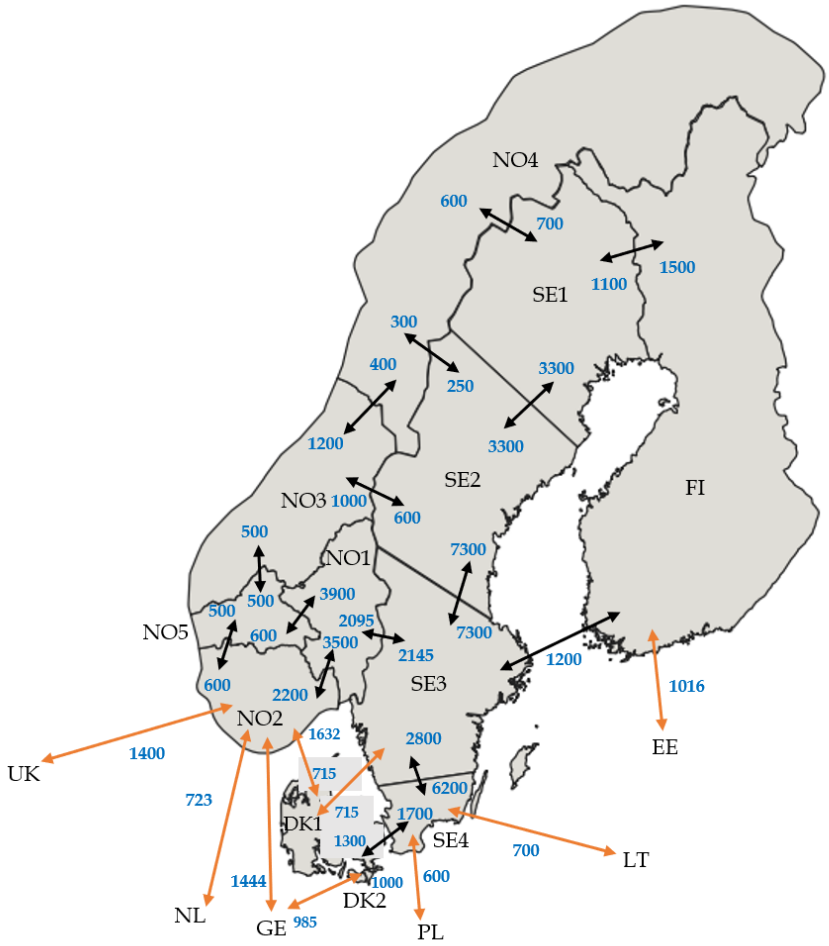

Figure 2.1: A map of the bidding zones in the Nordics and the transfer capacity between the borders in [MW]. Capacities taken from [6].

2.1.2 Generation

Hydropower accounts for just above half of the annual electricity production in the Nordic system, 221 TWh of the total production of 417 TWh in 2020 [7]. In 2020, wind power accounted for one seventh of the total energy production, whilst thermal (nuclear, bio, fossil, and other thermal) accounted for a third of the total electrical energy demand. All values are presented in Figure 2.2.

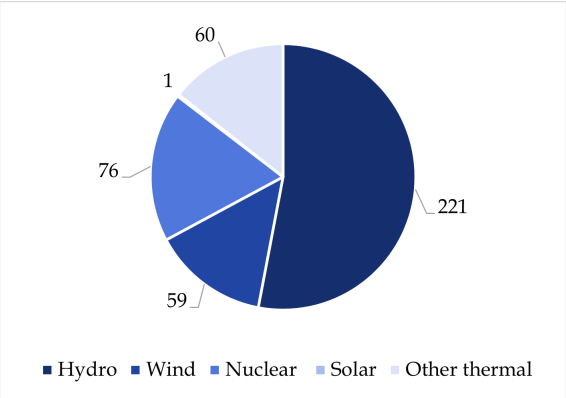

Figure 2.2: Total electrical energy production by source in the Nordic year 2020 [TWh][7]

Due to data availability for the model, the base cases are run on data from 2020. Therefore the installed capacity presented in Table 2.1 represents the installed capacities in 2020. Since then, more wind and solar power has been installed. Sweden has decommissioned, and Finland has commissioned nuclear power, and some thermal units have been removed [8], [9].

Table 2.1: Installed generation capacity per bidding zone per type 2020 [MW], [8], [10]

	Hydro	Nuclear	Other thermal	Solar	Wind onshore	Wind offshore	Total generation capacity
DK2			4 511	341	756	423	6 031
FI	3 148	2 794	9 180	7	2 145		17 274
NO1	3 883				222		4 105
NO2	11 564		5		1 087		12 656
NO3	4 760				1 902		6 662
NO4	5 345		270		654		6 269
NO5	8 259		367				8 626
SE1	5 325		273	13	1 314		6 925
SE2	8 075		620	35	3 421		12 151
SE3	2 583	7 725	4 055	440	2 647		17 450
SE4	345		2 144	210	2 598		5 297
Total	53 287	10 519	21 425	1 046	16 746	423	103 446
% of total	51.5	10.1	20.7	1.0	16.2	0.4	100

2.1.3 Loads

The total electrical energy demand of the Nordics (all of Denmark included) was 406 TWh in 2020, where households and services accounted for roughly 210 TWh, the industry for around 170 TWh, and the transport sector around 10 TWh, losses accounted for the rest of the demand [11]. As previously stated, most of the loads in

the Nordics are located in the southern parts due to the higher population density there.

Table 2.2 presents the load in each bidding zone during the peak load hour in Sweden 2020. This hour occurred at 07:00 (UTC) 28th of February, and the total load in the Nordic synchronous system was 58 GW. In the high load scenarios presented in Section 4.1 the loads were 50 GW and 56 GW.

Table 2.2: Load in each bidding zone at peak load hour 2020, [8]

	DK2	**FI**	**NO1**	**NO2**	**NO3**	**NO4**	**NO5**	**SE1**	**SE2**	**SE3**	**SE4**	**Total**
Load	1 972	12 298	6 755	5 625	4 262	2 795	2 424	1 449	2 352	14 422	4 005	58 359

2.1.4 Development of the Nordic Grid

The TSOs of the Nordic countries have all announced large plans to expand and upgrade the grid [12], [4], [13], [2]. This is driven by predictions of a need for more capacity now and even more in the future, as well as grid components reaching the end of their life span. The additional capacity needed in the grid is unclear and estimated in different scenarios, often with a wide range between the lowest and highest consumption and generation scenarios. Common between the scenarios is however that the estimated yearly load and generation are quite balanced in all countries. In the scenarios presented in the long-term market analyses, no Nordic country will produce a large surplus of electrical energy on a yearly basis nor have a large deficit.

To which degree the energy demand will increase is primarily dependent on some consumption categories, electric vehicles, server halls, and the electrification of heavy industries like forestry, mining, and the cement industry, including power to gas industries [14]. These categories are also expected to increase compared to today's demand [11]. On the other hand, the demand of households and services is the same in all scenarios presented in [14] and does not change between the years 2020-2050. However, this does not include home charging of electric vehicles, as it is presented as its own category [11].

To meet the increase in demand, the generation capacity will also be expanded, predominantly by increasing the wind capacity, both off- and on-shore. Solar is also predicted to increase, whilst hydro and thermal (not including nuclear) installed capacity will remain similar to today's values [14]. To which degree nuclear power will be a part of the 2045 energy mix varies, both in Finland and Sweden [14] [4]. Svk includes nuclear power in two of their scenarios for 2045. New nuclear power will be built in Sweden in one of those scenarios, *electrification plannable*. Many reactors will have reached their life expectancy by 2045, and with a life expectancy of 60 years, O3 and Forsmark 3 in Sweden will be decommissioned in 2045 [15]. The newly built Okilukto 3 in Finland is expected to be in commission in 2045, and Fingrid has included SMR in one of their scenarios. The predictions will be further investigated in Section 5.3, where the future scenarios used in this report

are presented.

2.2 Grid Transfer Capacity

Two things are considered when determining the Net Transfer Capacity, which is reported to Nordpool. The first is Total Transfer Capacity, which is how much active power is permitted to flow between areas given the system security criterion's [16]. These include thermal limitations on the equipment, voltage stability, and rotor angle stability. The second thing considered is the Transmission Reliability Margin. This is a margin that is calculated depending on insecurities in the measurements, the need for emergency exchanges between the TSOs, and deviations in flow due to having to match changes in load and frequency during operation. The Net Transfer Capacity is the Total Transfer Capacity minus the Transmission Reliability Margin [16].

This report will focus on the thermal limitations, which are dependent on how much current can be conducted for a specific time period without causing or sustaining damage. Voltage limitations are elaborated on in Section 2.2.2, and rotor angle stability refers to the disturbance through transient events which can follow a break-down or other disturbance to the grid. This is a dynamic phenomenon where generators can start to oscillate uncontrollably if the disturbance is not attenuated. The oscillations can impact the frequency, power flow and voltage in the grid, and can also cause damage to equipment in large areas [16]. All the above-mentioned aspects, as well as aspects affecting these, like network topology, load and generation pattern, and weather etc, are considered when determining the Total Transfer Capacity.

2.2.1 Congestion and Contingency

The Total Transmission Capacity is determined with regard to the N-1 criterion, which means that the grid needs to be dimensioned so that any contingency can occur without causing any unbalances. In the power system, contingency refers to a scenario where a power system component, such as a transmission line, transformer, or a generator, fails or is removed from service. Contingencies can happen for various reasons, such as equipment failure, human error, or natural disasters. The power system must be designed to handle these contingencies so that the system can continue to operate safely and reliably.

It is regulated in [17] that the system operators need to be prepared for N-1 contingencies and be able to keep the operational conditions within the allowed limits if unpredictable disturbances occurs. It is further stated that if a disturbance occurs and measures are taken to restore the system, that situation becomes the new N-0 state. Exceptions can be made to this if the fault only causes a local impact [17].

As a consequence, the N-1 criterion is therefore used by the TSOs when calculating the transfer capacity between bidding zones. The maximum allowed line loading, as shown in Equation 2.1, can be derived by dividing the flow that the network can accommodate after each possible contingency, k_{N-1} with the maximum capacity of the network, K [18].

$$\alpha_{N-1} = \frac{k_{N-1}}{K} \tag{2.1}$$

When the available capacities are calculated, these are reported to the energy market operator Nordpool, which can schedule the flow to accommodate the system's state. Congestion arises when the transfer capacity is insufficient to sustain the market interest, and price differences occur between different bidding zones as a consequence [19].

2.2.2 Static Voltage Stability

Static voltage stability refers to the ability of an electrical power system to maintain a stable voltage level under steady-state conditions, i.e., when the system is operating at a constant load and the power supply and demand are balanced. In other words, static voltage stability is concerned with the ability of the power system to maintain the desired voltage level without any significant deviations from the set value.

Voltage stability is essential to power system operation. Overvoltages can cause problems such as increased corona losses and damage to equipment. Undervoltages, on the other hand, can cause higher transmission losses, reduced capacity to transfer power, damage to equipment, and a higher risk for voltage instability or collapse. To reduce the risk of such problems, Svk has defined limits on operational safety concerning voltage [20]. Figure 2.3 displays the acceptable voltage ranges for different time intervals. As can be seen, the lower and upper limits for voltage level for an extended period are $[0.9875, 1.05]$ p.u.

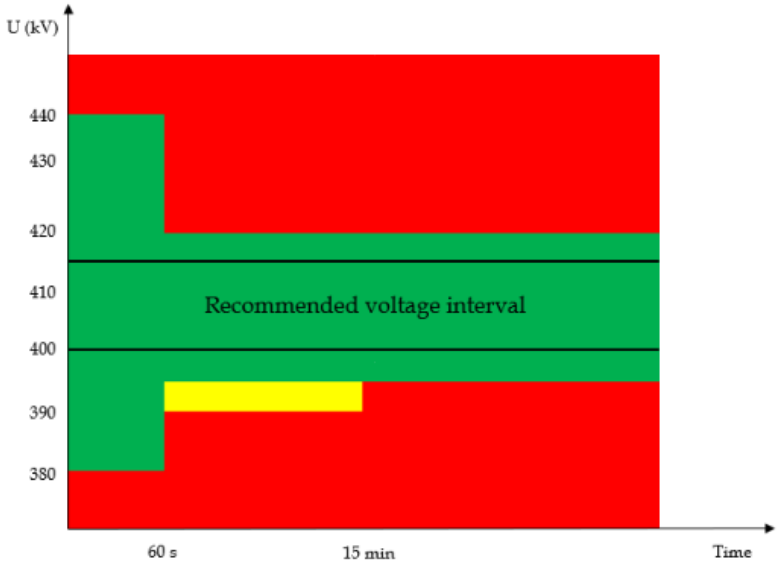

Figure 2.3: Acceptable voltage ranges [20]. Green, yellow, and red correspond to normal, alert, and emergency states, respectively.

3

Modelling of the Nordic Synchronous Power System

The model used for the studies performed in this thesis was first developed in the PyPSA-Eur project [21]. Section 3.1 describes how this was done. That model was based on open sources and included the whole power grid in the ENTSO-E area. The PyPSA-Eur model was then scaled down to only include the Nordic synchronous system and its interconnections in [22]. This chapter describes how choices were made for different components in the grid in the different iterations of the model. Changes implemented in this report for the different components are described in the subsections *Adaptations made* found for each component. Throughout the report, the initial model developed by [21] is referred to as the PyPSA-eur model, the scaled-down model over the Nordic area only developed by [22], is referred to as the Nordics model. The models developed in this report is referred to as this model, the 2020-model or the 2045-model.

The different components and approaches that have been altered are presented in the list below and are explained and evaluated further in Chapter 3 and 4.

- Buses: Network topology, slack bus, information on county
- Lines: Network topology, impedance, rating, lines out of operation
- External links: Existing and new links
- Loads: Sizing and distribution, redistribution
- Generators: Installed generators, output, reactive power limits
- Transformers: Size and impedance
- Reactive compensation: Shunts and series compensation
- Balancing

3.1 The PyPSA-Eur Project

The model used for the studies performed in this thesis is based on the PyPSA-Eur model, a model of the power grid in the ENTSO-E area, which also is based on open sources [21]. The network topology was taken from the ENTSO-E Interactive Map and distributed buses and lines with geographical coordinates. This was done using the `GridKit` toolkit [23]. It was also the `GridKit` that was used to place the generators at the nearest bus, given that the generator locations were decided using `powerplantmatching`, further described below. The information from the map was

extracted in May 2016. Some modifications to improve the network topology was done by the developers of the PyPSA-eur model [21].

Furthermore, the generator placement and capacities were decided using the `powerplantmatching` tool [24]. This tool creates an open-source database with data on powerplants in Europe which is used as input in the PyPSA-eur model. The input is from nine different sources with information on power plants in Europe. This data is then merged and standardized using `powerplantmatching`. If data is available from multiple sources, the sources are assigned a reliability score. The data from the source with the highest reliability is chosen, or the data is merged and used complementary. The data on the generation at a specific timestamp was taken from Open Power System Data (OPSD) project, which collects and standardizes data from the ENTSO-E Transparency Platform [25]. At the time of writing this report, the latest data available is from October 6th, 2020.

3.2 Buses

Buses were placed according to geographical information from ENTSO-E, using an extended version of the `GridKit` toolkit as explained in Section 3.1 [21]. The PyPSA-eur model only includes the transmission grid, which means voltage levels above and including 220 kV. In addition, information regarding which bidding zone each bus belonged to was added to the Nordics model. The voltage level was increased from 380 kV to 400 kV on buses and lines to represent the conditions in the Nordics [22].

Because of limited information on what bus the generators and loads throughout the system are connected to, the PyPSA-Eur project used a Voronoi diagram to assign generators and loads to buses [21], [23]. Figure 3.1 presents a general example of a Voronoi diagram. Each point p_k in the diagram has a corresponding Voronoi cell R_k whose distance to p_k is less than or equal to its distance to any other p_k [26]. In the PyPSA-Eur project, each point p_k corresponds to a bus in the system. Based on this, all generators and loads in a particular bus Voronoi cell R_k are assigned to the bus p_k.

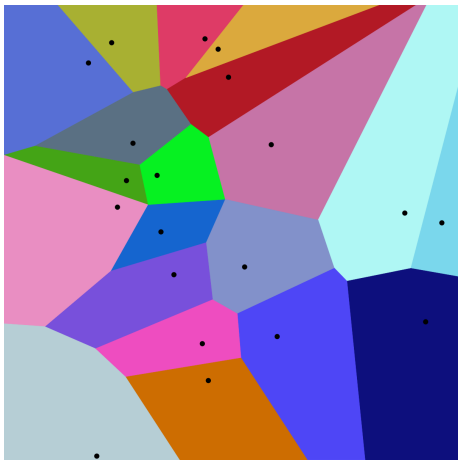

Figure 3.1: 20 points and their respective Voronoi cells [27].

3.2.1 Adaptations made

Errors in bus placements were found when investigating the grid topology. Some buses were missing, and in each spot where lines crossed over each other in the grid map [28], a "joint bus" was added. To validate the placements of the buses, the PSS/E model was compared to the ENTSO-E map and the grid map of each TSO, and the model was updated where inconsistencies were found.

Due to the lack of resolution around Oslo and Stockholm, simplifications in the model were done in these areas in the PyPSA-eur and the Nordics model. This included modeling much of the 300 kV/220 kV grid as one large bus with many lines connected to it. This bus was then connected to the 400 kV grid. These simplifications were kept in the 2020 model. In the 2045 model, the 400 kV changes were implemented.

Manually added buses had no impact on the Voronoi grid. Hence, no loads nor generators were assigned to these buses after having added them. Loads and generators had to be moved manually from buses close by. The slack bus was selected to be located in SE1 because it is a bidding zone with much available regulatory power. In addition to this, information regarding which county each bus belonged to was added, how this was done is further elaborated upon in Section 4.4.2.

3.3 Lines

The line types used in the PyPSA-Eur model were the same for all lines, depending on voltage level, and the voltage levels were restricted to either 220 kV, 300 kV, or 380 kV. The line types were kept the same in the Nordics model. However, the 380 kV voltage level was increased to 400 kV to represent the Nordic settings accurately.

The line impedances were given in [Ω/km], and the capacitances were given in [nF/km]. Since per unit values were chosen as input for PSS/E in this project, these

values were recalculated for each line into resistance [$R_{p.u.}$], reactance [$X_{p.u.}$], and charging [$B_{p.u.}$]. The Nordics model used the long line model for all lines [22].

The HVDC line between Finland and SE3 was modeled with VSC power electronics, 500 kV DC voltage, and it was assumed to be lossless. The power transmitted through this line was set to the values gathered from ENTSO-E for each case. HVDC links are always constant in the simulation software, and therefor will always transfer the power which it is set to. The HVDC connection that is part of Sydvästlänken was not in commercial operation until 21/7-2021 [29]. Sydvästlänken is present in the Nordics model and has been modeled in the same way as the FI-SE3 HVDC link, with the exception that the power going through the line is not pre-set from cross-border flows but has to be manually assigned. In the 2020 model this value is set to zero since the commissioning date is after the simulated dates.

3.3.1 Adaptations made

As mentioned in Section 3.2, certain inaccuracies were identified in the grid topology, and this affected how lines were drawn in the model. To address this issue, the joint buses in question were eliminated, and the ENTSO-E grid map was used to determine the intended path of the lines. By incorporating the lengths of the lines connecting the buses, new lines could be accurately added between the intended buses. Where uncertainties about the grid configuration arose due to lack of detail, OpenInfraMap [1] was used to determine which buses were supposed to be connected [30]. This map could also be used to see if lines were connected to busses or just passing by, with reservations that it is a community-driven source, and might not be entirely accurate. When adding new buses, the line length of existing lines was used in combination with Google Maps measuring function, and the wrongly placed line was removed. Then the grid topology was also compared to the grid maps provided by the TSOs to make sure updates to the grid made before 2020 were included in the model.

Sydvästlänken was not in operation in 2020 and therefore, not in operation in the 2020 model. In the 2045 model, both Sydvästlänken and FI-SE3 were modeled, and manual flows were assigned. The fixed transfer on these lines where determined through an iterative process to find the setting that transferred power in the same direction and with the same percentage of loading as the surrounding lines.

The line types, and thus the line parameters were all updated in this model according to Table 3.1. Based on the information provided by Svk, in the 400 kV grid, the 910AL59 is a standard line type, and in the 220 kV grid, it is either the 910AL59 or the 774AL59. It was assumed that all lines of one voltage level were of the same type. This was done for simplicity and lack of data providing information on which specific lines are of which types. Thus it was assumed that all 400 kV lines were of the 910AL59 kind, and all 220 kV lines were of the 774AL59 kind.

[1] OpenInfraMap is a branch of OpenStreetMap which is an open-source community-driven map service that provide information on infrastructure such as the power grid.

In the PyPSA-eur and the Nordics model, all lines of one voltage level were the same type and had the same rating. This method was kept, hence a decision regarding which line type to use and if a line type was simplex, duplex, or triplex had to be made. After studying implemented and future investment plans for 400 kV lines, triplex was chosen in most of the cases, and therefore, this was the choice made for the model as well. The same approach was used for the 220 kV lines, and plans of triplex, duplex, and simplex was found. The majority, however, was duplex and therefore this choice was assumed to be the best compromise.

Furthermore, the 300 kV grid only exists in Norway, and Statnett intends to upgrade most of the 300 kV grid to 400 kV level [13]. This is because most of the 300 kV lines built in Norway today are dimensioned so that they can be upgraded to 400 kV. Furthermore, most 300 kV concession plans in Norway are triplex [31], but the existing 300 kV grid is not built with triplex. Currently, only 15% of the 300 kV grid consists of duplex lines, while the remaining is simplex lines [13]. As a result, the first assumption for the 2020 scenarios was that all the existing 300 kV lines are simplex. However, after observing multiple overloads on 300 kV lines in Norway during the simulation, the 300 kV lines were all changed to duplex. This change will make it seem as many of the 300 kV lines have more available power than they should have. But, since the excising duplex lines could not be distinguished, it was decided that all should be modeled as duplex to avoid these lines overloading. In the future scenarios, where they operate at 400 kV, they are modeled as triplex lines due to the model's configuration. This works quite well since it was found that most new lines are triplex, and in the 2045 model, most 300 kV lines have been upgraded to 400 kV lines in Norway.

Table 3.1: Line types and electrical parameters

Line types	**Resistance, R [Ω/km]**	**Reactance, X [Ω/km]**	**Capacitance, C [nF/km]**	**I_{rated} [A]: 20°C**	**I_{rated} [A]: 0°C**
774AL59 - duplex (220 kV)	0.0384 [32]	0.30	11.84	1958.9	2 719.2
Feral 380 Grackle - simplex (300 kV)	0.0477 [33]	0.42	8.54	866.2	1 239.2
Feral 380 Grackle - triplex (300 kV)	0.0477 [33]	0.27	13.16	2 598.7	3 717.5
910AL59 - triplex (400 kV)	0.0326 [32]	0.27	13.22	3 241.9	4 517.9

In Table 3.1, the resistance values are the same as presented in each source, but the reactances and capacitances of the lines were calculated. The reactance is given by (3.1) - (3.3). $f = 50$ Hz is the nominal frequency, $a = 11.34$ m is the geometrical mean distance between the phases, assuming that the distance between the phases is 9 m which is a standard set-up for the 400 kV grid [34]. n is the number of lines per phase (different depending on which line type, simplex, duplex, or triplex). The distance between the lines in a phase is measured at 0.3 m and is denoted as $(D/2)$, this value complies with the Svk standard. d is the diameter of the conductor.

$$2\pi \cdot f \cdot L = X \tag{3.1}$$

where

$$L = 0.2 \cdot ln(\frac{a}{(d/2)_{ekv}} + \frac{1}{4 \cdot n})[\text{mH/km}] \tag{3.2}$$

and

$$(d/2)_{ekv} = \sqrt[n]{n \cdot (D/2)^{n-1} \cdot (d/2)}[\text{mm}] \tag{3.3}$$

Similarly, the capacitances were calculated using Equation 3.4, where $H = 15$ m is the geometrical mean height over the ground for the lines, and $A = 30$ m is the geometrical mean distance between each line and its image.

$$C = \frac{1}{18 \cdot ln(\frac{2H}{A} \cdot \frac{a}{(d/2)_{ekv}})} \tag{3.4}$$

These parameters were then used to calculate the per-unit values for each line going into PSS/E. When defining the line impedances which are used as input to PSS/E, it is important to consider the transmission line's length. This is due to the fact that different parameters dominate the line behavior for different lengths. In this report, three different models are used depending on the line length, l, and these models are defined in [35]. The short line model is used for $l < 80$ km. The medium line model is used for 80 km $\leq l \leq$ 250 km, and for 250 km $< l$, the long line model is used.

To calculate the impedance of short lines, the line length is multiplied by the per unit impedance of the line type, as shown in Equation 3.5.

$$Z = (R_0 + j\omega L_0) \cdot l = R + jX \tag{3.5}$$

For lines of medium length, Z is calculated as shown in Equation 3.5. Additionally, the shunt admittance needs to be taken into account. The equation for obtaining this is shown in 3.11 where G_0 and C_0 are the shunt conductance per phase per km and capacitance per phase per km, respectively.

$$Y = (G_0 + j\omega C_0) \cdot l \tag{3.6}$$

For lines longer than 250 km, additional considerations need to be made to account for the fact that L and C are distributed along the lines and not lumped together. Furthermore, the currents are not the same along the line. These considerations are displayed in Equation 3.7 through 3.10.

$$R' \approx R_0 l \cdot (1 - \frac{X_0 B_0 l^2}{3}) \tag{3.7}$$

$$X' \approx X_0 l \cdot (1 - \frac{X_0 B_0 l^2}{6}) \tag{3.8}$$

$$B' \approx B_0 l \cdot (1 + \frac{X_0 B_0 l^2}{12}) \tag{3.9}$$

$$G' \approx 0 \tag{3.10}$$

Z is calculated using the same Equation 3.5 as the short and medium line model but with R' and X' plugged in. The shunt admittance equation needs to be calculated in

a different way for the long-line case. This is shown in Equation 3.11. The per-unit values are then obtained by dividing each value by the system base.

$$Y' = G' + jB' \tag{3.11}$$

In order to calculate the rated current for the different line types, Equation 3.12 was used, where q_c represents the convection heat loss rate per unit length, q_r represents the radiated heat loss rate per unit length, q_s represents the heat gain rate from the sun per unit length, and R is the resistance in ohms per unit length. Equation 3.12 is the IEEE standard for calculating the current-temperature relationship of bare overhead conductors [36]. The method for obtaining q_c, q_r and q_s are displayed in Equations A.1 through A.10 in Appendix A.

$$I = \sqrt{\frac{q_c + q_r - q_s}{R}} \tag{3.12}$$

By using Equation 3.12 and varying the ambient temperature, the temperature dependency of the thermal rating of each line type used in the model could be derived. This is displayed in Figure 3.2. The current-temperature ratings for the line types 774AL59 and 910AL59 have been verified using a line rating calculator provided by an Svk employee.

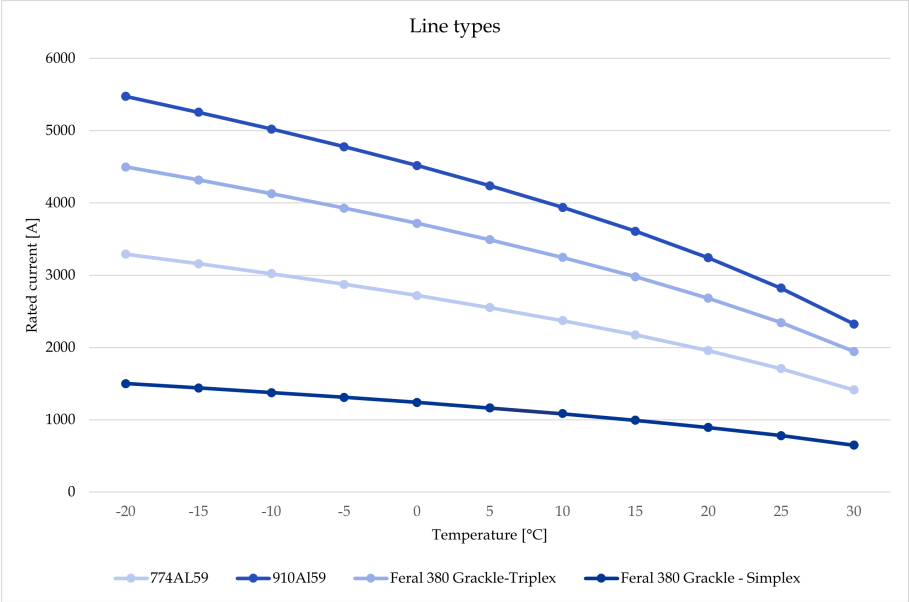

Figure 3.2: Line types used in the model along with their respective current-temperature relationship.

Having temperature dependant current ratings for the lines in the model allows for more sophisticated system analysis. Using the same current rating for a scenario in the summer compared winter scenario could lead to lines being misrepresented as heavily or lightly loaded because the rating is temperature dependent. As a result, the thermal ratings employed for winter scenarios are calculated based on an ambient temperature of 0 degrees Celsius, while the thermal ratings for summer scenarios

are determined using an ambient temperature of 20 degrees Celsius.

The thermal ratings of overhead lines are typically chosen to prevent two potential issues [36]. The first is excessive sag of the conductors, which occurs due to the thermal expansion of the conductors. This can result in violations of minimum distances from the ground, trees, or other conductors. The second is the annealing of the strands of the conductors. However, this report only focuses on the rated current provided by the calculations presented earlier.

3.4 External Links

In the PyPSA-eur model, the external links were not external since they are integrated in the European system. In the Nordics model [22], the external links are links with one connection within the Nordic synchronous system and one outside. The links are not modeled as links but rather as active power loads on the bus where the connecting cable is located. A positive value of the load represents export, and a negative value represents import. The loads are fixed to cross-border flow values retrieved from the ENTSO-E transparency platform, and if there is more than one connection between the same bidding zone and country, the flow is divided between these connections [22]. In 2020, the connection between Great Britain and NO2 was not in commission. A load was placed at the bus in Kvilldal but was set to zero. Furthermore, the Hansa PowerBridge connection between Hurva (SE4) and Germany is present in the model but will not be in commission until 2029 [2]. Since there is a connection between SE4 and Germany in commission, the load from this flow was divided equally between these connections.

3.4.1 Adaptations made

No adaptations have been made to the existing external links. The decision was made to keep the configuration in SE4 regarding Hansa PowerBridge and the load in Hurva. Since Hurva and Kruseberg, which is where the other HVDC link to Germany is connected, are located close by each other, the impact on the flow, in general, was deemed minimal, keeping in mind that this could mean a reduction or increase in flow by 300 MW between these buses. 300 MW is half of the transmission capacity of the existing HVDC connection. When the Hansa PowerBridge is commissioned, the transmission capacity between SE4 and Germany will increase by 700 MW to 1300 MW in total, which will be divided equally between the two buses.

HVDC links have the ability to adjust their voltage to 1 p.u. This was not taken into consideration in the Nordics model. In the 2020 model, the voltage regulation is entirely handled by generators with infinite reactive capability.

3.5 Loads

In the PyPSA-Eur model, the total load of each country was gathered from the ENTSO-E transparency page [25]. The loads were assigned to buses which, in the ENTSO-E and Svk map, were not considered generator buses [28], [2]. However, generators were often assigned to these buses as well in the model. How much load was allocated to each bus depends on 60 % of the gross domestic product (GDP) in that Voronoi cell and 40 % of the population. The GDP indicates the size of the industrial loads in that area, while the population represents household loads [21]. Typically, loads are connected to the lower voltage levels in the grid, but here all loads are directly connected to 400 kV, 300 kV, and 220 kV buses. All loads were assumed to have a unity power factor in the Nordics model. According to Svk, there should be no reactive power exchange between the transmission and distribution grid during normal grid operation, but an error margin of ±5 MVAr is allowed [37]. Thus the unity factor was kept in this model as well.

The resolution of the load distribution was improved upon in the Nordics model. By assigning bidding zones to each bus and using data directly from the ENTSO-E transparency page in the Nordics model, the loads were scaled per bidding zone and then assigned in the same way as the PyPSA-Eur model [22]. A second improvement in the Nordics model included removing the losses in each bidding zone. The hourly load data included the losses in the grid, but in PSS/E, the losses are not included in the loads. They are added additionally and compensated for by the slack bus. To mitigate this issue, the Nordics model iterates the simulation and calculates the losses in PSS/E per bidding zone. These losses were then removed from the total load in each respective bidding zone to avoid it being counted twice.

3.5.1 Adaptations made

The load distribution was mainly kept as in the Nordics model. However, when adding new buses, some of the load on buses close by were added to that bus instead. To mitigate imbalances in the data that arose when the net import/export, generation, and load in each bidding zone did not equal zero, manual loads and manual generators were added to each bidding zone. P_{set} was decided from the imbalance that arose in the bidding zones after having simulated a scenario once, and then this was iterated to reduce any discrepancies further. Both the balancing loads and generators had a power factor of 1 and were added at a 400 kV bus in the middle of each bidding zone, with several connecting lines.

During simulations, it was observed that all loads were connected to the 220 kV voltage side of transformer buses. In some cases, this lead to overloads. Simulations were run, and it was found that moving some of the load from the 300 kV/220 kV side to the 400 kV side helped with the overloads and the flow. The ratio decided upon was a 3:1 ratio (400 kV:300/220 kV). 75 % of the load was connected to the 400 kV side and 25 % to the 300 kV/220 kV side, the ratio was chosen after observing the power flow in the model and the cross border flows. This change only affected

loads connected directly to a transformer bus and did not apply to loads connected to other buses. Usually, loads are connected to lower voltages, but since the change did improve the model, the change was kept.

3.6 Generators

The toolkit `powerplantmatching`, as explained in Section 3.1, was used to decide the placement and capacity of the generators in the PyPSA-Eur model and the Nordics model. `powerplantmatching` aggregates all generation units on one site to one large generation unit. For instance, if there are several nuclear reactors in one place, these are seen as one large generator. The Voronoi cells were used to place the generators at the bus closest to their location, disregarding the underlying network and the voltage level of the generator [21].

Data on generation per type, per country, for the relevant hour was retrieved from the ENTSO-E transparency platform. This was compared to the available capacity of that generation type in the same country to decide the scaling factor according to Equation 3.13. Then, the scaling factor was multiplied with P_{max}^{gen} for the relevant generation units to set the active power output, P_{out}^{gen}. In the Nordics model, this was done on a bidding zone level, and the generators were set to have a power factor of $\pm$ 0.9 independently of generation type.

$$\frac{\textit{Generation [MW] per type in Country}}{\textit{Available generation capacity [MW] per type in Country}} = \textit{Scaling factor} \quad (3.13)$$

Improvements in the Nordics model included dividing all nuclear power plants into separate reactors and assuming all generators considered as storage units in the PyPSA-eur model as hydro generators since all hydropower plants with a reservoir were classified as storage units. Moreover, inconsistencies in the reported wind generation were discovered. They were compensated for by increasing the wind generation with 10 % of the reported wind generation for Finland, and 5 % for all other bidding zones [22]. Also, due to lack of generation per type per bidding zone data in Sweden on the ENTSO-E transparency platform, this data was manually extracted from Mimer [38], which is where Svk uploads their data on load and generation, and scaled with the reported totals of Sweden to be consistent with the ENTSO-E data [22].

3.6.1 Adaptations made

To comply with the regulation that synchronous generators should be able to produce reactive power corresponding to one-third of their active power output [39], the power factor of the generators was changed from 0.9 to 0.94, and Q_{min}^{gen} and Q_{max}^{gen} were set to depend on P_{out}^{gen} rather than S_{nom}^{gen} which was the setting in the previous models. However, issues with this approach arose when the reduced reactive capability had to be compensated for with switched shunts, especially in the 2045 model when very large loads were added. Therefore, to be able to compare the 2020 model

to the 2045 model, the switched shunts were removed and all generators were set to have infinite reactive capability. This way, no conflicts arose during simulations at buses with both shunts and generators connected. One of the drawbacks of this approach is that it is not realistic to have infinite reactive compensation at all buses, which also means no reactive power needs to be transferred between buses and thus reducing the loading on the lines.

Errors were also found regarding which generators were present in the model. To improve this, the installed generation per type and bidding zone was compared to data on the actual installed capacity per type. Discrepancies found were, to the best ability, adjusted for by comparing installed generators in the model to external sources. These sources were vattenkraft.info [40] for information on hydropower plants in Sweden, Vindbrukskollen [41] for information on wind power in Sweden, NVE [42] for information on hydropower and wind power in Norway, and Wikipedia for information on thermal power plants in Denmark [43] and Sweden [44].

3.7 Transformers

No data on transformer location, size, or parameters is available in the ENTSO-E grid map. The PyPSA-Eur model solved this by placing 2 GVA transformers between buses with different voltage settings in the same place. The size of the transformers was set to be high to avoid situations where the transformer capacity would cause constraints in the power flow. The reactance of the transformers was set to 0.1 p.u. and was calculated using the system base of 100 MVA.

3.7.1 Adaptations made

No changes were made to the capacity of the transformers. However, to get more realistic impedance values, the winding MVA of the transformers was set to 400 MVA since these are the largest typical transformer sizes in Sweden for 420 kV/145-245 kV voltages [45], and the reactance was set to 0.12 p.u using the winding MVA instead of the system MVA as the base. The same settings were used for all transformers.

3.8 Reactive Compensation

No reactive compensators were added in the PyPSA-Eur or Nordic models due to a lack of data. In the Nordics model, the reactive compensation was done by the generators, which were set to have a power factor of 0.9.

3.8.1 Adaptations made

Issues arose during simulations when both generators and switched shunts were assigned to the same buses in PSS/E. For this reason, the decision was made to remove previously added shunts and increase the reactive capability of the generators to be infinite, ensuring that the voltage at all generator buses is 1 p.u. Additionally, series

compensation was added at all 400 kV lines going from SE2 to SE3 [2]. The series compensation was set to reduce the reactance to 50 % of its uncompensated value [46]. The introduction of series compensation worsened the accuracy of the model in terms of cross-border flow, pushing even more flow through Sweden. The series compensation was not utilized in the low load cases since series compensation is used to increase the capacity of the lines, and during low load cases, the need for this is smaller.

In the 2045 model series compensation was not used due to Svk's long-term plan to remove it [2].

4

Base Case Scenarios and Model Validation

To understand the accuracy and discrepancy of the 2020 model with respect to the actual system, several cases are tested for validation and comparison. These cases, and the chosen validation method, are employed to evaluate the modifications made to the model as outlined in Chapter 3. This chapter will provide a comprehensive presentation of these scenarios and elaborate on the methodology employed to assess the model's performance.

4.1 Presentation of the 2020 Cases

The most up-to-date data available in the OPSD database is from October 6th, 2020. Hence the timestamps chosen for the cases were chosen before this. Four different scenarios with different load and generation mixes were selected to study the behavior in the grid during some of the more extreme cases that occur during a year. These cases primarily represent when large and small flows go from the north to the south and when there is more distributed generation due to more wind. The input data for the different cases are presented in Sections 4.1.1 - 4.1.4, and the timestamp of these cases are presented below.

- High load - high wind generation
  2020-02-21 18:00 UTC
- High load - low wind generation
  2020-02-27 18:00 UTC
- Low load - high wind generation
  2020-09-17 00:00 UTC
- Low load - low wind generation
  2020-08-01 05:00 UTC

Tables 4.1, 4.3, 4.5 and 4.8 summarizes the totals for the generation per type come from ENTSO-E [8]. However, in Sweden, the values per bidding zone is that total scaled with values from Mimer on the generation per bidding zone per type [38]. The choice to scale against the ENTSO-E data instead of using the values directly from Mimer was to make the totals in the data align with that of the other countries. In Tables 4.2, 4.4, 4.6 and 4.9, the 50 MW connection between NO4 and Russia is

not included, for all timestamps in this report the transferred power through this interconnection was zero [47].

4.1.1 High load - high wind - 2020-02-21 18:00 UTC

The high load, high wind scenario is one of Sweden's hours with the highest total wind power generation. According to the data presented in Table 4.1, the total generation in the Nordic synchronous system at this hour is 52.6 GW, of which 24 % is generated from wind. More than half of the generation, 52 %, comes from hydropower, where Norway is the biggest producer. The most significant surpluses of power are found in SE2 and NO2, and the most significant deficits are in NO1, FI, and SE4. The losses in the system are included in the loads.

Table 4.1: High load - high wind scenario. Generation and load data per bidding zone. Difference = Total generation - Load, thus, it represents the import/export need of each zone. The totals are sums of the bidding zones. All values in [MWh/h].

Type	Hydro	Nuclear	Other thermal	Solar	Wind-offshore	Wind-onshore	Total generation	Load	Difference
DK			1 272		1 368	2 604	5 244	4 578	666
DK2			677		363	623	1 663	1 854	-191
FI	2 152	2 798	2 096			1 787	8 833	10 755	-1 922
NO	15 391		463			2 067	17 921	18 824	-903
NO1	1 950		23			153	2 126	5 264	-3 138
NO2	6 630		13			750	7 393	4 979	2 414
NO3	2 004		99			828	2 931	3 741	-810
NO4	1 969		243			336	2 548	2 585	-37
NO5	2 836		85			0	2 921	2 254	667
SE	9 464	6 088	995			7 631	24 178	18 143	6 035
SE1	1 958		32			1 012	3 002	1 120	1 882
SE2	5 475					2 934	8 409	2 228	6 181
SE3	1 896	6 088	659			2 366	11 010	11 365	-355
SE4	290		147			1 319	1 757	3 430	-1 673
Total	27 161	8 886	4 075	0	363	12 108	52 593	49 575	3 018
% of total	51.6	16.7	7.7	0	0.7	23.0	100		

The cross-border flows between all bidding zones and connections to non-synchronized areas are presented in Table 4.2. The cross-border flow between bidding zones NO1-NO2 is marked in red and bold in this table. This is due to a lack of data in ENTSO-E. The value in red and bold is the mean value of the balance offset for that hour (difference = generation - load - other cross border flows) in the two bidding zones. The largest flows are found through Sweden, particularly SE3, which imports 5.6 GW from SE2 and distributes it to FI, NO1, and SE4. The total is the net import/export in MW for that bidding zone, and positive values mean net export. The total export for the Nordics is the sum of the totals, 2 893 MW. This value is different from the value presented Table **??**, this is due to data inconsistencies and is further elaborated on in Section 4.3

Table 4.2: High load - high wind scenarios. Cross border flows going from row to column. The total equals the net import/export of each bidding zone. Positive means export and negative means import. The values in red and bold is an estimation of the cross-border flow between NO1-NO2 due to lack of data in ENTSO-E. It is the mean value of the balance offset for that hour (difference = generation - load - other cross border flows) in the two bidding zones. All values in [MWh/h].

	DK1	SE4	EE	NO4	RU	SE1	SE3	NO2	NO3	NO5	NL	NO1	SE2	FI	DK2	LT	PL	DE	Total
DK2	-590	-236																585	-241
FI			984	-30	-186	-1 261	-1 202												-1 695
NO1							-842	**-1 132**	-111	-1 059									-2 012
NO2	432									419	425	**1 132**							1 276
NO3				-372						-28		111	-504						-793
NO4						-353			372				-118	30					-69
NO5								-419	28			1 059							668
SE1				353									58	1 261					1 672
SE2				118		-58	5 620		504										6 184
SE3	-696	3 690										842	-5 620	1 202					-582
SE4							-3 690								236	733	598	608	-1 515

4.1.2 High load - low wind - 2020-02-27 18:00 UTC

The high load - low wind case was chosen to illustrate the difference in energy mix when the load is high and the availability of wind power is lower. The data for this case is presented in Table 4.3.

Table 4.3: High load - low wind scenario. Generation and load data per bidding zone. Difference = Total generation - Load, thus it represents the import/export need of each zone. The totals are sums of the bidding zones. All values in [MWh/h].]

Type	Hydro	Nuclear	Other thermal	Solar	Wind-offshore	Wind-onshore	Total generation	Load	Difference
DK			3 038		538	322	3 898	5 018	-1 120
DK2			1 080			18	1 098	1 985	-887
FI	2 267	2 799	4 300			728	10 094	11 674	-1 580
NO	21 974		424			977	23 375	20 804	2 571
NO1	2 489		22			17	2 528	6 294	-3 766
NO2	8 168		8			370	8 546	5 481	3 065
NO3	3 415		74			408	3 897	4 038	-141
NO4	3 893		229			181	4 303	2 718	1 585
NO5	4 010		91				4 101	2 272	1 829
SE	12 145	6 895	1 469			1 530	22 039	21 290	749
SE1	3 499		45			519	4 064	1 323	2 741
SE2	6 636					771	7 407	2 278	5 129
SE3	1 968	6 895	937			156	9 956	13 809	-3 853
SE4	278		251			84	613	3 880	-3 267
Total	36 622	9 694	7 038	0	0	3 252	56 606	55 752	854
% of total	64.7	17.1	12.4	0	0	5.7	100		

From Table 4.3, one can see that compared to the high load - high wind case, the load is higher in this case, and the power generated from wind is almost 9 GW less. This is compensated for by more hydro, nuclear and thermal generation, and less export. 6 % of the total generated power comes from wind. The cross-border flows for the high load - low wind case are presented in Table 4.4. The cross-border flow between bidding zones NO1-NO2 is marked in red and bold in this table. This is

due to a lack of data in ENTSO-E. The value is the mean value of the balance offset (difference = generation - load - cross border flows) in the two bidding zones. The total export from the Nordics is 1 090 MW. What can be seen from Table 4.4 is that the flow from SE2-SE3 is exceeding the capacity limit by 112 MW, the capacity limit is 7 300 MW, but the flow is 7 412 MW.

Table 4.4: High load - low wind scenario. Cross border flows going from row to column. The total equals the net import/export of each bidding zone. Positive means export, and negative means import. The values in red and bold is an estimation of the cross-border flow between NO1-NO2 due to lack of data in ENTSO-E. It is the mean value of the balance offset for that hour (difference = generation - load - other cross border flows) in the two bidding zones. All values in [MWh/h].

	DK1	SE4	EE	NO4	RU	SE1	SE3	NO2	NO3	NO5	NL	NO1	SE2	FI	DK2	LT	PL	DE	Total
DK2	-313	-919																324	-908
FI			38	-44	-527	-1 094	195												-1 432
NO1							546	**-1 887**	-329	-2 116									-1 899
NO2	715									19	424	**1 887**							1 158
NO3				-1 014						251		329	314						-120
NO4						374			1 014				136	44					1 568
NO5								-19	-251			2 116							1 846
SE1				-374									1 933	1 094					2 653
SE2				-136		-1 933	7 412		-314										5 029
SE3	568	3 861										-546	-7 412	-195					-3 724
SE4							-3 861								919	-625	597	-111	-3 081

4.1.3 Low load - high wind - 2020-09-17 00:00 UTC

The data on the low load, high wind case is presented in Table 4.5. The load is significantly lower than in the high load cases, and wind power generates 26 % of the total generated power, most of it is generated in Sweden. Compared to the high load cases, the power surplus in NO2, SE1, and SE2, which are bidding zones with high installed hydropower levels, is smaller. The largest deficits are found in FI and NO1.

Table 4.5: Low load - high wind scenario. Generation and load data per bidding zone. Difference = Total generation - Load, thus it represents the import/export need of each zone. The totals are sums of the bidding zones. All values in [MWh/h].

Type	Hydro	Nuclear	Other thermal	Solar	Wind-offshore	Wind-onshore	Total generation	Load	Difference
DK			647		998	1 126	2 771	2 912	-141
DK2			236		282	305	823	1 013	-190
FI	383	2 261	1 281			1 714	5 639	7 229	-1 590
NO	12 691		177			480	13 348	11 781	1 567
NO1	792		4			112	908	2 657	-1 749
NO2	4 075		2			121	4 198	3 356	842
NO3	2 144		38			144	2 326	2 492	-166
NO4	2 113		50			103	2 266	1 716	550
NO5	3 565		84				3 649	1 559	2 090
SE	2 573	4 867	544			6 269	14 253	11 127	3 126
SE1	949		25			1 141	2 115	814	1 301
SE2	1 259					2 591	3 851	1 221	2 630
SE3	446	4 867	350			1 811	7 473	7 335	138
SE4	23		65			725	814	1 757	-943
Total	15 749	7 128	2 135	0	282	8 768	34 062	31 149	2 913
% of total	46.1	21.0	6.3	0	0.8	25.7	100		

The cross-border flows are presented in Table 4.6. Due to less surplus in the north of Sweden, there is not as much power transmitted from SE2 to SE3 as compared to the previous cases. The total export is 3 583 MW.

Table 4.6: Low load - high wind scenario. Cross border flows going from row to column. The total equals the net import/export of each bidding zone. Positive means export and negative means import. All values in [MWh/h].

	DK1	SE4	EE	NO4	RU	SE1	SE3	NO2	NO3	NO5	NL	NO1	SE2	FI	DK2	LT	PL	DE	Total
DK2	515	-728																0	-213
FI			655	0	-808	-577	-600												-1 330
NO1							-216	527	-289	-1 734									-1 712
NO2	1 158									-571	704	-527							764
NO3				-542						220		289	-66						-99
NO4						0			542				4	0					546
NO5								571	-220			1 734							2 085
SE1				0									693	577					1 270
SE2				-4		-693	3 414		66										2 783
SE3	499	2 453										216	-3 414	600					354
SE4							-2 453								728	466	0	394	-865

4.1.4 Low load - low wind - 2020-08-01 05:00 UTC

In this scenario, presented in Table 4.8, the load is small, and the power generated from wind is only 3 % of the total generated power. The only bidding zones with deficits are DK2, FI, SE3, and SE4, the others have a surplus. Compared to the low load - high wind case, an additional 7 GW is produced by hydro, whilst nuclear and thermal are producing about the same.

Table 4.7: Low load - low wind scenario. Generation and load data per bidding zone. Difference = Total generation - Load, thus it represents the import/export need of each zone. The totals are totals of the bidding zones. All values in [MWh/h]

Type	Hydro	Nuclear	Other thermal	Solar	Wind-offshore	Wind-onshore	Total generation	Load	Difference
DK			628	184	446	456	1 714	2 983	-1 269
DK2			109	76	53	57	295	1 116	-821
FI	1 326	2 706	1 083			23	5 138	7 104	-1 966
NO	13 119		338			812	14 269	10 516	3 753
NO1	2 158		21			3	2 182	2 123	59
NO2	3 259		12			748	4 019	3 098	921
NO3	2 583		32			49	2 664	2 225	439
NO4	2 484		168			12	2 664	1 651	1 013
NO5	2 632		106				2 738	1 420	1 318
SE	8 154	4 372	540			122	13 188	10 132	3 056
SE1	2 800		17			29	2 846	893	1 953
SE2	4 800					26	4 826	1 326	3 500
SE3	598	4 372	312			46	5 328	6 188	-860
SE4	71		96			21	188	1 725	-1 537
Total	22 710	7 078	1 957	76	53	1 014	32 888	28 869	4 019

Table 4.8: Low load - low wind scenario. Generation and load data per bidding zone. Difference = Total generation - Load, thus it represents the import/export need of each zone. The totals are totals of the bidding zones. All values in [MWh/h]

Type	Hydro	Nuclear	Other thermal	Solar	Wind-offshore	Wind-onshore	Total generation	Load	Difference
DK			628	184	446	456	1 714	2 983	-1 269
DK2			109	76	53	57	295	1 116	-821
FI	1 326	2 706	1 083			23	5 138	7 104	-1 966
NO	13 119		338			812	14 269	10 516	3 753
NO1	2 158		21			3	2 182	2 123	59
NO2	3 259		12			748	4 019	3 098	921
NO3	2 583		32			49	2 664	2 225	439
NO4	2 484		168			12	2 664	1 651	1 013
NO5	2 632		106				2 738	1 420	1 318
SE	8 154	4 372	540			122	13 188	10 132	3 056
SE1	2 800		17			29	2 846	893	1 953
SE2	4 800					26	4 826	1 326	3 500
SE3	598	4 372	312			46	5 328	6 188	-860
SE4	71		96			21	188	1 725	-1 537
Total	22 710	7 078	1 957	76	53	1 014	32 888	28 869	4 019
% of total	69.1	22.7	6.0	0.2	0.2	3.1	100		

The cross-border flows are presented in Table 4.9. From this, it is clear that more power flows from SE2 to SE3 than in the low load high-wind case. In this case, the total export is 4 695 GW, which is the case with the largest export of power.

Table 4.9: Low load - low wind scenario. Cross border flows going from row to column. The total equals the net import/export of each bidding zone. Positive means export and negative means import. All values in [MWh/h].

	DK1	SE4	EE	NO4	RU	SE1	SE3	NO2	NO3	NO5	NL	NO1	SE2	FI	DK2	LT	PL	DE	Total
DK2	-381	-1 050																582	-849
FI			943	-76	0	-1 363	-1 201												-1 697
NO1							1 014	507	-173	-1 287									61
NO2	1 160									-395	703	-507							961
NO3				-463						433		173	369						512
NO4						451			463				10	76					1 000
NO5								395	-433			1 287							1 249
SE1				-451									1 039	1 363					1 951
SE2				-10		-1 039	5 011		-369										3 593
SE3	351	3 820										-1 014	-5 011	1 201					-653
SE4							-3 820								1 050	733	597	7	-1 433

4.2 Comparison

Some patterns become evident when comparing the net import/export of the different zones for the cases presented in Figure 4.1. Sweden is a net exporter for all cases, and Norway is a net exporter for all cases except the high wind - high load case. Finland always imports roughly the same amount of power, and DK2 imports more during the low wind cases and is always a net importer. In total, the Nordic system is a net exporter for all cases. Norway's most significant exports occur during low wind scenarios. This aligns with the strategy to shut down hydro plants when there is a surplus of cheap power available and utilize the water reserves when there is less available power and the power is more expensive [48]. These are however only four different hours of the year, which means it it hard to say whether this is a pattern or coincidence. The behaviour could vary both seasonally and during the hours of a day, but it is interesting that Norwegian strategy appears in these cases.

The values in Figure 4.1 were calculated according to (4.1), where P^{gen}_{Input} is the data on the total generated power in each bidding zone, P^{load}_{Input} is the load per bidding zone including losses, and $P_{Import/Export}$ is the calculated import/export need from each bidding zone.

$$P^{gen}_{Input} - P^{load}_{Input} = P_{Import/Export} \tag{4.1}$$

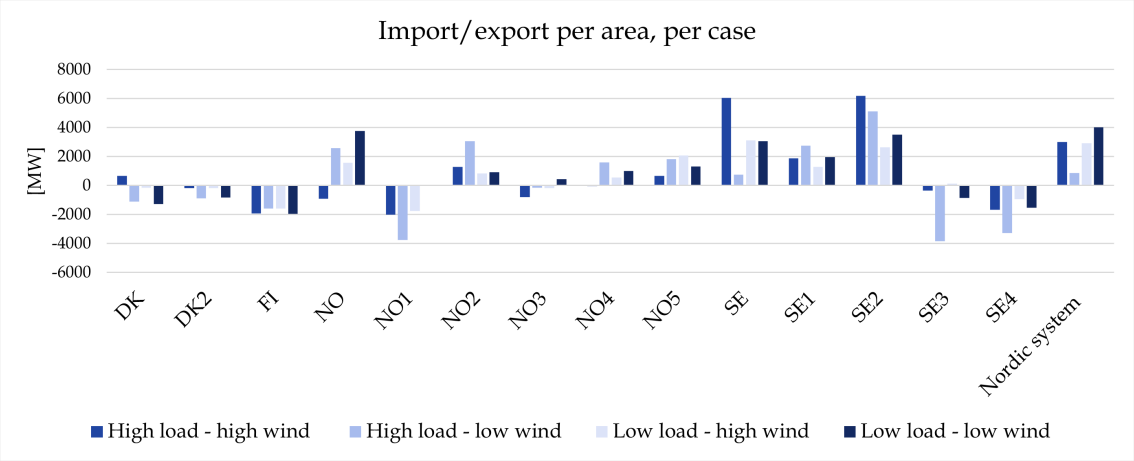

Figure 4.1: Comparison of the net import (negative values)/export (positive values) of each bidding zone and country. The last column represents the total Nordic synchronous system.

4.3 Quality of Data

Cross-border flows are the primary source of validation that this model is a good representation of reality, which is elaborated on in Section 4.4.3. A prerequisite for this to be a reliable form of validation is that the data going into the model is coherent with the data validated against. As seen in Figure 4.2, this calculated total is not always consistent with the sum of the reported cross-border flows in each bidding zone. The values in Figure 4.2 are calculated according to (4.2) where $P^{sum}_{Cross-borderflow}$ is the totals presented in Tables 4.2, 4.4, 4.6, and 4.9, and $P_{Import/Export}$ is the result of (4.1).

$$P_{Import/Export} - P^{sum}_{Cross-borderflow} = P_{Imbalance} \tag{4.2}$$

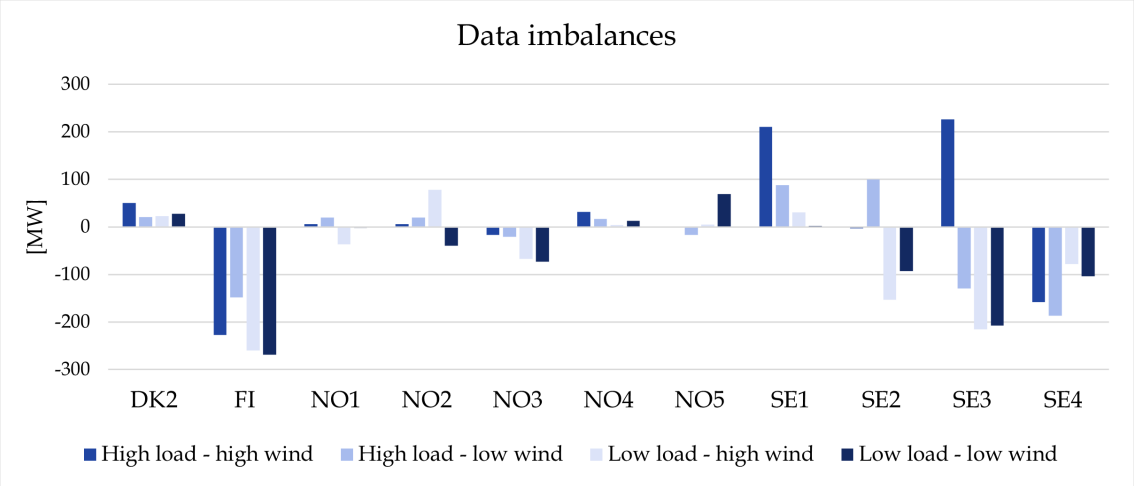

Figure 4.2: The diagram shows the data coherence between the bidding zones subtotals of generation and load presented in Tables 4.1, 4.3, 4.5, and 4.8, and the sum of the cross-border-flow for each bidding zone presented in Tables 4.2, 4.4, 4.6, and 4.9. The values are mismatches in the data in [MW].

From Figure 4.2, it is clear that the data going into the model is incorrect, which will impact the results in the validation. ENTSO-E was contacted to provide insight into the accuracy of the data and replied that the data on generation and load published on ENTSO-E transparency platform had to be reported within the hour and, therefore, could contain inaccuracies. ENTSO-E also stated that the measurements are taken using SCADA, which has an error margin of $\pm$ 5 %. Therefore, in order to be able to adjust the method to the inaccuracies, the mismatches in the cross-border flows were assumed to be correct, and the data on the load and generation more inaccurate. When the data on the ENTSO-E transparency platform was compared to data published on the TSO's own sites, discrepancies in the data became apparent. A recommendation would be not to use ENTSO-E data but instead use data published by the TSOs. The cross-border-flow data matches the data from Nordpool.

Assuming that the cross-border flows are correct, there is no way of knowing if the errors presented in Figure 4.2 are in the reported generation or the reported load. However, in Figure 4.2, some patterns present regarding if it is too much load/too little generation or vice versa. Compared to the sum of the cross-border flows, DK2 has too much generation or too little load reported in all four cases, and the opposite is true for FI, where the mismatch is considerably larger than in DK2. Overall, all Norwegian bidding zones are quite well-balanced, but the Swedish ones are not. There are also inconsistencies between the cases, whether the difference is positive or negative.

The 5 % measuring inaccuracy, when comparing the error in each bidding zone to the generated power in each bidding zone, is only exceeded in one case, the high load - high wind case in SE1, where the error is 7 % of the generated power.

4.4 Validation of the Model

In order to make sure that the model is a good approximation of reality, the model needs to be validated. This is done in the following sections. This validation is only viable for the base cases since the data used to validate against does not exist for future scenarios.

4.4.1 Installed capacities and line lengths

One way to validate the models' resemblance to reality is to compare the installed generation capacity of the model and the installed line length to the actual values. In Tables 4.10 and 4.11, the total line length and installed capacity for each country (excl. Denmark) in the model is compared to the TSO's own information on total line length.

Table 4.10: Total length of lines in the model for Sweden, Norway, and Finland along with the actual values [49], [50], [51].

	Model [km]	**Official number [km]**	**Difference [km]**
Sweden	14 733	16 000	- 1 267
Norway	8 666	11 000	- 2 334
Finland	7 041	6 400	641
Total	30 440	33 400	- 2 960

In Norway, the difference between the model and reality is quite significant, which could be explained by the fact that Norway's transmission grid includes some 132 kV lines, which are not included in this model. The total length of these lines is unknown, but they are mainly located in northern Norway where the total line length is $> 3\ 000$ km [13]. After studying the Statnett's grid map over this area [13], an estimation is that the 132 kV lines make up more than 50 % of the total line length in that area. Sweden and Finland differ less than Norway, but does still deviate from the official numbers with about 10 %. An explanation could be that some of the DC interconnections could be included in the total for Sweden, which is not the case for the totals in the model. Another reason behind the discrepancies is how the model defines lines. Each line has a from bus and a to bus, if the from bus and to bus are in different countries, the line gets assigned to the country that the from bus is in.

To summarize, the comparison of the overall line length per country indicates that the model is reliable in this sense. However, it is deemed to be an unreliable source of validation on its own due to the earlier mentioned uncertainties regarding what is included in the data. Furthermore, the fact that the official numbers in Table 4.10 are so even, suggests that they are rounded up or down. Because of this, the comparison between the model line length and the official numbers should be interpreted as an overall indication of how they match.

In Figure 4.11 the installed generational capacities per bidding zone in the model and from ENTSO-E reports are compared. The values for the Swedish bidding zones in the ENTSO-E column are not from ENTSO-E, as they do not publish generation data on a bidding zone level for Sweden. Instead, they are from the Long Term Market Analysis published by Svk.

Table 4.11: Installed generation capacities for Sweden, Norway, Finland, and DK2.

	Model [MW]	**ENTSO-E / Svk [MW]**	**Difference [%]**
DK2	6 047	6 057	0.17
FI	17 249	17 274	0.14
NO1	4 130	3 102	33.14
NO2	12 555	11 987	4.52
NO3	5 332	4 544	14.59
NO4	6 119	5 692	6.98
NO5	8 477	7 720	8.93
NO	36 613	33 045	9.75
SE1	8 765	6 925	20.99
SE2	14 551	12 151	16.49
SE3	16 907	17 450	3.11
SE4	4 678	5 297	11.68
SE	44 901	41 823	6.86

As can be seen in Figure 4.11, the installed capacity in the model matches very well with the reported values for DK2 and FI. However, obvious discrepancies are seen for both Norway and Sweden. These discrepancies show that the tool `powerplantmatching` lacks accuracy for Sweden and Norway. This was investigated to some extent but could have been investigated further.

4.4.2 Regions

To validate the model's accuracy on a regional level, the regions of the Nordic countries first had to be defined. This was done using available Geo-Data for the respective countries [52], [53], [54], that defines the region borders using coordinates. These sets of data were then merged into one single file containing all of the Nordic regions. This resulting file is displayed in Figure 4.3.

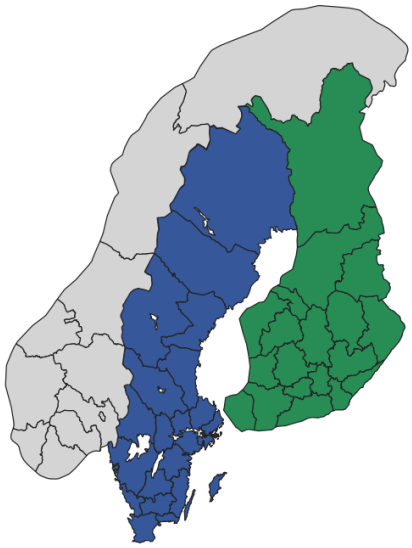

Figure 4.3: Norway, Sweden, and Finland divided into regions.

Using the information on regional borders shown in Figure 4.3, every bus in PSS/E was assigned to a geographical region based on its coordinates. The accumulated load per region for the different cases is compared to the percentage of annual consumption per region [55], [56], [57] in Figure 4.4, 4.5 and 4.6. The diagram illustrates how well the region's part of the total annual loads agrees with how the loads are distributed in the model. The numbers representing the model is the mean values of the four timestamps, where the load for each time stamp has been summed up on a regional basis and then divided by the total load for their respective country. DK2 have not been compared in the same way due to the small size.

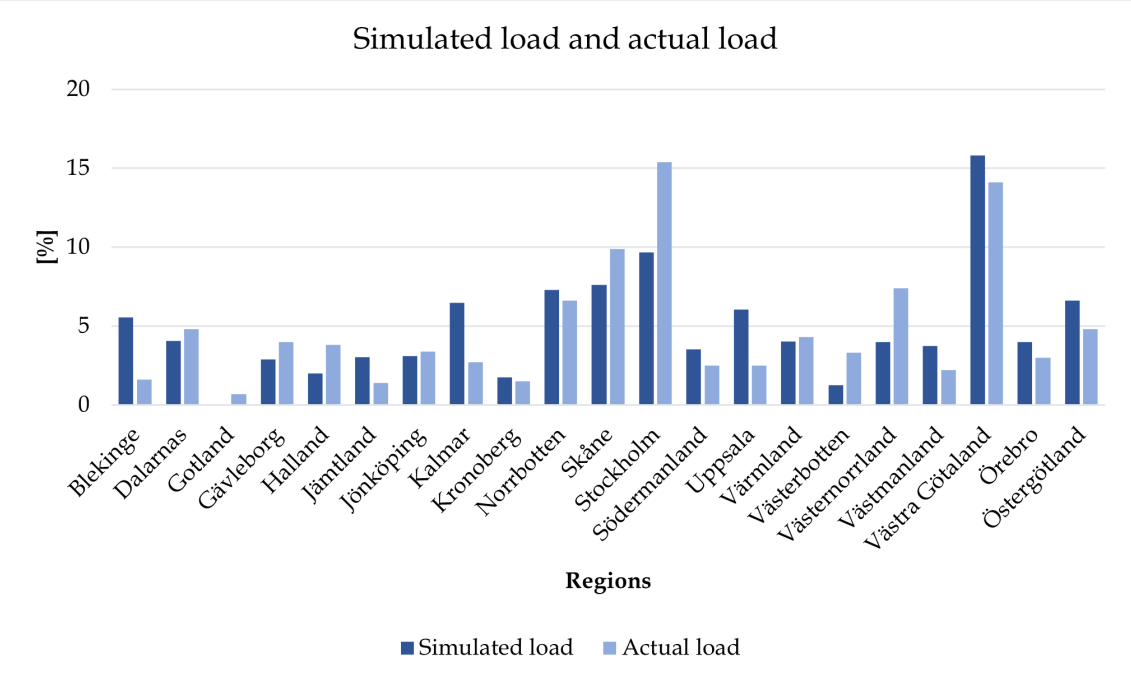

Figure 4.4: Simulated load along with actual load per region in Sweden.

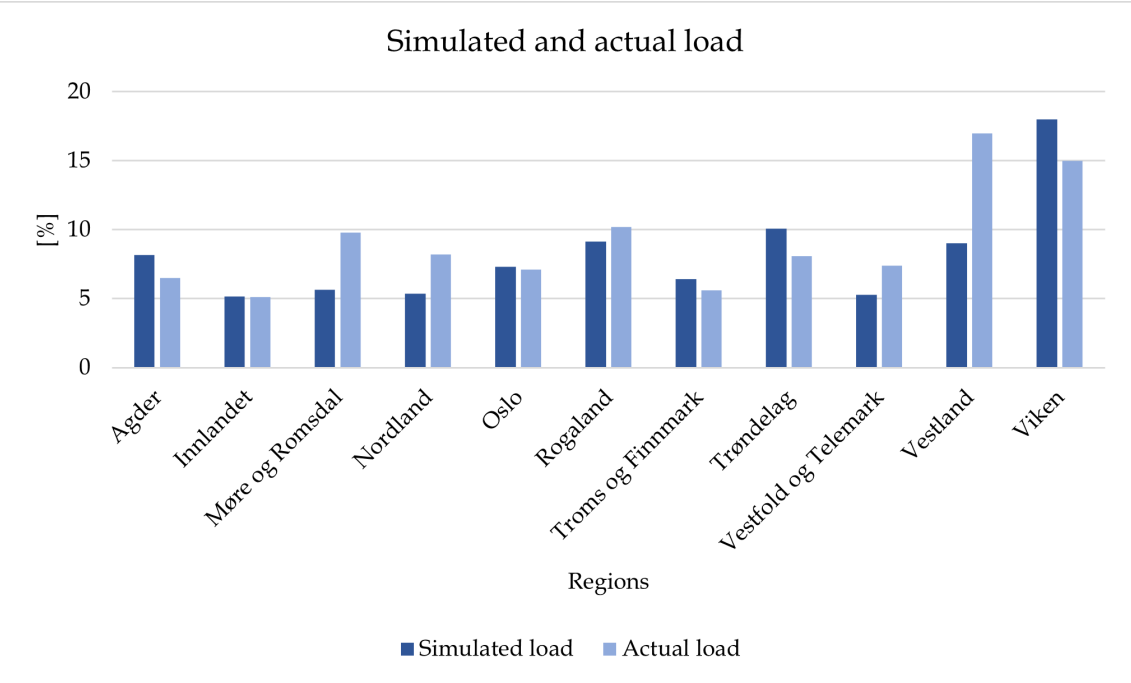

Figure 4.5: Simulated load along with actual load per region in Norway.

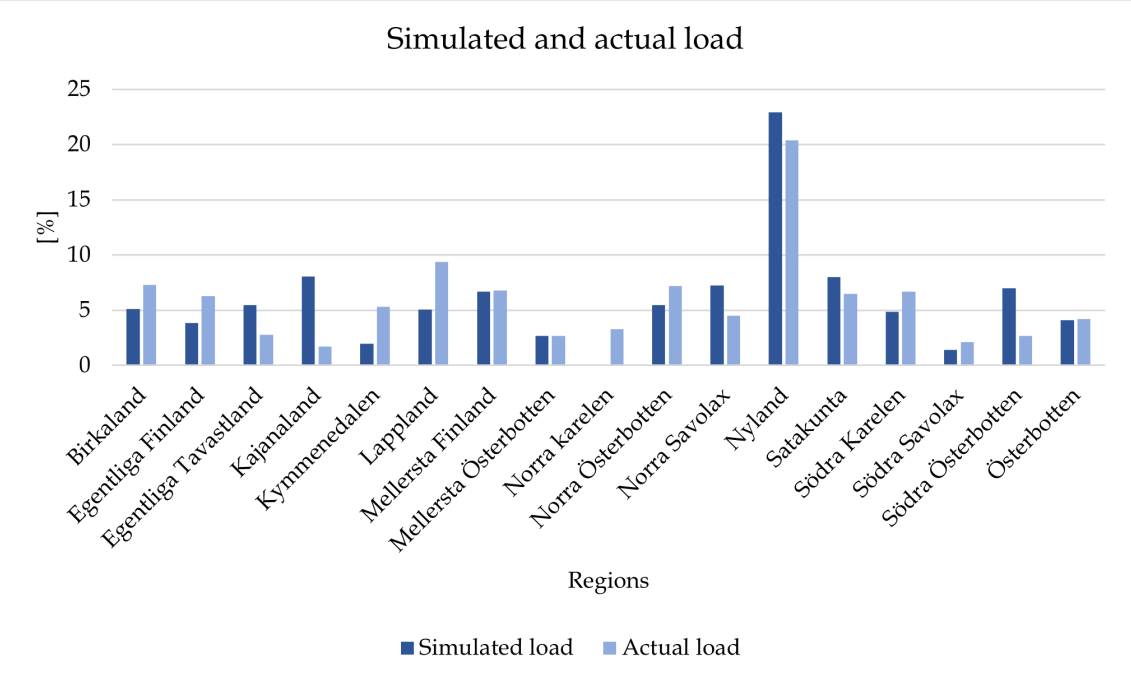

Figure 4.6: Simulated load along with actual load per region in Finland.

As seen in Figure 4.4, 4.5, and 4.6, Gotland in Sweden, and Norra Karelen in Finland, do not have any load assigned to them. This is explained by the fact that the loads are connected to a voltage level not included in the model, i.e., lower than 220 kV, no buses are located in Norra Karelen or Gotland. From the figures, it also becomes clear that load distribution in the model i similar to the yearly quotas but that there are some offsets. Sometimes some of the larger differences displayed in Figures 4.4-4.6 can be explained through adjacent regions having similar but opposite offsets from the yearly averages, Stockholm and Uppsala is one example of this, and Vestland and Viken is another. This indicates that there are errors in the load distribution, but on a regional level adjacent regions can make up for each other.

When assessing the regional accuracy of the model, it is important to note that comparing a load distribution on a yearly basis to the aggregated values for four different timestamps is not optimal. This is because the load distribution can differ over different seasons and times of day. Because of this, if the model is accurate, the aggregated values from the model should converge toward the yearly load distribution as more scenarios are run. However, with the data available now, some discrepancies on a regional level are apparent. These cancel each other when discussing the flow on a bidding zone level, since that is the resolution of the load data that is fed into the model. However, the discrepancies should be kept in mind when discussing local flows and how they impact, for example, the loading of lines.

4.4.3 Cross-border flows

In order to validate the model, the cross-border flows were examined and compared to the official ENTSO-E data. As explained in Section 4.3, the data on cross-border

flows were assumed to be accurate. Cross-border flows were chosen as the primary quantity to validate the model against, primarily because it provided comparable data that was not an input in the model, thus making it a good candidate for assessing the model's validity. It is also the only way to investigate the flows, hence, the accuracy of the cross-border flows should provide some insight into how well the model is performing.

To account for the imbalances found in the input data, each bidding zone is balanced using either a load or a generator. The method used was to run the simulation and sum the errors of the cross-border flows to see if more or less power than what was supposed to was being imported/exported. Then this sum was assigned to a load or generator, depending on polarity, placed in the middle of each bidding zone to account for this error. This was done in iterations until no balance error was larger than 5 MW in any bidding zone. This method removed errors related to inaccurate data but still allowed the flows to be evaluated. Important to realize, though, is that there is no way of knowing whether there were too much generation or too little load, or where this mismatch was located in each bidding zone.

To make sure the alterations done to the model were improving the model, the same simulations were run in the old model (Nordics model) and the new model (2020 model), as well as the new model before it was balanced. The unbalanced 2020 model was run two times, once with the slack bus being placed in SE3, as it were in the Nordics model [22], and once with the slack bus placed in SE1 as it were in the finalized 2020 model. The discrepancies between the ENTSO-E data on the cross-border flow and the flow between bidding zones in the different variations of the model for all scenarios are presented in Figures 4.7 - 4.10, and a comparison of the total improvement is presented in Table 4.13.

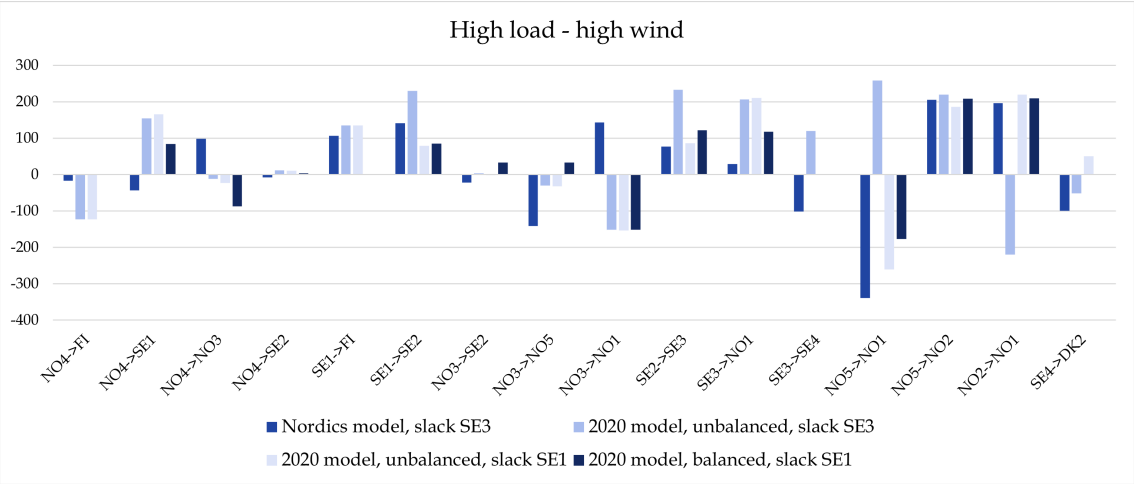

Figure 4.7: Offset between ENTSO-E data on cross-border flows and simulated values for the high load - high wind case for the different versions of the model.

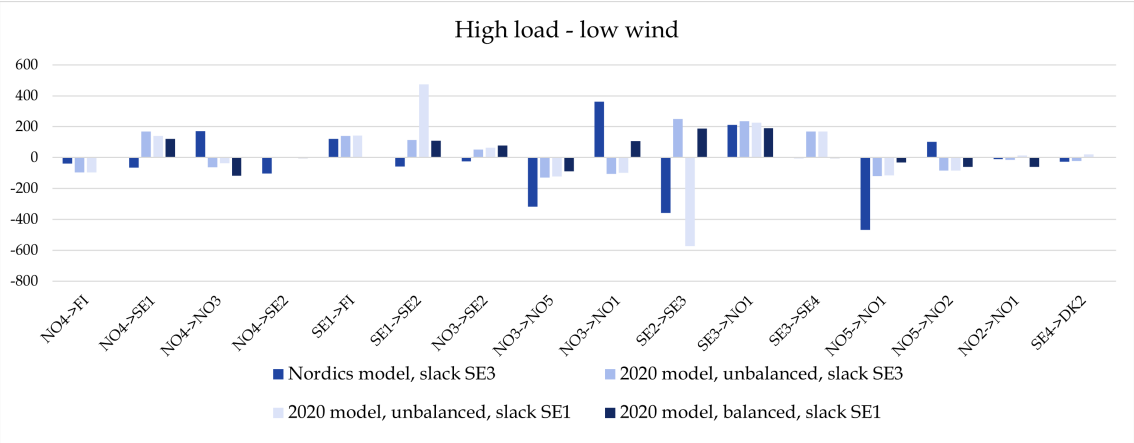

Figure 4.8: Offset between ENTSO-E data on cross-border flows and simulated values for the high load - low wind case for the different versions of the model.

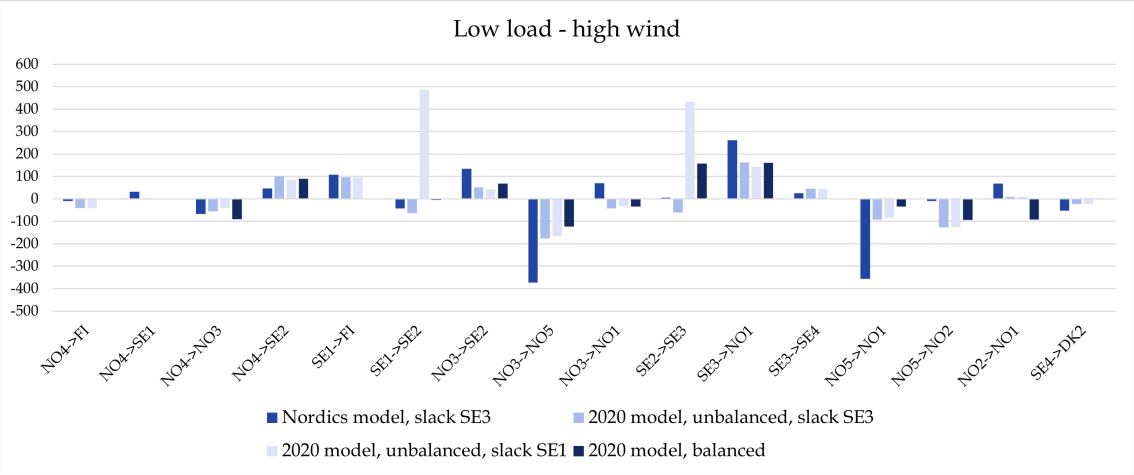

Figure 4.9: Offset between ENTSO-E data on cross-border flows and simulated values for the low load - high wind case for the different versions of the model.

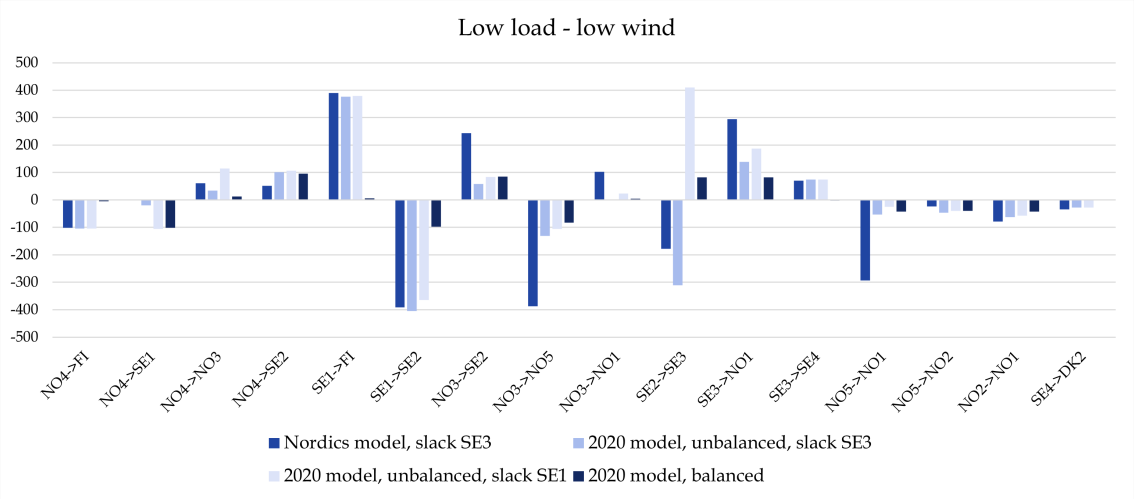

Figure 4.10: Offset between ENTSO-E data on cross-border flows and simulated values for the low load - low wind case for the different versions of the model.

From Figures 4.7 - 4.10, the importance of balancing becomes evident, as does the impact of the placement of the slack bus when the data is not balanced. The total error was improved in all cases after balancing the bidding zones, however some errors still remained. Moving the slack bus to SE1 worsened the cross-border flow in many instances, likely because SE3 is more central in the Nordic system, which means the error does not propagate over as many borders if the slack bus needs to compensate. However, the impact of the slack bus placement is negligible after balancing since no imbalances remain. The slack bus production in the different models and cases is presented in Table 4.12.

Table 4.12: The generated power by the slack bus in with the different slack bus placements, and after balancing [MW]

	High load - high wind	**High load - low wind**	**Low load - low wind**	**Low load - low wind**
2020 model slack in SE1	163.2	394.8	579.3	870.1
2020 model slack in SE3	146.3	320.8	503.4	738.4
2020 model balanced slack in SE1	1	1	1	1

Other patterns observed from Figures 4.7 - 4.10 include that before any changes were made to the model, there was always a "negative" flow between NO3-NO5 and NO5-NO1. These discrepancies were lessened in the 2020 models. What can be observed from Figures 4.7 - 4.10, and what is further confirmed in Table 4.13, is that with the implementation of all changes, the performance of the model was improved. The percentages in Table 4.13 are compared using (4.3). In Table 4.13,

the only included unbalanced 2020 case is the one with the slack in SE3 since it provided the best comparison to the Nordics model.

$$100 \cdot \frac{\sum_{Compared\_model} \|P^{Error}_{Cross-borderflow}\|}{\sum_{Nordics\_model} \|P^{Error}_{Cross-borderflow}\|} = \%_{\text{Error remaining}} \tag{4.3}$$

Table 4.13: The sum of the absolute values of all cross-border flow errors in the Nordics model, the unbalanced model with the slack bus in SE3, and the balanced model for all cases, as well as the remaining error compared to the Nordics model.

	High load - high wind	**High load - low wind**	**Low load - high wind**	**Low load - low wind**
Original Nordics model [MW]	1 766	2 438	1 661	2 698
2020 unbalanced, slack in SE3 [MW]	1 738	1 766	1 145	1 942
2020 unbalanced, slack in SE3 [%] of error remaining	122.3	72.4	68.9	72.0
2020 model balanced [MW]	1 316	1 159	949	782
2020 model, balanced [%] of error remaining	74.5	47.5	57.1	29.0

In one instance, the total error is larger than that in the Nordics model, it is the unbalanced high load - high wind case. However, the total error in the balanced model has been reduced for all cases, but some errors remain. These are compared in Figure 4.11. From this figure, it becomes clear that more power than what are supposed to flows through Sweden, and less flows through Norway. There is too much flow on the NO4-SE2, NO3-SE2, SE2-SE3, and SE3-NO1 connections which pushes power from the north of Norway through Sweden and then again into NO1. And then there is too little flow through on NO4-NO3, NO3-NO5, and NO5-NO1 connections which is where the power should have gone through. In the high load - low wind case, on the SE2-SE3 border, the power flow was exceeding the capacity limit to start with as stated in Section 4.1.2. This limit is even further exceeded in this model.

Another issue remaining in the balanced 2020 model is a loop error between NO1, NO2, and NO5, which remains in all cases, but is reversed in the high load - high wind case. In the balanced model, all errors in the flow to DK2, FI, and SE4 were eliminated. This is because these are positioned so that there are no alternative ways for the power to flow, hence if the generation and load are balanced compared to the cross-border flows, no errors will occur. Recognizing that this does not necessarily mean the exact amount of power flowing through the lines if multiple lines are crossing the bidding zone border.

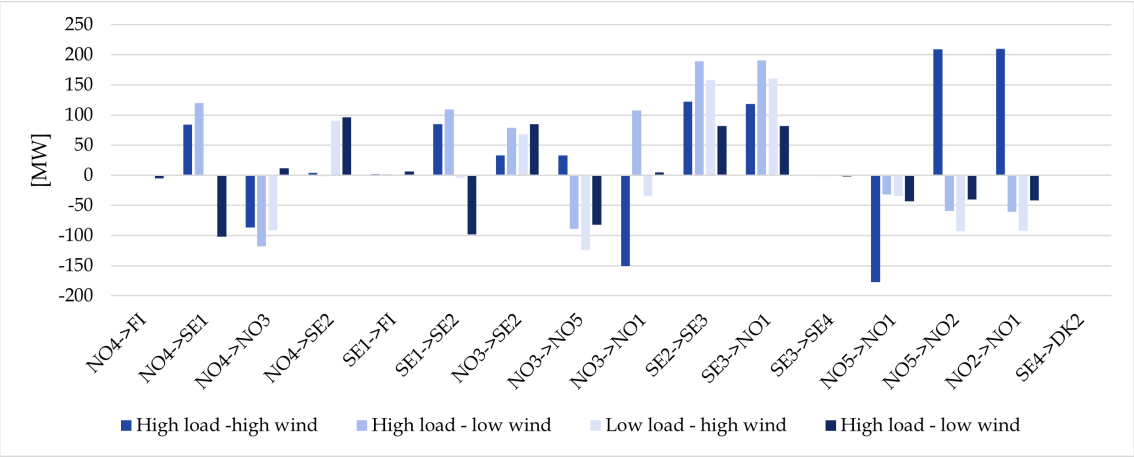

Figure 4.11: The discrepancies in the cross-border flows remaining in all four cases

The most significant error remaining in the balanced model was 210 MW from NO5 flowing through NO2 instead of directly to NO1 in the high load - high wind case. What the reason is behind this unclear, especially since in this instance the power flow offsets flow in a way that is not observed in any other case, which could indicate that there could be issues with the data, or possibly the load or generation distribution in this case. Where the same error is observed in all cases, errors in the impedance could be the explanation.

4.4.4 Limitations and reliability

There are several limitations of the model which should be considered when interpreting the results, and any conclusions should be made with caution considering these. Firstly, the model is only a model of the transmission grid which ignores all underlying network topology and the effect this has on the transmission grid. The underlying grid is modeled as fixed loads with a power factor of 1, and all generator units are connected to the closest bus. The method provides a good approximation but can lead to generators and loads being assigned to the wrong bus and, consequently, the wrong bidding zone/region. This impacts the regional resolution, further elaborated on in Section 4.4.2, but should not affect the model on a bidding zone level due to the re-scaling of the generation/load done per bidding zone, explained in Section 3.6.1. In addition to this, the load distribution is also an approximation, with the regional accuracy shown in 4.4.2, where it is clear that there are deviations. As mentioned in Section 3.5.1, there are also inaccuracies in the distributing of loads within the bidding zones, which impacts the accuracy on bus level negatively. The same issue can be found for the generators as well.

Secondly, impedances and ratings of lines and transformers are also approximations and assumed to be the same for all components of the same type, only distinguished by voltage level. As confirmed in Section 4.4.3, these changes are proving to improve the flow, however, the flows are still not entirely accurate. What could become problematic for, above all, the contingency analysis is that all lines on the same voltage level are assumed to have the same rating. This is not the case in reality, but due

to a lack of open data on, for instance, whether a line is simplex, duplex, or triplex, and the configuration of the model, this remains a limitation that is hard to mitigate.

Thirdly, the accuracy of the input data and the data validated against is not perfect, as further elaborated upon in Section 4.3, and the assumption that the cross-border flows are the more accurate could be wrong. This is a problem for the validation, however, in the future, there is no accurate data to input or compare against. For the purpose of comparing behavior between the 2020 grid and the 2045 grid, this should not be an issue, but it could impact the results from the ACCC and sensitivity analysis since they target specific branches and buses. The largest error in cross-border flow remaining was 210 MW, which should be considered when interpreting and discussing the results regarding specific branches. 210 MW is however a smaller error than the largest data imbalances, which indicates good performance given the circumstances.

Lastly, because the loads and generators are connected directly to 400 kV busses, line and transformer impedance that would typically affect the reactive power content of the grid, is ignored. This makes investigations of static voltage levels hard to perform. In addition, the issues of running the model with generators that had a power factor of 0.94 and shunts also complicated evaluating the static voltage performance. For this reason, the approach was changed to give the generators infinite reactive power limits and evaluate the difference in how much reactive power is injected in the different cases and scenarios to see how the need for reactive power could come to change. This approach eliminates the need to transfer more reactive power than what is consumed in the line, in any given line in the model. This makes lines seem less loaded than they would be, if there had not been a reactive power source on the other end.

Considering all limitations described above and the validation performed in Sections 4.4.1 - 4.4.3, the model's reliability could be interpreted. The model does lack in bus level accuracy, but the power flow between bidding zones is replicating what is expected at large. Consequently, the model provides a good starting point for the 2045 grid model and provides results that could be used to compare the needs and behaviors of the 2045 grid to the 2020 grid. The resolution when it comes to loading on specific lines should however be interpreted with care. Especially considering the largest error identified is 210 MW and the thermal rating on all lines is standardized.

4.4.5 Summary of adaptations made

A summary of the adaptations made to the model and the impact this had on the model is presented in this section. The main parameter used to evaluate the impact of the changes was cross-border flows. However, in some instances, changes were made that did not improve the cross-border flow accuracy. Instead they were implemented to replicate the power systems state, such as topological accuracy and the addition of series compensation.

Line features After reviewing the previously used line impedances and thermal ratings, it was concluded that they had to be altered to replicate the most commonly used line types in the Nordic grid. Four lines were chosen, and their length-dependent impedances were calculated and implemented. Furthermore, their thermal rating was calculated for two different ambient temperatures, one for the winter scenarios and one for the summer scenarios. Finally, the ratings were validated against values provided by a contact at Svk. Hence, the changes were deemed to improve the accuracy of the model.

Grid topology Enhancements were made by adding missing buses and lines from the PyPSA-eur and Nordics models. Moreover, faulty lines and buses were removed. Additionally, bus names were included in the model and each bus was also assigned a region. Although these modifications initially resulted in a decline in accuracy, they ultimately improved the overall correctness of the model.

Series compensation Series compensation was added, but it increased power flow through Sweden more than Norway, which was already an issue. Since series compensators are used in the grid, this was kept in the high-load cases. However, it was removed in the low-load cases because the need to series compensate is not as prominent when the lines are less loaded, and therefor it was assumed that no series comensation wa needed in the low load cases.

Assigning of loads to new buses When new buses were incorporated into the system, loads were shifted from nearby buses. This adjustment had minimal impact on the power flow, but it enhanced the accuracy of the model. The buses were added since they were missing in the Nordics model, when comparing it to the TSO's and the ENTSO-E grid maps.

Adding and removing generators The Nordics model initially had inaccuracies in the installed capacity, with some missing generators. To address this, additional generators were included and some were removed, resulting in improved overall model accuracy. However, these adjustments had minimal impact on the cross-border flows within the system.

Reactive compensation Initially, the reactive power output of the generators was reduced to comply with regulations, and shunts were introduced where necessary. However, a different approach was adopted to ensure consistency between the 2020 and 2045 grid models. In this new method, infinite reactive power capability was assigned to the generators. While this change allowed for compatibility between the two models, it decreased the accuracy of the overall system representation as it did not replicate actual power system operations. Additionally, this adjustment contributed to less loading on the lines since less reactive power needed to be transmitted between buses. If only the 2020 model is used, it is possible to revert to the previous approach.

Transformer impedance To achieve more realistic impedance values, the winding MVA of transformers was adjusted to 400 MVA. In addition, in this update, the reactance was set to 0.12 p.u using the winding MVA, as opposed to the previous approach of using the system MVA. This change aimed to improve the accuracy of the impedance values and ensure a more realistic representation in the model.

Balancing of generation and load in bidding zones To address inaccuracies in the net import/export of the bidding zones, manual adjustments were made by introducing additional loads or generators. This corrective measure aimed to improve the accuracy of the power flow. However, the exact cause of the error or its specific impact on regional accuracy within the bidding zones remains unknown. Nevertheless, including manually added loads or generators helped enhance the power flow accuracy of the model.

Deactivation of deactivated lines To replicate the system state at the different time stamps used, the lines that were out of order at the time according to the Nordic Unavailability Collection System (NUCS) [58] were deactivated for each case. This improved the accuracy.

Change of location of slack bus Adding the slack bus to a new bus with no generation except for the generation from the slack made it easier to see how much the slack was generating. At first, the model's power flow accuracy was negatively affected by relocating the slack bus from SE3 to SE1. This occurred because errors in the system balance had to be compensated for by the slack bus, and these errors propagated over longer distances affecting the inter-area flows. However, when the bidding zones were balanced, the placement of the slack bus had minimal impact on the overall accuracy.

Redistribution of loads After observing overloaded lines in the 220/300 kV grid, some of the load at the 220/300 kV side of transformers were relocated to the 400 kV side. A positive effect on both the overloading of the lines, and the cross-border flow was observed. However, this might be different from how the loads are typically distributed.

5

Future Power System Scenarios and Modelling

Building the future power grid and the future power system scenarios included three steps. The first was to model the future grid, the second was to combine scenarios over the installed capacity and yearly energy need, and the third was to determine the generated power and the load for each case. The TSO's own predictions for the grid and future generation and load scenarios were the sources used to produce all cases. A summary of the sources used is presented in Appendix C

5.1 Overview of Future Power System Scenarios

The goal is to compare three different scenarios for 2045, two with vastly increased generation and consumption, with a varied generation mix, and one with more distributed generation where the generation capacity and loads are not increased as much. This should provide insight to how well the grid expansion plans are adapted to different future scenarios.

There are significant uncertainties when predicting what energy production and consumption will look like in the future. For example, between Statnett's long term market analysis in 2020/2021 [7] and the one released in March 2023 [59], the base consumption scenario in the 2023 report is equal to the high scenario in the report from 2021. This uncertainty is also addressed in Svk's system development plan, where the electrification of large industries, the extent of increased energy efficiency, and how the electrification of the transport industry will look are rendered as insecurities [2].

Comparing different scenarios presented in different reports, the insecurities are further confirmed, often the scenarios for the same country varies between different reports. For the scenarios in this report, the most recent predictions made by the country's own TSO are primarily used, and similar scenarios for the different countries are matched. Where these scenarios lack information on a bidding zone level, predictions made for the countries are considered, along with information regarding specific projects. One general finding is that predictions made by the TSOs about the generation and load increase in their own country, are often larger than predicted increases made by other organisations or other TSOs. Fingrid and Svk have each presented four different scenarios for the generation and loads in the future. In

this report, similar cases are matched and used in full. Energinet has presented one scenario which is used in all cases. However, Statnett has not made similar scenarios for installed capacities.

When scenarios have been used for the future generation assumptions, they also include load scenarios where the yearly consumption is split into different categories. Section 5.3 presents all load and generation scenarios.

5.2 General Assumptions For All Cases

The hydropower capacity is almost built to maximum capacity, with the only exception being in Norway, where Statnett predicts that the capacity could be increased by 5 GW to 39.5 GW, primarily in the southwest parts of Norway, which is NO2 and NO5 [60], [59]. No scenarios in Sweden, Finland, or Denmark increase the hydro capacity further.

Statnett presents four different load scenarios in the 2022 long-term market analysis [59] but does not specify predictions about the installed capacity on bidding zone level. Instead, they specify that, in their base case, solar, hydro, and onshore wind will account for 32 TWh of increased yearly production in 2045, 7 TWh of which is onshore wind, 12 TWh of which is hydro and 12 TWh of which is solar. They further state that the insecurity in their scenarios mainly depends on the volume of offshore wind connected. For this reason, the base case assumptions about these generator categories (solar, hydro, and onshore wind) will remain the same in all cases, and only the offshore wind will differ in Norway between the different production scenarios. Thermal plants in Norway will be removed because of the goal of an emission-free power system, and the existing thermal plants in Norway today are powered by fossil gas.

In SE3, according to Svk's calculations in the 2020 long-term market analysis [14], 12.1 GW of installed solar will generate 11.5 TWh in a year. SE3 is located at roughly the same latitude as NO1, NO2, and NO5, and it is reasonable to believe that the same amount of installed capacity would generate as much energy. The predicted installed solar capacity will therefore be evenly spread out in the southern bidding zones in Norway, NO1, NO2, and NO5, and less in NO3 since it is located further north. Onshore wind in SE3 is expected to produce 3.48 TWh per installed GW in 2045. Assuming that the production per installed capacity is the same in Norway, and the increase in yearly energy production is the same, this would mean a total installation of 2 GW onshore wind. The largest volumes of wind power concessions requests are found in NO3 and NO4, hence 1 GW will be placed in each of these bidding zones.

The installed offshore wind was also only given in TWh. To convert this into installed capacity, information about a planned offshore wind farm in Norway was used. There, the estimated yearly generation from 1 GW of installed wind was 4.3 TWh [61]. This number was then reversed to find the needed installed capacity

for each scenario in Norway. The distribution is then decided by information on exciting plans to build offshore wind farms.

In DK2, the generation and load scenarios are the same for all cases. Energinet has not presented the same speculations using different scenarios as the other TSOs, but has one prediction for the time period 2022-2050 [62], therefore the same data will be used in all scenarios for DK2.

5.3 Selected Future Power System Scenarios

5.3.1 Scenario 1: Small scale production - low electrification

Scenario 1 is the most conservative scenario in terms of new installed capacity and increase in load. The installed capacity of each generation type in each bidding zone is presented in Table 5.1.

Table 5.1: Installed capacity in the small scale renewable scenario. 2020 values inside parenthesis. All values in [GW]

	Hydro	Nuclear	Wind onshore	Wind offshore	Solar	Other thermal	Total
DK2			1.2 (0.8)	6.5 (0.4)	9 (0.3)	1.4 (4.5)	19.7 (6.0)
FI	3 (3.1)	8 (2.8)	14 (2.1)	1 (0)	14 (0)	3 (9.2)	43 (17.3)
NO1	3.9 (3.9)		0.2 (0.2)		4 (0)		8.1 (4.1)
NO2	14.1 (11.6)		1.1 (1.1)	3.1 (0)	4 (0)		22.3 (12.7)
NO3	4.8 (4.8)		2.9 (1.9)	0 (0)	1 (0)		8.7 (6.7)
NO4	5.3 (5.3)		1.7 (0.7)	0 (0)		0 (0.3)	7 (6.3)
NO5	10.8 (8.3)			1.4 (0)	3 (0)	0	15.2 (8.6)
SE1	5.4 (5.4)		4.6 (1.3)	0 (0)	1.6 (0)	0.2 (0.3)	11.8 (6.9)
SE2	7.6 (8.1)		7.8 (3.4)	0.3 (0)	3.0 (0)	0.8 (0.6)	19.5 (12.2)
SE3	2.3 (2.6)	0 (7.7)	6.8 (2.6)	0.3 (0)	17.3 (0.4)	2.7 (2.6)	29.4 (17.5)
SE4	0.2 (0.3)		2.0 (2.6)	0.8 (0)	7.2 (0.2)	0.8 (2.1)	11.0 (5.3)
Total	57.4 (53.3)	8.0 (10.5)	42.3 (16.7)	13.4 (0.4)	64.1 (1.0)	8.9 (10.4)	199.9 (103.4)
% of total	28.7 (51.5)	4 (10.2)	21.2 (16.2)	6.7 (0.39)	32 (0.97)	4.5 (10.1)	100

The common denominator between Svk's and Fingrids scenarios *small scale renewable* respectively *local power* is that the load increase is not as large as in the other cases, but it is still increasing due to the electrification of industries and transportation. However, new heavy electricity-demanding industries are not built, nor is the infrastructure around hydrogen, which the other scenarios assume [4]. In Fingrid's scenario, small-scale nuclear reactors have been introduced. Common for both cases is the increase in solar power and the limited increase in offshore wind capacity [4], [14].

In Norway, the *low* consumption scenario is assumed, with a limited increase in offshore wind production. In the lowest scenario, the increase in installed offshore wind capacity is limited to 4.5 GW. In 2023, a total of 4.2 GW is planned in Norway, 2.8 GW in NO2, and 1.4 GW in NO5. In this case, another 0.3 GW is added to

NO2 in order to increase the total to 4.5 GW.

Table 5.2 presents the yearly energy demand for different consumption categories. Because the data comes from different sources, the consumption categories do not match completely, and the reference values are from different years.

Table 5.2: Yearly electrical energy demand per consumption category for the small scale scenario. All values in [TWh], reference values in Finland from 2019 [4], in Norway from 2022 [59], and in Sweden from 2020 [14]

	Denmark	**Finland**	**Norway** [1]	**Sweden**	**Total**
Household	3 (4)	46 (45)	65 (80)	72 (79)	186 (208)
Losses	Inc. in household	Inc. in household	Inc. in household	14 (11)	14 (11)
Transport	6 (0)	8 (1)	24 (3)	13 (0)	51 (4)
Industry	7 (6.0)	59 (41)	72 (56)	68 (50)	206 (153)
Electrolysis	11 (0)	16 (0)	17 (0)	Inc. in industry	44 (0)
Server halls	3 (0)	Inc. in industries	10 (1)	6 (1)	19 (2)
Total	30 (10)	129 (86)	188 (140)	173 (141)	520 (377)

From Table 5.2, it is clear that no load category is expected to become very large, and household loads are decreasing or remaining roughly the same. Transport, Industry, Electrolysis, and server halls are increasing in all countries, but none with more than 20 TWh/year.

5.3.2 Scenario 2: Fossil free scenario

In the fossil free production case, for Sweden, it is the *electrification plannable* in Svk's long-term market analysis that is used [14], and for Finland, the *power to product* scenario presented by Fingrid in their electricity system draft scenarios [4]. These are both scenarios that predict a significant increase in, above all, industrial loads, where electricity is the primary energy carrier. Hydrogen production will be important in both cases, and both cases include continued nuclear production. The equivalent load scenario for Norway is the *high* scenario [59]. The installed generation capacity per type and per bidding zone is presented in Table 5.3.

[1] Mean value of 2040 and 2050 scenarios.

Table 5.3: Installed capacity in the fossil free scenario. 2020 values inside parenthesis. All values in [GW]

	Hydro	Nuclear	Wind onshore	Wind offshore	Solar	Other thermal	Total
DK2			1.2 (0.8)	6.5 (0.4)	9 (0.3)	1.4 (4.5)	19.7 (6.0)
FI	3 (3.1)	4 (2.8)	53 (2.1)	10 (0)	25 (0)	4 (9.2)	99 (17.3)
NO1	3.9 (3.9)		0.2 (0.2)		3 (0)		7.1 (4.1)
NO2	14.1 (11.6)		1.1 (1.1)	14.0 (0)	3 (0)		32.2 (12.7)
NO3	4.8 (4.8)		2.9 (1.9)	4.0 (0)	1 (0)		12.7 (6.7)
NO4	5.3 (5.3)		1.7 (0.7)	4.0 (0)		0 (0.3)	11.0 (6.3)
NO5	10.8 (8.3)		0 (0)	1.2 (0)	3 (0)	0 (0.4)	14.0 (8.6)
SE1	5.4 (5.4)		7.4 (1.3)	1.5 (0)	0.1 (0)	0.2 (0.3)	14.6 (6.9)
SE2	7.6 (8.1)		8.8 (3.4)	1.5 (0)	0.5 (0)	0.8 (0.6)	19.2 (12.2)
SE3	2.3 (2.6)	8.4 (7.7)	6.4 (2.6)	4.8 (0)	7.3 (0.4)	3.3 (2.6)	32.1 (17.5)
SE4	0.2 (0.3)		2.8 (2.6)	2.3 (0)	3.2 (0.2)	0.9 (2.1)	9.4 (5.3)
Total	57.4 (53.3)	12.4 (10.5)	85.5 (16.7)	49.8 (0.4)	55.1 (0.9)	10.6 (21.4)	270.8 (103.3)
% of total	21.2 (51.5)	4.6 (10.2)	31.6 (16.2)	18.4 (0.39)	20.3 (0.97)	3.9 (10.1)	100

This scenario predicts a large increase in installed wind capacity, both on- and offshore, and solar. The increase is expected in all countries, but what stands out is the increase in installed onshore wind in Finland. In this scenario, Finland expects to install 51 GW of new onshore wind. The increase in offshore wind in NO2 is also comparatively large. Nuclear power is expected to be part of the generation mix, but not in any new bidding zones compared to today. In total, the installed capacity is expected to be more than double what was installed in 2020.

The predicted yearly loads for this generation scenario are presented in Table 5.4. Most significant is the electrolysis production in Finland, which is estimated to use 126 TWh of energy yearly. In addition, the energy consumption of transport, industries, and server halls is estimated to increase in all countries. The household loads are increasing in Finland and decreasing in Norway and Sweden. Loads are increasing in all countries, but the most significant is the increase in load in Finland, mainly due to hydrogen production.

Table 5.4: Yearly electrical energy demand per consumption category for the fossil free scenario. All values in [TWh], reference values in Finland from 2019 [4], in Norway from 2022 [59], and in Sweden from 2020 [14]

	Denmark	Finland	Norway [2]	Sweden	Total
Household	3 (4)	59 (45)	74 (80)	73 (79)	209 (208)
Losses		Inc. in household	Inc. in household	20 (11)	20 (11)
Transport	6 (0)	10 (1)	24 (3)	21 (0)	61 (4)
Industry	7 (6)	79 (41)	87 (56)	135 (50)	308 (153)
Electrolysis	11 (0)	126 (0)	38 (0)	Inc. in industry	175 (0)
Server halls	3 (0)	Inc. in industry	29 (1)	11 (1)	43 (2)
Total	30 (10)	274 (86)	252 (140)	260 (141)	816 (377)

5.3.3 Scenario 3: Renewable production

In this scenario, presented in Table 5.5, the production and consumption increase even more than in the previous case, mainly due to large offshore wind farms. In Svk's 2020 LMA, this corresponds to the *electrification renewable* scenario, and in Fingrid's prognosis, the *hydrogen from wind* scenario. Both scenarios share a common prediction that hydrogen will emerge as a crucial energy carrier, accompanied by a highly developed infrastructure to support its utilization. The *extra high* scenario will be used in Norway.

Table 5.5: Installed capacity in the renewable production scenario. 2020 values inside parenthesis. All values in [GW]

	Hydro	Nuclear	Wind onshore	Wind offshore	Solar	Other thermal	Total
DK2			1.2 (0.8)	6.5 (0.4)	9 (0.3)	1.4 (4.5)	19.7 (6.0)
FI	3 (3.1)	2 (2.8)	76 (2.1)	9 (0)	19 (0)	4 (9.2)	113 (17.3)
NO1	3.9 (3.9)		0.2 (0.2)		4 (0)		8.1 (4.1)
NO2	14.1 (11.6)		1.1 (1.1)	15 (0)	4 (0)		34.2 (12.7)
NO3	4.8 (4.8)		2.9 (1.9)	5 (0)	1 (0)		13.7 (6.7)
NO4	5.3 (5.3)		1.7 (0.7)	5 (0)		0 (0.3)	12.0 (6.3)
NO5	10.8 (8.3)			5 (0)	3 (0)		18.8 (8.6)
SE1	5.4 (5.4)		8.7 (1.3)	4.5 (0)	0.9 (0)	0.2 (0.3)	19.7 (6.9)
SE2	7.6 (8.1)		10.4 (3.4)	4.5 (0)	0.9 (0)	0.8 (0.6)	24.2 (12.2)
SE3	2.3 (2.6)	0 (7.7)	5.4 (2.6)	9.5 (0)	12.1 (0.4)	2.5 (2.6)	31.8 (17.5)
SE4	0.2 (0.3)		2.2 (2.6)	10 (0)	5.3 (0.2)	0.8 (2.1)	18.5 (5.3)
Total	57.4 (53.3)	2 (10.5)	109.8 (16.7)	74.0 (0.4)	59.2 (1.0)	9.7 (10.4)	312.1 (103.4)
% of total	18.4 (51.5)	0.64 (10.2)	35.2 (16.2)	34.7 (0.39)	19 (0.97)	3.1 (10.1)	100

[2] Linear interpolation between 2040 and 2050 scenarios.

The renewable production scenario predicts no new nuclear power plants to be built in Sweden. All currently existing nuclear power plants will be decommissioned by 2045, and the nuclear power in Finland will be limited. Sweden and Norway will build about 30 GW of offshore wind each, and there will also be a lot of new onshore wind and solar installed. Notably, Finland's onshore wind capacity increases even further compared to Scenario 2, to 76 GW of installed capacity. In total, the installed generation capacity is almost three times that of 2020.

The load scenario for this case, presented in Table 5.6, is characterized by increased industrial loads, including more electrolysis and server halls. Fingrid's scenario is based on the assumption that the hydrogen industry will be very big in Finland, and an extensive infrastructure will exist around this [4].

Table 5.6: Yearly electrical energy demand per consumption category for the renewable scenario. All values in [TWh], reference values in DK2 from 2022 [62] Finland from 2019 [4], in Norway from 2022 [59], and in Sweden from 2020 [14]

	DK2	**Finland**	**Norway** [3]	**Sweden**	**Total**
Household	3 (4)	56 (45)	84 (80)	73 (79)	216 (208)
Losses		Inc. in household	Inc. in household	22 (11)	22 (11)
Transport	6 (0)	10 (1)	24 (3)	21 (0)	61 (4)
Industry	7 (6)	71 (41)	100 (56)	159 (50)	337 (153)
Electrolysis	11 (0)	202 (0)	40 (0)	Inc. in industry	253 (0)
Server halls	3 (0)	Inc. in industry	35 (1)	11 (1)	49 (0)
Total	30 (10)	339 (86)	283 (140)	286 (141)	938 (377)

The yearly energy consumption is predicted to increase by 561 TWh to a total of 938 TWh. Compared to the fossil free case, the industrial loads and electrolysis will increase the most. Together, those categories make up 63 % of the estimated energy need. The increase in household loads in Norway is because they assume the maximum population growth scenario in their *extra high* load scenario. In the two other scenarios, this category has decreased [59].

5.4 Modeling of the 2045 Grid

The 2045 model used the 2020 model as a starting point but was developed and adapted to the conditions of the 2045 scenarios. This involved three different aspects; grid topology, generation, and loads. Adding and removing buses, lines and transformer was done, as well as changing voltage levels in Norway, to adapt the grid topology. As for the generation, generators were added and removed to fit the

[3] Mean value of 2040 and 2050 scenarios.

different scenarios, and a method to determine the power output of each generator was developed. A similar approach was used for the loads.

When deriving the thermal rating of the different lines used in the model, one input factor, as mentioned in Section 3.3.1 is ambient temperature. Since no specific dates are used in the future cases, this ambient temperature has been set to 20°C. This was done based on the assumption that high load scenarios are more likely to occur during high wind scenarios rather than during winter, and this means that this line rating could be limiting in high load scenarios.

5.4.1 Modeling of the grid topology

As a starting point for the 2045 model, the finalized 2020 model was used. Then the Nordic TSOs 10-year development plans were used to find out the grid reinforcements that were planned that would change the grid topology. For instance, an update of a substation would not be considered if the voltage level of the substation is not supposed to change. Likewise, with the lines, reinforcements of old lines where the new one went between the same substations were left the same as before. What was considered were all instances where new lines are planned. The removal of old ones was only considered if new ones of the same were not planned in the same places. Grid changes labeled "under consideration" have all been included in the model.

To begin with, in DK2, Energinets long-term analysis [12] for the grid in DK2 includes changes to the grid topology in up until 2040. In combination with this, a map over the possible 2040 grid was used [63]. One reinforcing line was added, and one new bus at Ejbygård, with two branches connecting it to Hovegård and Avedøreverket.

In Finland, Fingrids Main grid development plan 2022-2031 [64] was used. No further grid development plans were taken into consideration when developing the grid in Finland. The report "Electricity system vision" by Fingrid [65] includes sketches of the grid reinforcements needed for the different scenarios in Finland. However, these were very undefined and different for each scenario. Because of this, they have not been implemented.

Statnetts predictions for Norway, presented in their System development plan 2021 [13], included two different grid models for the Norwegian grid; one over the planned transmission grid in 2030 and one over the future target grid. The model that was used in this report was the target grid. This model predicts almost all 300 kV lines to be upgraded to 400 kV lines and adds some new lines and some parallel lines as well. For instance, the 400 kV line going through NO4 is a double 400 kV line all the way to Skaidi in this scenario.

To implement this upgrade, the 300 kV grid was initially upgraded to a 400 kV grid in the 2045 model. This was done in the code for the whole 300 kV grid at once.

Where the 300 kV grid remained, the now 400 kV grid was removed and the 300 kV grid was added back with the voltage level set to 301 kV, to prevent the code to change it to 400 kV. A consequence of this method was that the old transformer buses were still connected through a transformer, despite the fact that they were both 400 kV buses now. This was solved by removing the transformer in question and adding two lines with zero impedance between the two buses to enable the power to flow between the connected lines as if it were one bus. In addition, the NO2-GB interconnection was added as a load at the bus Kvilldal.

In Sweden, Svk's system development report 2022-2031 [2] was used. This report included possible development projects until 2040, which were all included in the 2045 model. Furthermore, information was also gathered from the information document about the NordSyd [66] project in Sweden, which is an investment package that aims to renew and increase the transmission capacity between SE2-SE3. After the project is finished, the plan is that the current eight 400 kV lines and three 220 kV lines should be twelve 400 kV lines instead. The approximate stretches and some new buses are planned, but how the existing 220 kV grid should be redrawn is not as defined. Therefore, to include these plans, the 400 kV lines and buses are implemented, and the 220 kV grid changes are implemented to the best possible extent. However, the 220 kV lines and buses are not removed completely. Instead, one line connecting SE2 and SE3 on each 220 kV "leg" is removed to force all transmission between SE2 and SE3 to go through the 400 kV lines. This eliminated the need to reassign generators and loads.

5.4.2 Modeling of the generators

The scenarios were modeled as either a high or low wind scenario, where initial assumptions were made about how much each generator type would generate in such conditions. This value is a factor of the installed capacity of a generation type and is called availability factor in this report. In the following sections, the assumptions made for each generation type in the high and low cases are described. Generally, all generator types were handled in the same way in all bidding zones. The power output from each generator in one bidding zone is determined in the same way as in the 2020 cases. The total generated capacity was divided by the installed capacity for each type in each bidding zones.

5.4.2.1 Hydro

Hydropower largely remains the same in the 2045 cases, with some extra generation added in NO2 and NO5, no changes were made to the other bidding zones.

5.4.2.2 Nuclear

The installed nuclear power is very different in the different scenarios. In Sweden, nuclear is not added in any new places in either of the cases. However, it is assumed that the nuclear generation will be in the already existing places in Scenario 2, which is the only case with nuclear power in Sweden [14]. In Finland, Scenario 1 assumes

a lot of new small modular reactors, but there are no available plans on where these plants would be located. Therefore, smaller nuclear reactors were distributed over some buses in Finland in this scenario.

5.4.2.3 Other thermal

No expansion of this type of generation is planned in any of the Nordic bidding zones except for SE3 in the fossil-free and small-scale renewable case. This is due to its environmental impact and operational cost. In the 2045 model, it is removed altogether in some bidding zones and is scaled down in others to reduce the capacity in order to align with future scenarios. No new plants have been added to the model in this generation category.

5.4.2.4 Solar

Solar installation is evenly distributed over the southern bidding zones, which are projected to have high level of solar installed. These are DK2, NO1, NO2, NO3, NO5, SE4 and SE3. In Finland, the installed solar was distributed over all buses in the southern part, and in SE1 and SE2 some 400 kV buses were chosen. The installed capacity at each bus was the total installed capacity in that bidding zone divided by the number of buses.

Solar is an intermittent source of power, which has a seasonal and daily production pattern. According to [14] the average power output from solar is about 10 % of the installed capacity. Because the power output is varying and not controllable, one set fraction was used for all cases. The assumption was that the solar would generate at 20 % of its capacity in all cases.

5.4.2.5 Offshore wind

The offshore wind generation units in the model have all been added manually. This was done by matching the future capacity of offshore wind per bidding zone for each scenario with the capacity and location of planned offshore wind projects. The resources used to find the locations and capacities of planned offshore wind projects were Vindbrukskollen [41], the Norwegian Water Resources and Energy Directorate (NVE) map of wind farms in Norway [42], and the Finnish Wind Power Associations map of wind farms in Finland [67].

The locations of the implemented offshore wind farms are pointed out in Figure 5.1, a list of the wind farms can be found in Table E.1 in the appendix.

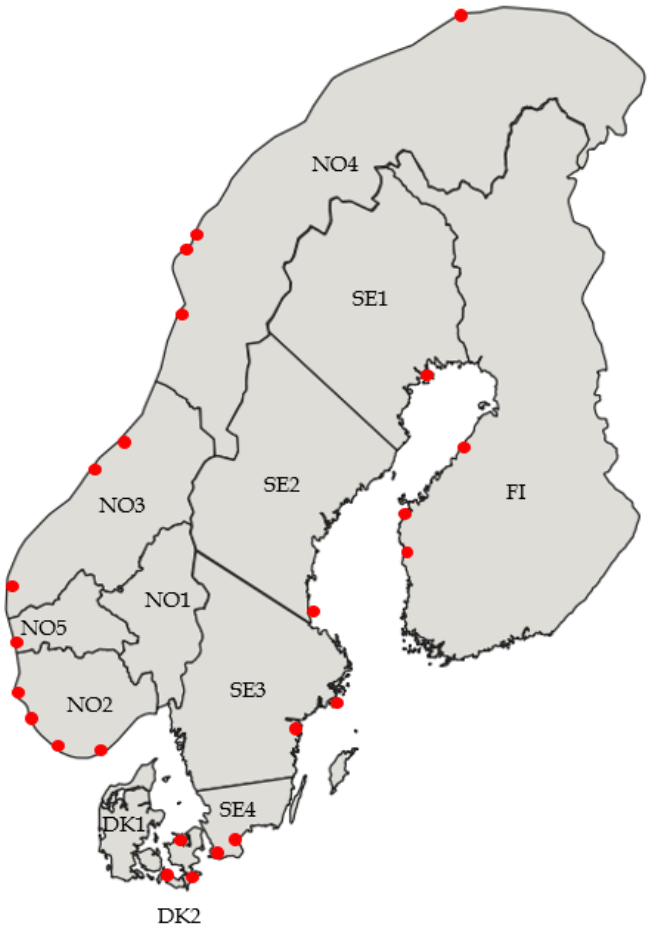

Figure 5.1: Locations of implemented offshore wind farms.

The scenarios are based on the availability of wind power. The assumption is that the availability factor of offshore wind is equal in all bidding zones in each case. When comparing the 2020 high wind cases, the wind power was generating between 50-90 % of the capacity in the different bidding zones. In the future high wind scenarios, offshore wind was set to generate at 80 % of the installed capacity, or have an availability factor of 0.8. Svk assumes the availability of wind power during the top load hour to be at least 9 % in 90 % of the cases [6]. This is the guideline for the low wind scenarios when the power estimations for the wind power have been made. The availability factor used for offshore wind in this report is 10 %, or 0.1.

5.4.2.6 Onshore wind

In order to align generational capacities with the anticipated future cases, onshore wind has been added to the bidding zones that are expected to have increased onshore wind penetration by 2045. The onshore wind plants have been added systematically and are of uniform size across bidding zones where large amounts of onshore wind are estimated to be installed, these bidding zones are FI, SE1, SE2, and SE3. Here the difference in installed capacity between 2020 and 2045 was divided by the

number of buses in that bidding zone and then added as separate generators to these buses. In DK2, NO3, and NO4, some buses were selected to which the onshore wind was added.

As for the generation from the onshore wind, in the low wind cases, the generators were set to generate at 5 % of the installed capacity. The availability was chosen below the 9 % availability which Svk uses because that only covers 90 % of the cases, and the aim was to see how the grid would behave in very low wind scenarios. In the high wind cases, the onshore wind was set to generate at 70 % of the installed capacity or have an availability factor of 0.7.

5.4.3 Losses

In the 2020 model, the losses were removed from the loads in each bidding zone. This was to provide a more accurate way of validating the model. When simulating the 2045 scenarios, the presented losses are the losses obtained from the load flow in PSS/E. These are shown in Table 5.9-5.18. No losses were subtracted from the loads in the 2045 scenarios, which means the load is marginally higher than it should be.

5.4.4 Modeling of the loads

In the different cases, further described in Sections 5.5.1-5.5.5, the load will be modeled as high load in the high wind scenarios and low load in the low wind scenarios. The decision to do it like this is based on the belief that more loads will be adapted with regard to how much power is available rather than the other way around. By doing it this way, the worst-case scenarios are likely not modeled, which should be considered when interpreting the results.

When looking at the different consumption categories for the Nordic countries, the most dramatic increases are in industry and electrolysis. These are interconnected since industries will rely on electrolysis to supply power when generation is low due to the intermittency of the future power mix. This allows for flexibility when modeling the different scenarios. For example, if generation is low due to low wind speeds across the Nordic countries, the electrolysis loads can be reduced to balance generation and consumption. The planned future industrial loads are displayed in Table 5.7 along with their average consumption and respective bidding zone and county.

Table 5.7: Planned industrial loads in the Nordics.

Industry	Average consumption [MW]	Bidding zone	County
H2 Green Steel [68]	1 369	SE1	Norrbotten
Northvolt 1 [69]	360	SE1	Västerbotten
Hybrit 1 Oxelösund [70]	1 000	SE3	Södermanland
Hybrit 2 Kiruna [70]	1 000	SE1	Norrbotten
Hybrit 3 Kiruna [70]	1 000	SE1	Norrbotten
Hybrit 4 Gällivare [70]	1 278.5	SE1	Norrbotten
Hybrit 5 Luleå [70]	1 000	SE1	Norrbotten
Hybrit 6 Skellefteå [70]	1 000	SE2	Västerbotten
Northvolt 2 [71]	200	SE3	Västra Götaland
Melkoya landanlegg [72]	262.50	NO4	Troms og Finnmark
Haltenområdet [72]	57.10	NO3	Trondelag
Tjeldbergodden metanolfabrikk [72]	171.20	NO3	More og Romsdal
Troll B og C [72]	91.3242	NO5	Vestland
Oseberg feltsenter og Oseberg Sor [72]	45.66	NO5	Vestland
Kollsnes gasprosseseringsanlegg [72]	45.66	NO5	Vestland
Kårsto delelektrifisering [72]	159.82	NO2	Rogaland
Kårsto fullelektrifisering [72]	296.80	NO2	Rogaland
Yara Heroya [72]	570.78	NO2	Vestfold og Telemark
INEOS Rafsnes [72]	79.90	NO2	Vestfold og Telemark
Borregaard [72]	34.25	NO1	Viken

The loads displayed in Table 5.7 are the manual additions of load in future cases. The remaining load is dealt with in a more general manner. First, the average load for each country and case is calculated by dividing the yearly load in TWh of each country by 8 760, the number of hours in a year. Then this value is multiplied with a case factor of 0.8 or 1.2 for the low and high load cases, respectively. These factors were obtained by checking the total load in the 2020 high load and low load scenarios, respectively, and dividing it by that year's average load. The values were then made to be less extreme since this report will not look into the more extreme cases, but rather adapt the loads with regards to the generated power.

The future load cases for Norway, as published by Statnett, are not published on a bidding zone basis but on a country-wide basis. To distribute load between bidding zones, load distribution factors were applied to all non-manually added loads, this was done in both Norway and Sweden, in order to stay consistent. This method has been verified by comparing Sweden's distribution to the published predictions. It was concluded that by applying the load distribution factors, a good approximation was achieved. One reason to why this method works is that the manually added loads are factored into the distribution. This causes the load distribution to shift between bidding zones in the way it is expected to. For example, in Case 3:a, Electrification renewable - low wind, SE3 represents 33 % of the national load compared to the 41 % that SE3 represents in the corresponding 2020 scenario.

Another assumption made concerns the flexibility of the future electrolysis and industrial loads. In order to deal with issues concerning under and over production in the different cases, the electrolysis and industrial loads have been tailored to balance the cases. The range assigned to electrolysis and industrial loads are 0 % - 200 % and 80 % - 120 %, respectively. The uncertainties connected to this assumption

concern whether this range is feasible, on the other hand, it can be established that without this allowed range of flexibility, some scenarios will not be able to converge.

The household loads, along with the losses, transport and server halls, are all included in the total load and were distributed in the same way as in the 2020 cases, and scaled to be either 80 % of the yearly average in low load cases, and 120 % in high load cases.

The methodology used for balancing load and generation together with import and export in all future cases and scenarios is described in Figure 5.2.

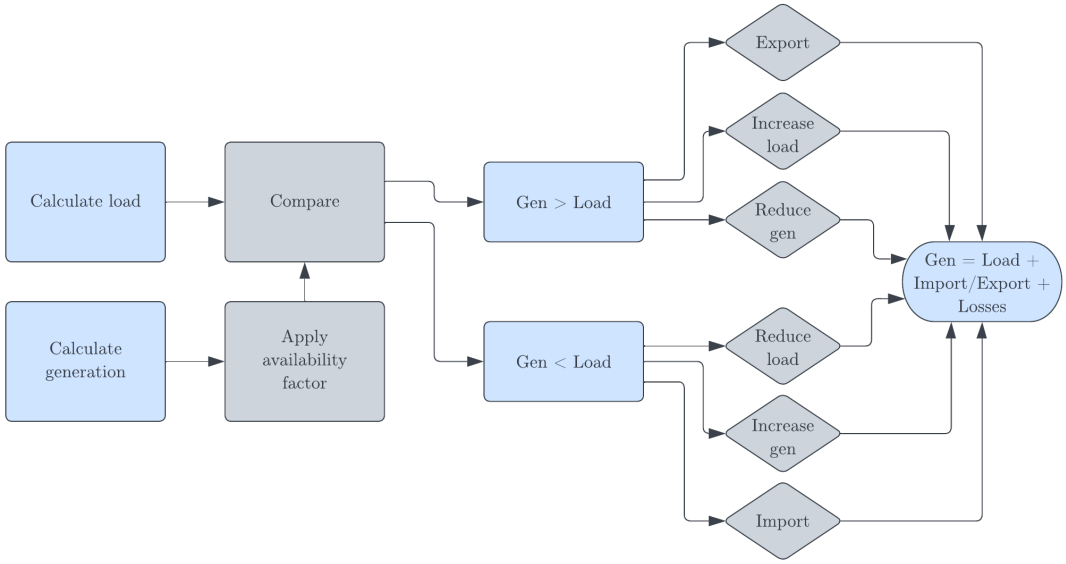

Figure 5.2: General methodology for balancing load and generation in future cases and scenarios.

5.5 Findings Regarding the Sufficiency of the Grid Planning and the Matching of Generation and Load

In this section, the findings from running the scenarios in PSS/E will be presented. Scenarios 2 and 3 were divided into two cases, one low wind, and one high wind. Scenario 1 was only tried as a high wind case due to lack of time to simulate the low wind case. Using the method described in Sections 5.4.2 and 5.4.4, the generation per type and per bidding zone, the load per bidding zone, and the manual loads were used as input in PSS/E. When the load and generation scenarios matched, this configuration's impact on the grid was evaluated and adjusted accordingly to avoid large overloads in the grid. Adaptations made to mitigate these overload issues and necessary grid reinforcements are presented in order for branches not to overload.

This section only considers the overloads in N-0 conditions, however, the rating in N-0 conditions is 70 % of the rated capacity, just like in the 2020 model.

5.5.1 Case 1: Small scale renewable - high wind

In the small-scale renewable case, the expected total energy demand of the synchronized Nordic region in 2045 is 520 TWh. This means the average load is 59 GW. Some assumptions have been made when constructing this case, these are listed below. The first assumption when estimating the production and consumption was that the non-hydrogen-related loads would be 120 % of their yearly average as explained in Section 5.4.4. The second assumption was regarding the hydrogen-related loads, which means the loads in the electrolysis row of Table 5.2. Since the electrolysis load is included in the industry row for Sweden, this value has been approximated as 20% of Sweden's industrial load. The third assumption is regarding the flexibility of the hydrogen loads. Since this is a high wind scenario and the power availability is high, the hydrogen loads have been set to 150 % of their original value to account for the excess generation in this case. The fourth assumption concerns the availability factors for the different generation categories. Onshore and offshore wind have been assigned availability factors of 0.7 and 0.8, respectively, as described in Sections 5.4.2.5 and 5.4.2.6. The availability factor for solar has been set to 0.2, and the remaining generation categories, hydro, nuclear, and other, have been assigned their availability factors from the 2020 high wind scenario.

Finland is expected to increase its nuclear capacity from 2.8 GW to 8 GW in this case. This capacity is added through many small modular reactors. Table 5.9 presents a summary of the scenario's load and generation. As can be seen in the difference column of Table 5.9, the Nordics are a net exporter in this scenario. This power is exported to Estonia through Finland and to Lithuania through Sweden. In Table 5.8, the export and import through the interconnectors to other countries is presented.

Table 5.8: Interconnectors to other countries and the active power flow through them in Case 1. Positive indicates export, and negative indicates import. All values are in MW.

	DE	DK1	EE	LT	NL	PL	UK
DK2	585	-590				0	
FI			984				
NO2		432			0		0
SE3		-696					
SE4	0			100		0	

Table 5.9: Generated and consumed active power in each bidding zone in Case 1. Loads are excluding losses. Difference = Total - Load - Losses, indicates import/-export of the bidding zones. Losses are gathered from PSS/E load flow simulations. All values are in MW.

	Hydro	Nuclear	Other thermal	Solar	Wind-offshore	Wind-onshore	Total	Load	Losses	Difference
DK2	0	0	0	480	2 400	2100	4 980	4 582	118	279
FI	2 057	8 011	0	2 800	800	9 800	23 469	18 078	555	4 835
NO1	1 969	0	0	800	0	140	2 909	5 323	64	-2 479
NO2	8 130	0	0	800	2 480	770	12 180	9 052	77	3 050
NO3	2 023	0	0	0	0	2 030	4 253	5 811	57	-1 615
NO4	1 962	0	0	0	0	1 190	2 858	4 415	34	-1 590
NO5	3 719	0	0	600	1 120	0	5 439	3 741	39	1 658
SE1	1 981	0	0	320	0	3 220	6 023	8 632	221	-2 830
SE2	5 137	0	0	600	240	5 460	11 437	4 636	327	6 474
SE3	1 686	0	0	3 460	240	4 760	9 780	16 198	216	-6 633
SE4	168	0	0	1 440	640	1 400	4 013	4 114	33	-133
Total	28 836	8 011	0	11 500	7 920	30 870	87 345	84 586	1 744	1 015
% of total	33	9.2	0	13.2	9.1	35.3	100			

With this generation and load setup, there was still some overloading in the north of Sweden. In order to not overload any lines, reinforcement was needed between Djuptjärn (SE1) and Viitalajärvi (FI), and in SE1, from Harspånget, via Porjus to Vitas, where Hybrit loads were located.

In Figure 5.3, the cross-border flows of the 2045 small scale scenario are displayed. In Finland, the extensive onshore wind power installations have contributed to a surplus of electricity generation. As a result, Finland exports its excess power to neighboring regions. To accommodate this situation and prevent an overwhelming amount of active power flow through SE1, the high-voltage direct current (HVDC) link between FI and SE3 has been set to 1200 MW. The overloaded areas are also displayed in red in Figure 5.3. At the locations in question, the grid had to be strengthened further in order to comply with N-0 conditions.

Despite the increased wind and solar production capacity in SE3, it still relies on importing power. This is due to multiple factors. Firstly, the scenario assumes a high overall load in SE3. Secondly, the decommissioning of nuclear power plants in this scenario further amplifies the need for power imports. With a reduced nuclear power contribution, SE3 relies on imports from primarily SE2 to maintain the power balance in this scenario.

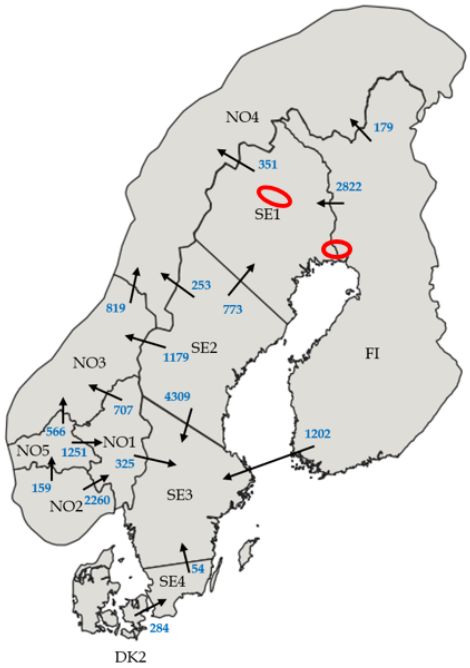

Figure 5.3: Active power flows between bidding zones for the high wind case in the small scale scenario, Case 1. All values are in MW. Red circles indicate highly loaded areas.

5.5.2 Case 2a: Fossil free case - low wind

In the fossil free case, the expected total energy demand in 2045 in DK2, Finland, Norway, and Sweden is 817 TWh. This means that the average load is 93 GW in this scenario. The initial assumptions are as described in Sections 5.4.2 and 5.4.4, for low wind cases. This means the power output from offshore wind is 10 %, from onshore wind 5 %, from solar 20 %, and the total load was set to 80 % of the yearly average. All values are presented in Table 5.11.

Hydropower was set to generate, on average, 76 % of maximum capacity, nuclear 79 %, and other thermal 55 %. The interconnectors were set to full import, totaling 7.7 GW. This created a balanced case in terms of generation and load, but the way the power had to flow in order to get from generation/import location to load caused extensive overloads. This overload was primarily found between NO1 and SE3, SE2 and SE1, and SE1 and FI.

The reason for this is that Scenario 2 in Finland predicts considerable growth in installed wind capacity, especially onshore, and a large increase in loads. With an availability factor of 5 % for the onshore wind and only a 20 % cut in loads, the import need to Finland through SE1 became about 6 GW, given that the HVDC connection between Finland and SE3 was utilized to the maximum degree, and that Finland was importing 1 GW from Estonia. Most of this deficit was covered with hydropower and import from other countries, much of which is located in the south

of Norway.

To prevent the transmission lines from overloading in this case, all lines between SE1 and SE2, and SE1 and Finland needed doubling, and the transmission line between Hasle and Borgvik (NO1-SE3) needed tripling. Some reinforcements in the north of Finland were also needed, but within the bidding zones, the grid was well-equipped for this scenario.

As an alternative to grid reinforcements, load flexibility in Finland was considered. In this scenario, 126 TWh of Finland's yearly energy demand is estimated to come from electrolysis. On average, this contributes to 14.4 GW of load, which is assumed to be flexible. Hence, after having reduced the total load to 80 %, another 7 GW was removed from Finland's total load. The 7 GW of reduced load also meant that for the system as a whole, the import need was reduced by the same amount, which is why all interconnectors were set to zero, as can be seen in Table 5.10. The final generation and load outcome after these adaptions are presented in Table 5.11.

Table 5.10: Interconnectors to other countries and the active power flow through them in Case 2a. Positive indicates export, and negative indicates import. All values are in MW.

	DE	DK1	EE	LT	NL	PL	UK
DK2	0	0				0	
FI			0				
NO2		0			0		0
SE3		0					
SE4	0			0		0	

Table 5.11: Generated and consumed active power in each bidding zone in Case 2a. Loads are excluding losses. Difference = Total - Load - Losses, indicates import/-export of the bidding zones. Losses are gathered from PSS/E load flow simulations. All values in MW.

	Hydro	Nuclear	Other thermal	Solar	Wind-offshore	Wind-onshore	Total	Load	Losses	Difference
DK2	0	0	500	480	300	150	1 430	3 320	10	-1 900
FI	2 300	3 500	2 900	5 000	1 000	2 650	17 350	17 943	150	-743
NO1	2 200	0	0	600	0	20	2 820	4 309	528	-2 017
NO2	10 000	0	0	600	300	110	11 010	7 135	139	3 736
NO3	3 500	0	0	200	300	290	4 290	4 671	152	-533
NO4	3 500	0	0	0	200	170	3 870	3 540	93	237
NO5	7 500	0	0	600	0	0	8 100	3 011	106	4 983
SE1	3 500	0	100	20	150	370	4 140	6 430	49	-2 339
SE2	6 000	0	300	100	150	440	6 990	3 820	276	2 894
SE3	1 800	6 300	1 550	1 550	660	320	12 180	14 200	326	-2 346
SE4	150	0	350	640	180	140	1 460	3 691	117	- 2 348
Total	40 450	9 800	5 700	9 790	3 240	4 660	73 640	72 071	1 947	-376
% of total	54.9	13.3	7.7	13.2	4.4	6.3	100			

With these adjustments, the export need from Norway remained high, and in order to not overload any lines, grid reinforcements were needed within NO1 and from Hasle to Borgvik, as well as between Halden and Trollhättan. This is shown in Figure 5.4.

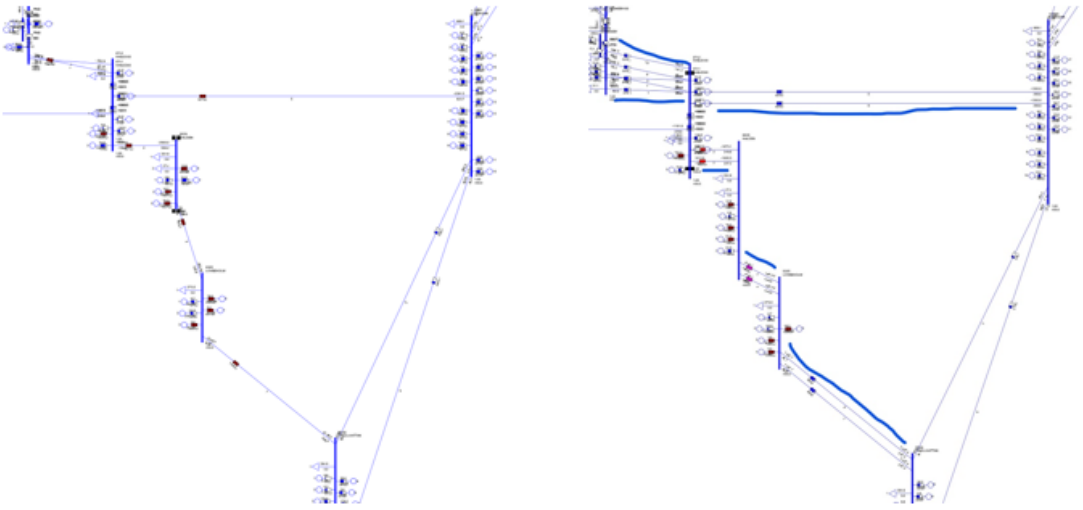

Figure 5.4: Before and after adding extra lines in the NO1-SE3 area, snapshot of the .sld file in PSS/E.

When all the adaptations were made, the final cross-border flows are presented in Figure 5.5. NO1 was exporting 5 522 MW to SE3, which mostly came from NO5 and NO2. SE2 imported some power from Norway and exported power to SE1 and SE3. Since Finland's load was lowered to almost be balanced with the generation in Finland, the flow between FI and SE1 is low. However, Finland imports at maximum capacity from SE3.

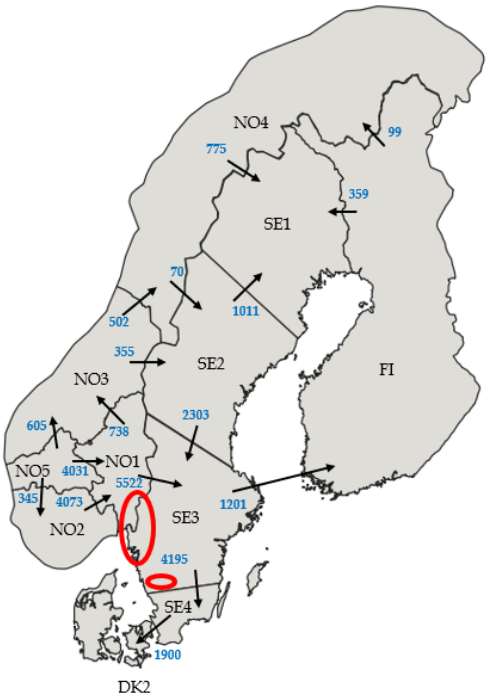

Figure 5.5: Active power flows between bidding zones for the low wind case in the fossil free scenario, Case 2a. All values are in MW. Red circles indicate highly loaded areas.

5.5.3 Case 2b: Fossil free case - high wind

Case 2b assumes the same installed capacity and yearly averages as Case 2a, but the wind generation is much higher, and as a consequence of that, the load is also much higher. The same method for the generation output as in Case 2a is used, but in this case, the offshore wind is generating power at 80 % of the installed capacity, onshore wind 70 %, and solar 20 % of the installed capacity. The load is estimated to be 120 % of the yearly average load, and since 7 GW of power was removed from Finland's load in the low wind case, it is added in this case. Table 5.13 presents each bidding zone's generation, loads, and losses. The export used to balance this case is displayed in Table 5.12.

Table 5.12: Interconnectors to other countries and the active power flow through them in Case 2b. Positive indicates export, and negative indicates import. All values are in MW.

	DE	DK1	EE	LT	NL	PL	UK
DK2	585	590				0	
FI			1 000				
NO2		700			1 000		1 000
SE3		700					
SE4	600			700		600	

Table 5.13: Generated and consumed active power in each bidding zone in Case 2b. Loads are excluding losses. Difference = Total - Load - Losses, indicates import/-export of the bidding zones. Losses are gathered from PSS/E load flow simulations. All values in MW.

	Hydro	Nuclear	Other thermal	Solar	Wind-offshore	Wind-onshore	Total	Load	Losses	Difference
DK2			100	480	2 450	2 160	5 190	4 192	72	926
FI	500	1 500	500	5 000	8 200	37 160	52 860	45 156	771	6 933
NO1	1 500	0	0	600	0	144	2 244	8 653	154	-6 563
NO2	1 000	0	0	600	11 000	792	13 392	10 131	159	3 102
NO3	1 500	0	0	200	3 200	2 088	6 988	6 860	108	20
NO4	1 000		0	0	3 200	1 224	5 424	4 740	38	684
NO5	4 500	0	0	600	600	0	5 700	4 131	92	1 477
SE1	1 000	0	0	20	1 200	5 328	7 548	11 000	173	-3 625
SE2	1 200	0	0	100	1 200	6 336	8 836	4 647	350	3 839
SE3	500	6 300	500	1 460	3 900	5 376	17 684	14 435	466	3 135
SE4	20	0	0	640	1 800	2 016	4 828	6 733	67	- 2 342
Total	12 720	7 800	1 100	9 700	36 750	62 624	130 606	120 680	2 451	7 563
% of total	9.7	6	0.84	7.4	28.1	47.9	100			

In Finland, the generated power from wind and solar is in total 50 GW, and the load is 45 GW. The HVDC connections in Finland can export 2.2 GW of power. This means the other power sources need to be quite limited in a scenario like this, if the wind is not curtailed nor the load increased, to not overload the lines going into SE1. Hydro and other thermal are therefore set to 500 MW each, and nuclear is reduced by 2 000 MW compared to Case 2a, to 1 500 MW.

From 5.13, it can be seen that in the other countries, the hydro was also reduced significantly, the total power generated from hydro was 12.7 GW, compared to 40 GW in Case 2a. Other thermal was also lowered to 1.1 GW in total. As mentioned before, nuclear was reduced in Finland but is kept the same in Sweden compared to Case 2a.

When running this case, the importance of smart placements of the large offshore wind farms in relation to the placements of the loads was proved, and some adjustments needed to be made to avoid overloading lines along the coast in Finland and in NO2. Issues with the distribution of the onshore wind also became apparent when the power output increased. Since, in some bidding zones, the new onshore wind was installed at all busses in that bidding zone, regardless of grid topology, some lines became overloaded because of this. These lines were the 220 kV lines in Finland and SE2, which have much less transmission capacity as compared to the 400 kV lines and are also, to a larger extent, placed radially with few connections to 400 kV buses. To mitigate this problem, these generators were moved to other 400 kV buses nearby in SE2, and to buses nearby and further south in Finland.

Many of the overloads were mitigated with these adaptations, but some remained. The area where NO1 and SE3 connects were still overloaded. Due to reduced hydropower generation, high loads, and large export from Norway to mainland Europe, much of the power consumed in NO1 was imported from SE1, more than what the

grid was equipped for. Adding one line between Borgvik (SE3) and Hasle (NO1) solved this issue.

In addition to this, one branch between Viitalajärvi (FI) and Djuptjärn (SE1) was added to supply the large Hybrit load placed at Djuptjärn. Another reinforcement was also needed between Porjus and Harspånget to be able to supply the Hybrit loads located at Porjus, Vitas and Ritsem, which are downstream from each other, all located in SE1. Two branches in the 220 kV grid, one in SE2 and one in DK2, were also needed to connect all generation. The same problem that was observed in the 2020 cases was shown here as well. The load located at the bus Forre in NO2 became too big for the transmission capacity surrounding it. Here, instead of adding a line, half of the remaining load was moved to Lyse, a bus next to Forre. The areas in question are displayed in red in Figure 5.6.

Figure 5.6 shows the cross-border flows after implementing all changes. The flow between SE1 and FI was high, 4 557 MW from FI to SE1, and the export from FI to SE3 was at maximum capacity. The large import from Finland to Sweden meant the flow through Sweden was going south. SE3 was exporting 3 173 MW to NO1, which had a substantial import need, and 4 121 MW to SE4 which was exporting through the interconnectors and had a power deficit. NO2 had a small net exchange with the neighboring bidding zones, but a large surplus in power, this is all exported through the interconnectors.

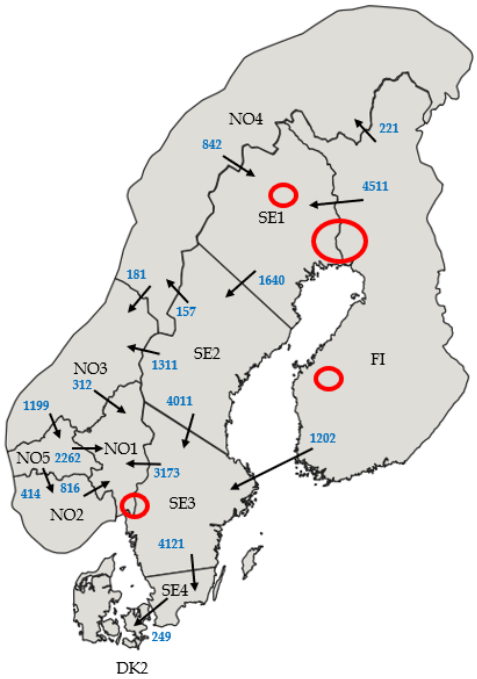

Figure 5.6: Active power flows between bidding zones for the high wind case in the fossil free scenario, Case 2b. All values are in MW. Red circles indicate highly loaded areas.

5.5.4 Case 3a: Electrification renewable - low wind

In Scenario 3, the synchronized Nordic region is expected to have a total energy demand of 938 TWh by 2045. This corresponds to an average load of 107 GW. It is assumed that the general consumption level will be 80 % of the average load.

Scenario 3 poses significant challenges to the Nordic transmission grid, particularly during periods of low wind generation. This is because most of the installed capacity relies on intermittent production, primarily from onshore wind sources. Therefore, a substantial mismatch between load and generation was observed when the low wind generation profile was applied to the installed capacity. This discrepancy necessitated the modeling of demand-side flexibility to achieve a balance between power generation and consumption.

By introducing flexibility by adjusting electrolysis loads and industrial loads, the model aims to address the challenges posed by intermittent renewable energy generation. So in order to balance the generation and consumption of power, the electrolysis loads have been set to zero. The total load and generation in each bidding zone is presented in Table 5.15. Furthermore, the manually added industrial loads have been set to operate at 80 % of their average load. In addition to demand-side management, the Nordic countries rely on power imports in this scenario. Table 5.14 summarizes the power imports facilitated through interconnections with other countries.

Table 5.14: Interconnectors to other countries and the active power flow through them in Case 3a. Positive indicates export, and negative indicates import. All values are in MW.

	DE	DK1	EE	LT	NL	PL	UK
DK2	0	-582				0	
FI			-357				
NO2		0			0		-510
SE3		-149					
SE4	0			-500		-600	

Table 5.15: Generated and consumed active power in each bidding zone in Case 3a. Loads are excluding losses. Difference = Total - Load - Losses, indicates import/-export of the bidding zones. Losses are gathered from PSS/E load flow simulations. All values in MW.

	Hydro	Nuclear	Other thermal	Solar	Wind-offshore	Wind-onshore	Total	Load	Losses	Difference
DK2	0	0	29	534	375	227	1 165	2 191	12	-1 038
FI	1 650	1 937	474	3 800	450	3 800	12 111	7 876	908	3 326
NO1	2 145	0	0	800	0	10	2 955	4 486	235	-1 767
NO2	7 755	0	0	800	750	55	9 360	5 767	118	3 473
NO3	2 640	0	0	200	250	145	3 235	4 740	92	-1 598
NO4	2 915	0	0	0	250	85	3 229	3 536	38	-346
NO5	5 940	0	0	600	250	0	6 790	3 179	63	3 546
SE1	2 970	0	13	180	225	435	3 992	6 821	155	-2 984
SE2	4 180	0	0	180	225	520	5 105	4 446	148	509
SE3	1 265	0	193	2 420	475	270	4 547	7 638	138	-3 229
SE4	110	0	36	1 060	500	110	1 892	4 446	35	-2 590
Total	31 570	1 937	746	10 574	3 750	5 657	54 383	55 131	1 949	-2 698
% of total	20.1	1.27	0	6.7	29.5	42.7	100			

When the adaptations were made, there were still some overloads remaining. These were between Djuptjärn (SE1) and Viitalajärvi (FI), in the NO1-SE3 area, and in SE1. The overload between Djuptjän and Viitalajärvi was very large, and two extra lines were needed between those buses. Initially, it seemed as if adding those lines between Djuptjärn and Viitalajärvi would be enough to mitigate the issue in this area, but after having added those lines, more flow went through there due to the reduction in impedance, which meant that the line going from Pikkarala (FI) to Viitalajärvi, and from Djuptjärn to Svartbyn (SE1) also needed to be reinforced. The Pikkarala-Viitalajärvi stretch needed two extra lines as well. In the NO1-SE3 area, one line was added between Halse and Borgvik, and between Halse and Halden, and Halden and Loviseholm. In SE1, the line between Harspånget and Projus needed reinforcing. The reinforced areas are displayed in red in Figure 5.7.

The cross-border flows are displayed in Figure 5.7. Considering that this is a low wind scenario and Finland relies heavily on onshore wind production, it is reasonable that Finland would need to import power from neighboring bidding zones. However, this is mitigated through the flexibility measures mentioned earlier, so instead, Finland is a net exporter in this scenario. Furthermore, since this is a low wind case, the hydro plants in northern Sweden have to carry a large percentage of the national load, which causes a north-to-south flow. The hydro plants in southwest Norway also deliver a lot of power to NO1 and SE3.

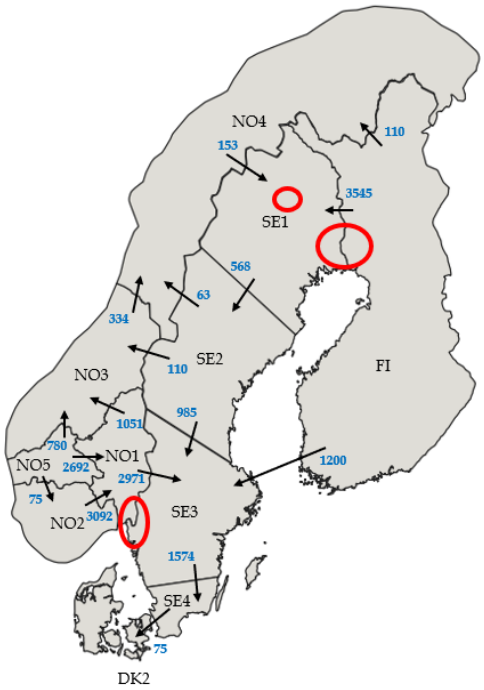

Figure 5.7: Active power flows between bidding zones for the low wind case in the electrification renewable scenario, Case 3a. All values are in MW. Red circles indicate highly loaded areas.

5.5.5 Case 3b: Electrification renewable - high wind

When estimating the electricity demand in this scenario, the general consumption level (industrial and electrolysis not included) will be 120 % of the average load. As can be seen in Table 5.18 where the load and generation are presented, this scenario produces much power during high wind conditions. To accommodate this production, the electrolysis loads have been doubled in Norway, Finland, and DK2. In Sweden, the industrial load has been increased by 50 % since electrolysis and industrial loads are not separated, as can be seen in Table 5.6. In addition, the total system needs to export power to balance generation and load in this scenario. Table 5.16 provides a summary of the power exports to neighboring countries.

Table 5.16: Interconnectors to other countries and the active power flow through them in Case 3b. Positive indicates export, and negative indicates import. All values are in MW.

	DE	DK1	EE	LT	NL	PL	UK
DK2	0	14				0	
FI			1016				
NO2		432			0		1400
SE3		0					
SE4	0			700		600	

Table 5.17: Generated and consumed active power in each bidding zone in Case 3b. Loads are excluding losses, indicates import/export of the bidding zones. Difference = Total - Load - Losses. Losses are gathered from PSS/E load flow simulations. All values in MW.

	Hydro	Nuclear	Other thermal	Solar	Wind-offshore	Wind-onshore	Total	Load	Losses	Difference
DK2	0	0	0	480	2 570	2 147	5 196	5 452	132	-388
FI	1 657	2 003	0	3 800	5 850	45 600	58 909	54 960	1 468	2 480
NO1	2 154	0	0	800	0	120	3 073	8 386	259	-5 572
NO2	7 786	0	0	800	9 750	660	18 995	13 735	259	5001
NO3	2 651	0	0	200	3 250	1 020	7 840	8 827	173	-1 160
NO4	2 927	0	0	0	3 250	1 020	6 944	6 568	24	350
NO5	5 964	0	0	600	3 250	0	9 813	5 641	233	3 939
SE1	2 982	0	0	180	2 925	5 220	11 129	10 436	173	519
SE2	4 197	0	0	180	2 925	6 240	13 541	7 313	683	5 544
SE3	1 270	0	0	2 420	6 175	3 240	12 854	20 617	334	-8 097
SE4	110	0	0	1 060	6 500	1 320	9 240	7 597	98	1 545
Total	31 696	2 003	0	10 520	46 445	67 307	157 540	149 537	3 841	4 162

Table 5.18: Generated and consumed active power in each bidding zone in Case 3b. Loads are excluding losses, indicates import/export of the bidding zones. Difference = Total - Load - Losses. Losses are gathered from PSS/E load flow simulations. All values in MW.

	Hydro	Nuclear	Other thermal	Solar	Wind-offshore	Wind-onshore	Total	Load	Losses	Difference
DK2	0	0	0	480	2 570	2 147	5 196	5 452	132	-388
FI	1 657	2 003	0	3 800	5 850	45 600	58 909	54 960	1 468	2 480
NO1	2 154	0	0	800	0	120	3 073	8 386	259	-5 572
NO2	7 786	0	0	800	9 750	660	18 995	13 735	259	5001
NO3	2 651	0	0	200	3 250	1 020	7 840	8 827	173	-1 160
NO4	2 927	0	0	0	3 250	1 020	6 944	6 568	24	350
NO5	5 964	0	0	600	3 250	0	9 813	5 641	233	3 939
SE1	2 982	0	0	180	2 925	5 220	11 129	10 436	173	519
SE2	4 197	0	0	180	2 925	6 240	13 541	7 313	683	5 544
SE3	1 270	0	0	2 420	6 175	3 240	12 854	20 617	334	-8 097
SE4	110	0	0	1 060	6 500	1 320	9 240	7 597	98	1 545
Total	31 696	2 003	0	10 520	46 445	67 307	157 540	149 537	3 841	4 162
% of total	20.1	1.3	0	6.7	29.5	42.7	100			

In this case, several overloads remained. Many were in Norway, one in DK2, two in Finland, and two in SE1. In NO1, reinforcements were needed between Hasle and Halden, Flesåker and Sylling, and Sylling and Olso. NO1 was exporting to SE3, but the load in NO1 was also large, particularly in Oslo, which had a load of 2.6 GW. One line in NO2 between Saturdal and Kvilldal was overloaded, and one in NO5 between Eldfjord and Dagali. These areas are displayed in red in Figure 5.8.

In Finland, at the bus Pyhänsel, the load was just above 3 GW, which meant that a second line was needed between Pyhänsel and Pikarala and between Pyhänsel and Isokangas. In DK2, a second line was needed between Glentgard och Gorlosegard, and in SE1, the line between Harspånget and Porjus needed reinforcing, as well as the line between Ligga and Messaure.

The cross-border flows are displayed in Figure 5.8. Some changes are apparent when compared to the flows from the low wind scenario described in Section 5.5.4. Firstly the North-South flow is no longer present. Instead, power flows from SE2 to both SE1 and SE3, this is due to the industrial loads present in SE1 and the generally high load of SE3 combined with the decommissioning of the nuclear power plants. Secondly, DK2 and SE4, along with NO1, also export power to SE3. Finland generates a lot of onshore wind power, but the increased electrolysis loads consume it and thus only exports power through the HVDC link connected to SE3.

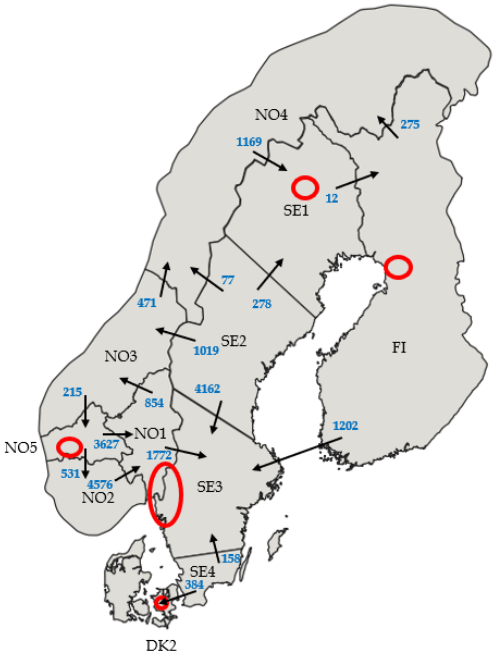

Figure 5.8: Active power flows between bidding zones for the low wind case in the electrification renewable scenario, Case 3b. All values are in MW. Red circles indicate highly loaded areas.

5.6 Demand For Reactive Compensation

In this section, the need for reactive compensation provided by the generators is presented for each case. The generators are set to have infinite reactive capability, which means that the voltage for all generator buses will be controlled to 1 p.u. With this configuration, the need to transmit reactive power from one bus to another is reduced, which means that the reactive power induced or consumed by the generators at one bus is only to compensate for the reactive power induced or consumed by the transmission lines leading to that bus.

In Figures 5.9-5.10, the reactive compensation of all cases is compared. Figure 5.9 presents the total reactive compensation for all cases. It shows that the absorbed reactive power in all 2020 cases is around -10 000 MVAr, with high wind cases needing to absorb slightly more than low wind cases. In the 2045 cases, there is an increased

need to consume reactive power, in these cases, there was a need to absorb around -15 000 MVAr.

The injected reactive power differs more, from Figure 5.9 it is clear that in the 2020 low load cases and the high load - high wind case, the need for induced reactive power is low compared to the 2020 high load - low wind case. Then, comparing the 2020 cases to the 2045 cases, it is clear that there is a need for more induced reactive power, especially in the high wind cases. Case 3a, the renewable low wind case, has a comparatively low need for injected reactive power among the 2045 cases.

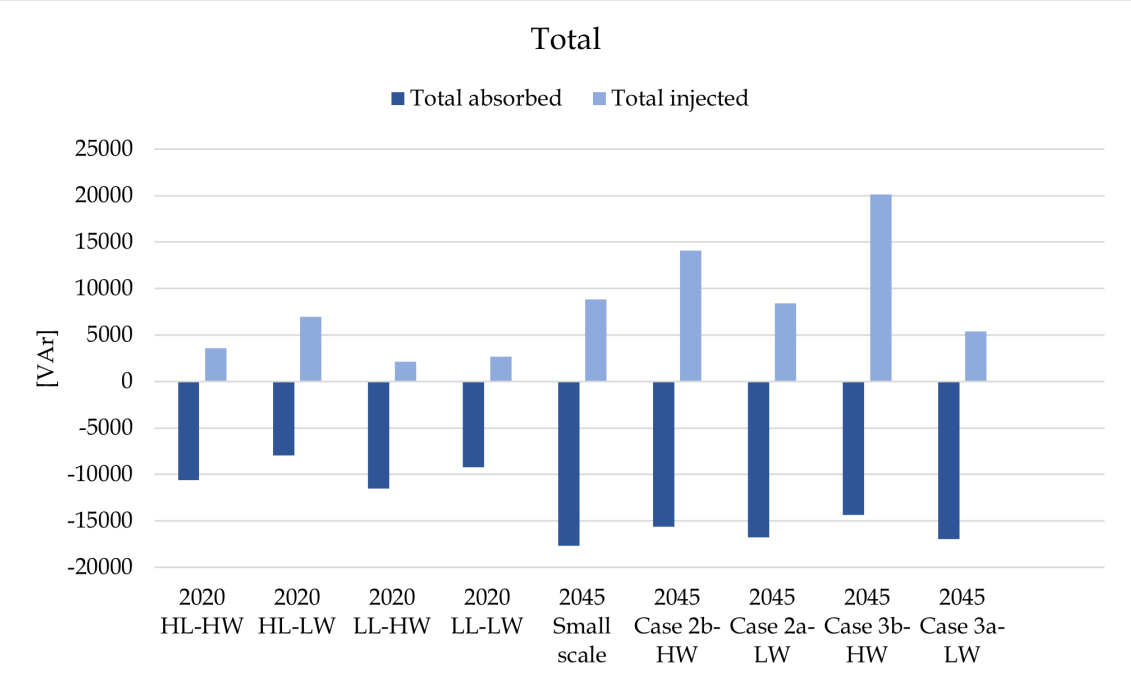

Figure 5.9: The total injected and absorbed reactive power for all cases. All values in [VAr]

When comparing the total injected reactive power as a percentage of the generated power in each case, the individual differences in induced reactive power that was apparent in Figure 5.9 disappear, as can be seen in Figure 5.10. Almost all cases inject around 10 % of the generated power. The 2020 low load cases and the high wind - high load inject slightly less. However, the cases' need for absorbed reactive power is quite different. This is the reversed pattern compared to the totals. There is a clear tendency that the low load cases need more absorbed reactive power compared to how much active power is being generated. The exception is the small scale case, which is a high load case but has a comparatively large need for absorbed reactive power compared to the other high wind cases in 2045.

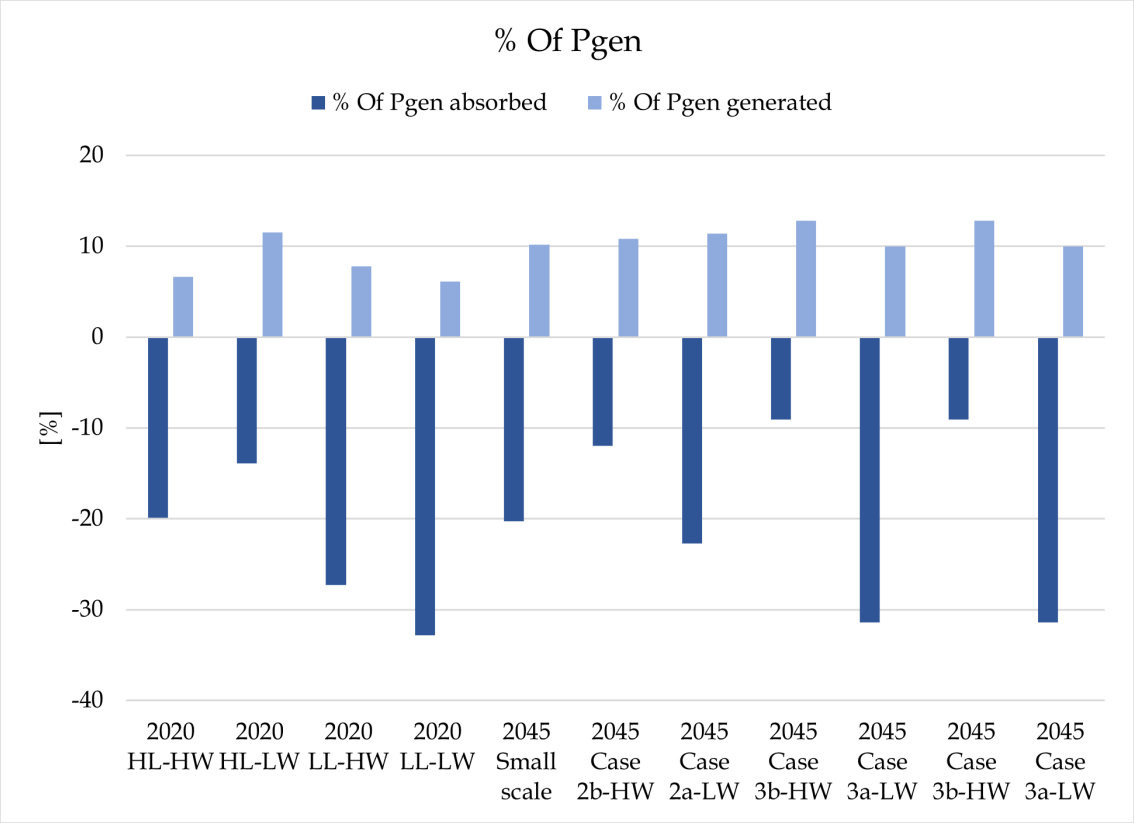

Figure 5.10: The total injected and absorbed compensation in each case, as percentages of the generated active power.

5.6.1 Reactive compensation at specific buses compared to the 2020 cases

To be able to determine where further reactive compensation in the grid is needed in 2045, the reactive compensation at each bus was investigated, both in the 2020 and 2045 cases. The maximum values for injected and absorbed reactive power of each 2020 case, at each bus, was found. Of all buses, the buses with the most injected or absorbed reactive power are presented in Table 5.19.

Table 5.19: Buses with most injected and absorbed reactive power in the 2020 cases

Buses injecting reactive power	**Bidding zone**	**Injected reactive power [MVAr]**	**Buses absorbing reactive power**	**Bidding zone**	**Absorbed reactive power [MVAr]**
SAURDAL	NO2	300.0	RAMSELE	SE2	-437.5
AURLAND	NO5	292.3	FORSMARK	SE3	-289.3
BÄSNA	SE3	232.0	OLKILUOTO	FI	-287.0
SAMNAGER	NO5	214.1	RINGHALS	SE3	-270.4
ÖSTANSJÖ	SE3	207.6	PIKKARALA	FI	-262.8
NYBRO	SE4	204.2	LETSI	SE1	-256.5
BREARED	SE4	200.9	HJÄLTA	SE2	-240.3
MORGARDSH	SE3	189.7	ALAJÄRVI	FI	-219.5
ODENSALA	SE3	183.3	OSKARSHAMN	SE3	-212.5
BORGVIK	SE3	175.4	STORNORRFORS	SE2	-204.7
KRISTIANSAND	NO2	167.9	RÄTAN	SE2	-200.7
LÅNGBJÖRN	SE2	162.9	KILFORSEN	SE2	-198.2
FLESAKER	NO1	152.1	BORGVIK	SE3	-181.6
BETÅSEN	SE2	145.8	PORJUS	SE1	-163.9
FOLLO	NO1	139.2	MOLIDEN	SE2	-154.4
ÅKER	SE3	133.5	VIITALAJÄRVI	FI	-154.0
UDDEBO	SE3	125.6	STACKBO	SE3	-152.4
LINDOME	SE3	103.3	JUKTAN/BLAIK	SE2	-150.4
MINNE	NO1	101.0	SVARTBYN	SE1	-149.2
NYSÄTER	SE2	98.7	ÖSTANSJÖ	SE3	-141.1
MIDSKOG	SE2	97.3	HARSPÅNGET	SE1	-136.7
VÅGÅMO	NO3	95.2	LOVIISA	FI	-135.9
OSLO	NO1	95.0	HERSLEV	DK2	-131.7
TRÅNGFORS	SE2	91.3	BÄSNA	SE3	-131.3
SEITENOIKEA	FI	91.1	ULVILA	FI	-130.7

From Table 5.19, the ten buses injecting respectively absorbing the most power is mapped in Figure 5.11. What can be seen from this table and figure is that the places with the most injected power are located at buses with typically large loads, south in the grid. Meanwhile, the buses with the most absorbed reactive power are located at large generator buses, like by nuclear reactors, or further north.

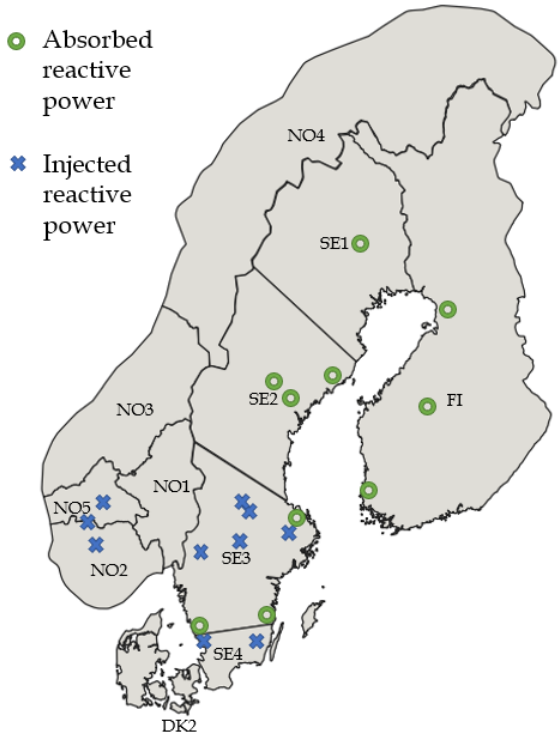

Figure 5.11: The bus locations where the most reactive power is injected and absorbed in the 2020 cases.

The results from 2020 can be used to compare the results from 2045. In the 2045 results, the maximum reactive power absorbed or generated at each bus is removed from the maximum absorbed or generated reactive power in either of the 2020 cases. This is because since the 2020 cases are working, all the reactive compensation needed is expected to exist in the grid today. What is interesting to see is how the need for reactive compensation can come to change and where reactive compensators could be needed. The ten places with the largest increased need for either injected reactive power or absorbed reactive power for Scenarios 2 and 3 are shown in Figures 5.12 and 5.13.

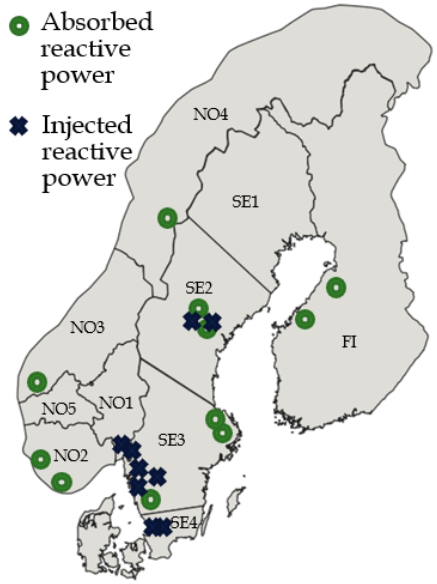

Figure 5.12: The bus locations where the most reactive power is injected and absorbed compared to 2020 in the fossil free scenario, Case 2a and 2b.

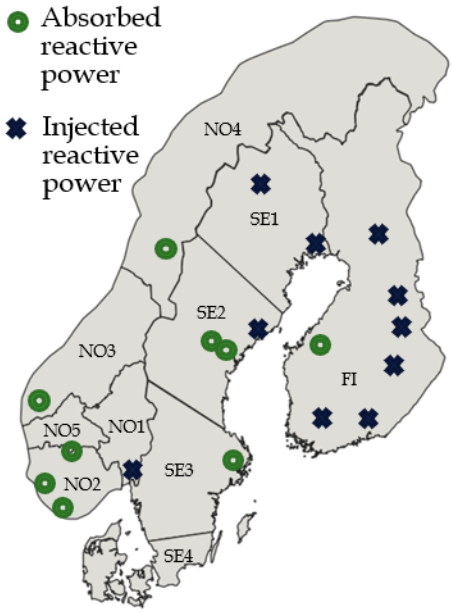

Figure 5.13: The bus locations where the most reactive power is injected and absorbed compared to 2020 in the electrification renewables scenario, Case 3a and 3b.

When comparing the locations for the most absorbed reactive power between Scenarios 2 and 3, presented in Figures 5.12 and 5.13, it is clear that they are quite similar. They are also distributed over the Nordics, with no particular areas that require more absorbed reactive power. When looking at the injected reactive power, however, the two different scenarios differ a lot when studying where the need for

reactive power will change. In Scenario 2, the most significant need for reactive power injection is found in the NO1-SE3 area, which has heavily loaded lines in this scenario. In Scenario 3, the largest change in the need for injected reactive power is more commonly found in eastern Finland, which is an area with heavily loaded lines in this scenario.

5.6.2 Reactive compensation at specific buses compared to actual reactive compensation capability

According to the grid code, generators connected to the grid need to be able to absorb or inject reactive power within the interval of $\pm$ 1/3 of P_{gen} [39]. In this section, the injected reactive power at each bus is compared to the generated power at each bus to study where a reactive power shortage could arise. This is done for Scenarios 2 and 3, where the largest value at each bus between the cases for each scenario was compared.

Figure 5.14 shows the locations where the exceeding need for reactive power is the largest, both injecting and absorbing for Scenario 2, fossil free. Table 5.20 presents the bus names and the exceeding need for reactive power for Scenario 2.

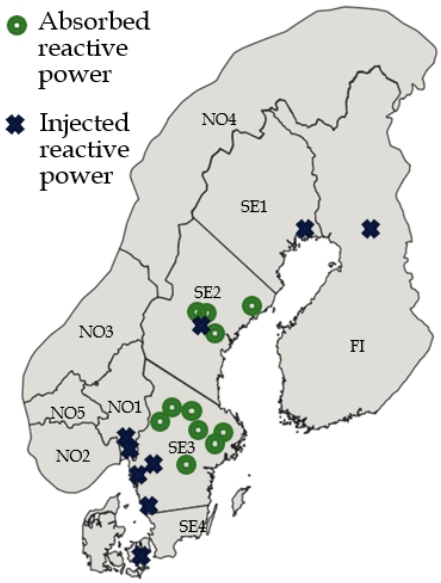

Figure 5.14: The bus locations where the need for reactive power exceeds the grid code requirement for reactive power compensation the most in Scenario 2, fossil free.

Table 5.20: The locations were the need for reactive power exceeds what is required by the grid code to be produced by the generators, and the exceeding reactive power need in [MVAr] in Scenario 2.

Buses absorbing reactive power	**Bidding zone**	**Exceeding reactive power [MVAr]**	**Buses injecting reactive power**	**Bidding zone**	**Exceeding reactive power [MVAr]**
GRÖNVIKEN	SE3	-549.9	BJAEVERSKOV	DK2	421.9
TANDÖ	SE3	-549.7	RATANSKV	SE2	418.1
ODENSALA	SE3	-476.2	HASLE	NO1	387.1
HJÄLTA	SE2	-448.0	LOVISEHOLM	SE3	319.2
FALLVIKEN	SE3	-414.3	DJUPTJÄRN	SE1	295.3
MIDSKOG	SE2	-403.7	PIRITTK	FI	264.3
KILFORSEN	SE2	-387.9	HORRED	SE3	254.6
STORFINNSFORS	SE2	-358.1	HALDEN	NO1	235.1
STACKBO	SE3	-255.5	OSLO	NO1	230.9
LINDBACKA	SE3	-226.9	BORGVIK	SE3	229.6
HAGFORS	SE3	-201.2	JÄRPSTRÖMMEN	SE2	201.4
BETÅSEN	SE2	-198.6	PETÄJÄSKO	FI	198.9
TUNNSJÖ	NO4	-150.3	BETÅSEN	SE2	193.4
PYHÄNSEL	FI	-132.0	UDDEBO	SE3	188.2
PETÄJÄSKO	FI	-131.0	GLAN	SE3	187.6

As can be seen in Figure 5.14, the largest exceeding need for absorbed reactive power is found in SE2 and SE3. These are areas connected by many long transmission lines. If these are not heavily loaded, more reactive power needs to be absorbed. In SE3, there are also some new buses with less generation connected to them, for instance, Grönviken and Tandö. This means that the reactive power compensation capability is quite low at these buses, which could be one reason for the result. In Case 2a, the low load case, the generation in SE2 is high compared to the load. This could be an explanation for the need for absorbed reactive power in this region as well. The exceeding need for injected reactive power is primarily concentrated to the NO1-SE3 area, and this is an area with limited generation and heavily loaded lines. Comparing the results presented in Figure 5.14 to the results presented in Figure 5.12, the NO1-SE3 area is present in both.

In Figure 5.15, the exceeding need for reactive power is shown, and in Table 5.21, the buses are named, and the exceeding reactive power need is shown.

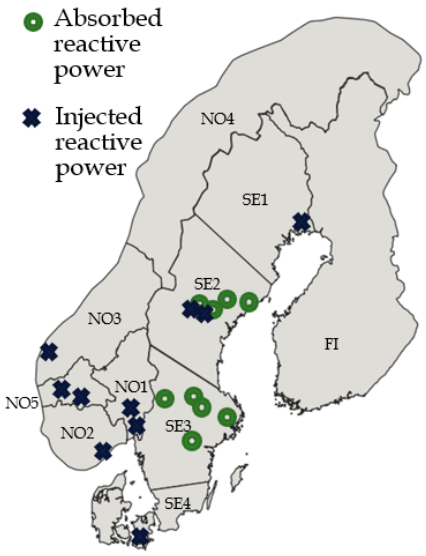

Figure 5.15: The bus locations where the need for reactive power exceeds the grid code requirement for reactive power compensation the most in Scenario 3, electrification renewable.

Table 5.21: The locations were the need for reactive power exceeds what is required by the grid code to be produced by the generators, and the exceeding reactive power need in [MVAr] in Scenario 3.

Buses absorbing reactive power	**Bidding zone**	**Exceeding reactive power [MVAr]**	**Buses injecting reactive power**	**Bidding zone**	**Exceeding reactive power [MVAr]**
TANDÖ	SE3	-551.6	DJUPTJÄRN	SE1	329.7
GRÖNVIKEN	SE3	-539.3	RATANSKV	SE2	315.0
ODENSALA	SE3	-522.7	BAMBLE	NO2	279.3
HJÄLTA	SE2	-489.3	BJAEVERSKOV	DK2	243.0
MIDSKOG	SE2	-452.1	OSLO	NO1	225.7
KILFORSEN	SE2	-448.8	JÄRPSTRÖMMEN	SE2	224.3
STORFINNSFORS	SE2	-415.4	ÅLFOTEN	NO3	218.5
LINDBACKA	SE3	-325.6	SAMNAGER	NO5	209.5
FALLVIKEN	SE3	-317.7	HASLE	NO1	207.0
STACKBO	SE3	-279.1	USTA	NO5	206.0
HAGFORS	SE3	-216.8	ROD	NO2	182.7
BETÅSEN	SE2	-194.8	DAGALI	NO5	169.2
HAMRA	SE3	-149.4	KVILLDAL	NO2	167.2
TUNNSJO	NO4	-143.0	MUNGA	SE3	164.9
TOVÅSEN	SE2	-123.2	HEDENLUNDA	SE3	162.3

The same pattern regarding the exceeding need for absorbed reactive power in Scenario 3, as in Scenario 2 is shown Figure 5.15. These buses are also located in SE2 and SE3, and the largest exceeding need is about the same, around -550 MVAr.

When comparing where the change was the largest compared to the 2020 cases, presented in Figure 5.13, the buses in Noway are changed to buses in Sweden. The same reasoning as explained when studying Scenario 2 can be applied here. As for the exceeding need for injected reactive power, this is primarily found in Norway, and this differs a lot from the largest change in need for injected reactive power presented in Figure 5.13 where the largest changes was primarily found in eastern Finland. This means that even if the reactive power need change a lot in Finland, it will still be able to compensate for this change since many new generators are installed where this need exists.

6

Contingency and Sensitivity Studies

6.1 Theory on ACCC and Sensitivity Studies

The conducted study involves two main analyses: contingency studies (ACCC) and sensitivity studies. These analyses serve different purposes in the model investigation.

Contingency studies were carried out using the ACCC studies function in PSS/E. This function helps understand the impact of contingencies on power system branches and how they affect the loading on other branches. The primary goal of these simulations is to identify the branches that are most likely to experience overloading, both under normal operating conditions (base case) and during contingencies.

Once the heavily loaded branches are identified through contingency studies, a sensitivity analysis is performed. This analysis focuses on evaluating how changes in loads placed on different buses affect the power flow on the analyzed line. The purpose is to determine favorable locations for load and generation placement to avoid overloading lines in normal operation and during contingencies.

6.1.1 ACCC studies

ACCC studies are performed to assess the impact planned or unplanned contingencies in the power system have on the loading of the branches and the voltage at the buses. In this report, the focus will be on the thermal limits since, at each generator bus, there is infinite reactive power controlling the voltage to 1 p.u. The only contingencies performed are single contingencies on lines and transformers. The ACCC analysis starts by defining which contingencies are supposed to be performed. Then each contingency is simulated, and the steady-state voltage at the buses and the power flow through the lines are calculated and registered for all pre-defined lines and buses. In these studies, the Nordic synchronous zone was simulated at once.

To perform the ACCC studies, a .dfx file needs to be generated in PSS/E. The input to create this file is a SUB, a MON and a CON file which all are text files specifying which zones to include in the study, what the study should monitor, and which contingencies to perform. These files were individually created for each

model, however, the content of them was kept the same. The SUB file defines different subsystems of buses on which the study should be performed. The SUB file used for the ACCC analysis included all the bidding zones in the Nordic system as one subsystem, meaning everything was monitored in the same simulation. In the MON file, it was decided to monitor the bus voltage deviating from 0.95-1.05 p.u., as well as all branch flows. In the CON file, it was specified only to check single contingencies. The information on the voltage level was not used.

The ACCC studies were performed using the `ACCC_WITH_DSP3` function in PSS/E with a 0.1 mismatch tolerance, locked taps, disabled interchange control, the adjust DC taps flag was enabled, switched shuts adjustments were enabled (but non exists in the model), and the Full Newton-Raphson (FNLS) solution was used because it is the most accurate. The dispatch was disabled in order to see how the system would act in a worst-case scenario without mitigating potential overloads.

In order to directly write the results to an Excel sheet, `pssexcel.accc` was used, and all branch flows for all contingencies were exported. These were then sorted to find the worst loading case on each line, which could be during N-0 or N-1 conditions.

6.1.2 Sensitivity studies

The sensitivity studies performed in this study investigate how the branch flow on a predetermined branch is affected by adding load or generation on surrounding buses. When performing the sensitivity studies in AC mode, the sensitivity factors are represented as first-order partial derivatives to a power flow study with a set of voltage angles and magnitudes as input. As the representation of the model is a linearized one, the sensitivity factors can be assumed to be linear as well, which means that if the sensitivity factor of adding one MW load on one bus is x, for instance, the sensitivity factor when adding a 100 MW load can be estimated to 100x.

When a load is added in the PSS/E, another load needs to decrease, or more generation must be generated. In this simulation, a subsystem of ten buses with larger hydro units in the north of Sweden and Norway was defined to spread out the generation to compensate for the added load or generation. These were:

- Harspånget (SE1)
- Hjälta (SE2)
- Tuggen (SE2)
- Stornorrfors (SE2)
- Holen (NO2)
- Hekni (NO2)
- Nea (NO3)
- Grytten (NO3)
- Eldfjord (NO5)
- Dagali (NO5)

The sensitivity study was performed on all branches using the `sensitivity_flow` function. The settings were to run it in AC, calculating the sensitivity factor in MVA, at all buses, using the above-mentioned buses as the opposing subsystem. The cut-off for the sensitivity factor was set to 0.1 MW for a 1 MW load. If the impact from a bus was less than that, the impact was not registered. Setting the limit to this value meant that the impact from some buses was excluded, but the buses having the most influence on the branch flow were included. As mentioned earlier, the sensitivity factor could be assumed to be linear, and hence the effect of any sized load or generator could be evaluated.

In the next step, the results from the ACCC analysis that was used was the information on the minimum remaining capacity for each line in either N-0 or N-1 conditions. This information was used in combination with the information on which impact load placement had on the loading of a line gained from the sensitivity analysis. If the effect of an added load or generator on a specific line exceeded what was available, the placement was disregarded as suitable. On the other hand, if the contribution of the load/generator did not exceed the available power on any line, the placement was deemed suitable. Each bus was then checked to see if a load or generator placed there would make any line overload. If no lines did, it was considered a suitable placement.

6.2 Results from the ACCC and Sensitivity Analysis on the 2020 Model

6.2.1 ACCC

In the 2020 model, the high load cases are run with a higher capacity on the lines due to colder weather. Before this adaptation was implemented, there were some overloads, however, when running the ACCC analysis on all four cases, there were no overloads in the 400 kV grid. In the high load cases, there are no overloads at all. In the low load cases, there are some overloads in the 300 kV grid in Norway. The connection between Evanger (NO5) and Samnanger (NO5), is the only overloaded line in the low wind - low load case, it exceeds its transfer capacity by 105 MW (16 % overload). The same line is overloaded in the base case in the low load - high wind case too, by 95 MW (15 % overload).

In addition to this, the two lines between Refsdal (NO5) and Modalen (NO5) and between Modalen (NO5) and Evanger (NO5) overload if the transformer in Aurland (NO5) is out of operation. Then the overload of the lines is 52 MW and 43 MW, respectively. The area where these buses are located is in the area where NO3 and NO5 connect, and it is also a place with much generation. At the same time, it is only two different 300 kV lines connecting the 400 kV bus in Fardal. What is gathered from this is that there were only overloads in the 300 kV grid in Norway, whereas all other lines managed well. A reason for this could be that during the

high load cases, the line ratings in this model become very high during both base cases and contingencies. For instance, in a 400 kV line during contingencies in the high load cases, the rating on the 400 kV lines is 3 300 MVA, due to the lower temperatures, which is very high.

6.2.2 Sensitivity

From the ACCC analysis of the 2020 cases, it was found that the loading of the lines was not particularly high in either case, even in high load - low wind case where the official transmission capacity limit is exceeded. There were few overloads and generally a low loading on the lines. In order to evaluate ideal places for load and generation in this circumstance, the load/generation had to be very high. The selected buses presented in Figure 6.1 are buses on which either load or generators could be placed without causing overloads on either of the lines when looking at the minimum available capacity on the lines in either N-0 or N-1 conditions.

To limit the number of buses selected for loads and generation, the load tested was 2 500 MW and the generation 2 500 MW. In some areas, such as around Stockholm (SE3), there are suitable placements for both load and generation, whilst in other areas, for example in Norway, suitable placements for load and generation are divided. From Figure 6.1 it is clear that generators are better suited in NO2, whilst loads are better suited in the northern parts, indicating that there is a limiting branch between NO2-NO5 and NO2-NO1. In Finland and SE4, there are suitable spots for generation.

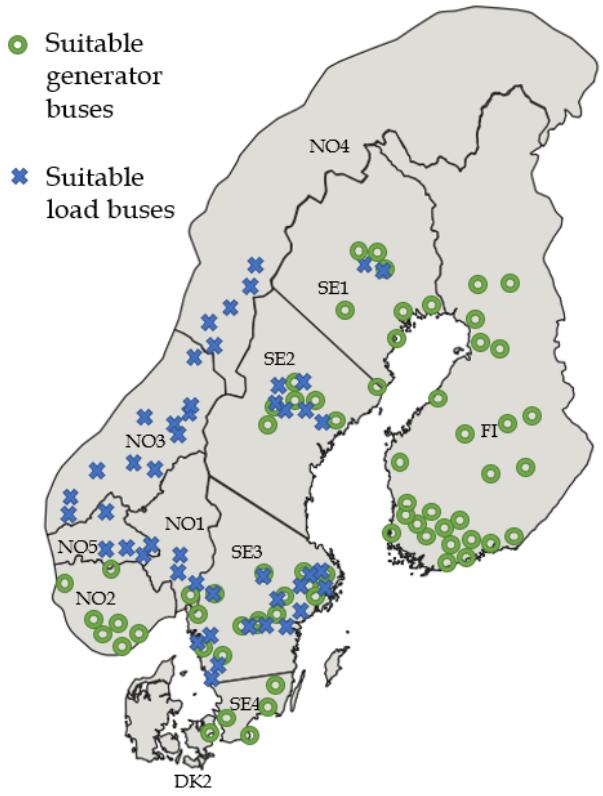

Figure 6.1: Suitable placements for load and generation in the 2020 grid. Loads and generator that are deemed to fit at these spots are each 2 500 MW

The results are quite coherent with known current grid conditions, where more loads are suitable in the north and more generation in the south. The division in Norway is explained by the results from the ACCC analysis, which pointed out lines within NO5 which are important for the power transfer through NO5 to be overloaded. However, one thing that seems inconsistent with current grid conditions is that this study finds the area around Stockholm and Uppsala and the area around Gothenburg suitable for both generation and load. This is not coherent with the current grid situation, as these are areas with known congestion. A possible explanation for this could be that these areas are areas with many connecting lines, the grid is meshed here. If hours are chosen that are not the worst case scenarios for these areas, this could instead mean that there is a lot of available capacity in the surrounding lines, meaning that it is possible to fit larger loads or generators. Or the reason for the congestion in the actual grid is not thermal, but rather due to other limitations like voltage or rotor angle stability.

Another thing that can be noticed is that in the north of Norway, there are no suitable buses for either generation or load. This is because in the low load - high wind condition, the NO4-SE1 connection was out of commission, which meant there is only one line feeding the area north of Ofoten (NO4). This line was very lightly loaded with a capacity of 2 300 MW in the base case scenario. Adding either a 2

500 MW load or generator makes this line overload in either case, making all buses in this area be disregarded as suitable.

6.3 Results from the ACCC Analysis on the 2045 Model

Sections 5.5.1-5.5.5 described how the 2045 cases were adapted to avoid overloading lines in N-0 conditions. In this section, it will be described how well these adapted models perform in N-1 conditions. As mentioned earlier, N-1 only refers to contingencies on branches. It has been identified that many issues with congestion occur in the 220 kV grid, which in some areas are about to be faced out apart from connecting generation to the 400 kV grid. Considering this, the ACCC and sensitivity studies on the 2045 grid will be performed with the 400 kV grid in focus.

The analyses were performed using the same method as in the 2020 cases. When performing the ACCC analyses, the grid after the necessary reinforcements described for each case is the grid being analyzed. The decision was made to prioritize the ACCC and sensitivity studies on Scenarios 2 and 3 and not perform it on Scenario 1, the small scale renewable scenario, because the expansion is limited in that scenario. Also, only a high load and wind case is investigated, which means that the results from a study on Scenario 1 would only be suitable in a high load, high wind case.

6.3.1 Case 2a: Fossil free - low wind

In Case 2a, the worst overloading during a contingency occurs between Loviseholm (SE3) and Halden (NO1), in the NO1-SE3 area. When any of the two parallel lines between these buses are out of service, the other one overloads with 437 MVA. The second worst contingency is in the same area, between Halden and Hasle (NO1), which results in an overload of 120 MVA. In addition to this, there are also overloads occurring between Ringhals (SE3) and Horred (SE3) when either of the parallel lines between these buses are disconnected. Apart from these instances, there is no other overloads in the 400 kV grid for this scenario.

In reality it would be reasonable to assume that areas around nuclear plants like Ringhals are dimensioned in such a way that overloads should not occur, even during contingencies. How this is mitigated is hard to find out based on open sources though, whether it is the connections or dispatches or similar.

6.3.2 Case 2b: Fossil free - high wind

In Case 2b, the worst overload occurred between Porjus (SE1) and Harspånget (SE1), which was a distance that was reinforced further due to overloading in this case. The overload occurred when either of the parallel lines was out of commission. The second worst overload occurred on the line between Ofoten (NO4) and Ritsem (SE1) when the line between Vitas (SE1) and Porjus was off. In this both of these

instances, the overloads occur on lines that transfer power to the loads located at the buses Ritsem and Vitas. The total load is 3 225 MW in this case, and only two transmission lines connect these buses.

There is also overloading on the lines from Djuptjärn (SE1) to Viitalajärvi (FI), the line between Högåsen (SE2) and Järpströmmen (SE2), and between Borgvik (SE3) and Hagfors (SE3).

6.3.3 Case 3a: Renewable - low wind

Case 3a performed well in N-1 conditions. There are only two parallel lines between Tegneby (NO1) and Hasle (NO1) which overload during N-1 conditions, which is when the other parallel line is not connected. An explanation to why there is less overloads in this scenario is because more flexibility in the electrolysis loads is assumed, reducing the need to use almost the full capacity of the hydro power in Norway to supply loads in Sweden and Finland. Hence there is a reduced need to transmit power, especially over the NO1-SE3 border.

6.3.4 Case 3b: Renewable - high wind

Focusing on the 400 kV grid regarding the overloads in Case 3b as well, there are comparatively many lines that overload in this case compared to the other cases. The overloads are mainly found in NO2 and NO5, as well as in SE1 and SE2. The worst overload occurs on the parallel lines between Arendal and Bamble in NO2 when either is off the other overloads with about 300 MVA. Furthermore, almost all overloads occur within bidding zones, only in one instance does the overload occur on a line crossing two bidding zones. This is the line between Stornorrfors (SE2) and Trolltjärn (SE1), which transmits a lot of offshore wind power from SE1 to SE2.

In Finland, some lines are close to overloading, these are lines in the north of Finland, leading to the interconnection to Sweden, and a line going from the Finnish west coast into the county (Seinäjoki-Alajärvi). In this area, some offshore wind were rearranged and spread out more evenly over buses along the coast.

6.3.5 Findings - all cases

Typical for all cases is that the overloads often occur on the lines added to make the N-0 cases not overload and between busses with parallel lines. Naturally, the lines added to avoid overloading were added as parallel lines, which, if the overload were high to begin with, was not enough to withstand N-1 conditions. In areas with a more meshed grid, overloads are quite unusual in N-1 conditions. However, the lines that do overload are often located close to the reinforced lines for each case.

6.4 Results from the Sensitivity Analysis on the 2045 Model

To investigate suitable placements for loads and generation in Scenarios 2 and 3, a similar approach as in the 2020 cases was used. However, to display the possible differences and similarities between the two scenarios, the matching of suitable buses was only done between the high and low wind cases in the same scenario. Moreover, the sensitivity analysis was only done on the 400 kV branches. The results from the sensitivity analyses are presented in Figures 6.2 and 6.3. These figures display the locations where load and generation of a specified size fit in the grid without overloading any line in either N-0 or N-1 conditions for Scenarios 2 and 3.

The sizes of the loads and generators was determined through trying different sizes and see how many buses were sorted as suitable after having compared the suitable buses between the cases for the same scenario. A size was chosen when approximately 10 buses were found suitable. The different sizes in the different cases could be an indication of how congested the grid in each scenario is.

In Scenario 2a, 2 000 MW load and 500 MW generation were tested, and from the figure, it is clear that the grid is very saturated in terms of generation since suitable spots are only available in the area in and around NO5, and this is limited to 500 MW. Loads also fit in this area, but there are also suitable spots in the southernmost area in NO2 and central Sweden, which fits loads of 2 000 MW.

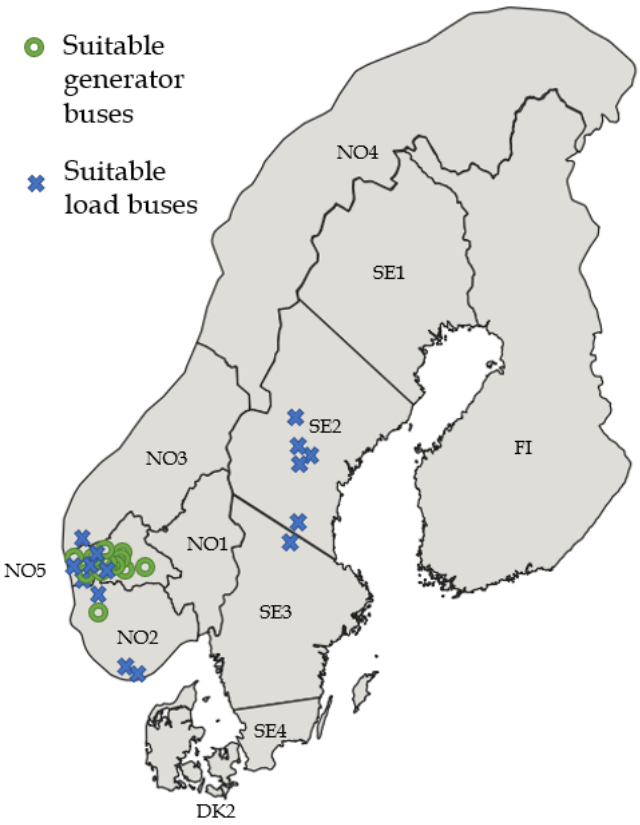

Figure 6.2: Suitable placements for 2 000 MW loads and 500 MW generation in Scenario 2 - fossil free

Figure 6.3 shows suitable placements for 2 000 MW loads and 1 000 MW generators in Scenario 3. Here the suitable load locations are concentrated to NO2 and NO5, with one exception in SE2, and the generator locations are concentrated to SE2 and SE3, with one exception in NO2.

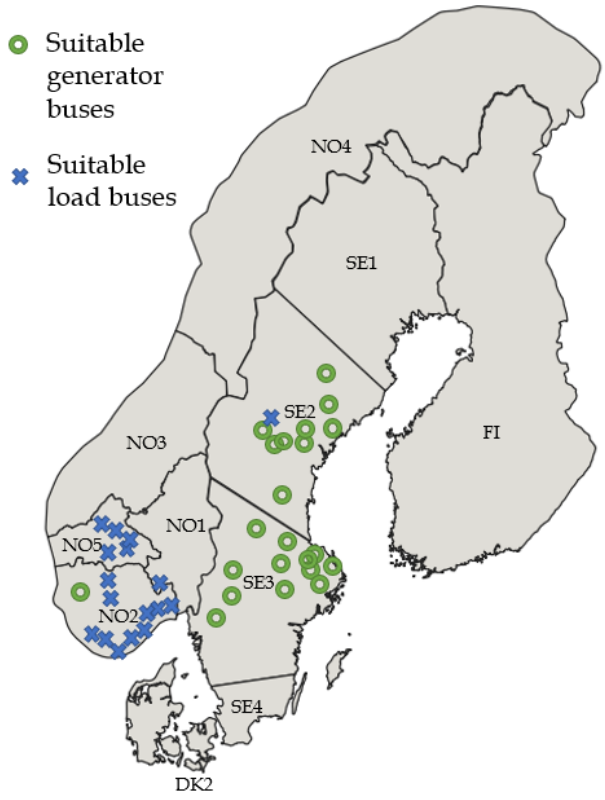

Figure 6.3: Suitable placements for 2 000 MW loads and 1 000 MW generation in Scenario 3 - electrification renewable

When comparing the results on the recommended load and generation locations from the 2020 cases presented in Figure 6.1 to the recommended load and generation locations in Scenario 2 and 3, the most apparent difference is that in the 2020 grid, there are more locations suitable for both large loads and generators, and the locations are more spread out. Especially in Scenario 2, the identified locations are concentrated to one area for load and generation. There are also no suggestions for adding loads or generators in the northernmost bidding zones or Finland. The difference in the sizes of loads/generators that can be added in the 2020 and 2045 model indicate that the 2045 grid is more congested than the 2020 grid.

7
Discussion

The previous chapters present the process of building, testing, and validating the different models. In Section 4.4.4, the results from the validation were interpreted, and it was concluded that the power flow was as expected at large but that the detail in the model was not perfect. Furthermore, the way the reactive power is handled in the model is not realistic, however, the method does provide insight into how the need for reactive power compensation could change in the future. In addition to this, patterns in the discrepancies of the flow identified in the 2020 model will be taken into consideration when discussing the 2045 flows. Much of the insecurities in the models are related to the placement and sizing of loads and generators as well, especially in the 2045 model. The fact that detailed grid plans for 2040 are not available yet also impacts how the results can be interpreted.

Two patterns were consistent in the 2020 model, first, there was an increased flow through Sweden compared to Norway, and a loop flow was observed in the NO1, NO2, and NO5 areas, shown in Section 4.4.3. With the changes implemented in the 2045 model, with even more lines being added through Sweden, the impedance is decreased further and could come to push even more flow through Sweden. Series compensation was observed to worsen the power flow accuracy, thus the removal of series compensation in the 2045 models might mitigate this source of error, but this is not verified due to the absence of data regarding future power flows.

7.1 Method of Validation

In Section 4.4 the methods used to validate accuracy of the 2020 model are explained. The validation process conducted for the 2020 model of the Nordic transmission grid in Section 4.4 aimed to evaluate its performance by comparing various key parameters against official data. The parameters considered in the validation included cross-border flows, installed line lengths, installed generational capacities, regional load distribution, and network topology.

The validation of cross-border flows against official data is crucial as it ensures that the model accurately represents the inter-area exchange of power between bidding zones. The model generally performs well in this area, but some errors persist. This could be due to inaccurate impedances, causing the flow to be pushed through transmission lines it is not supposed to. It could also be due to loads and generators

being aggregated in a way that is not a good equivalent representation of the system. Another possible source of inaccuracies is that data on unavailable lines could be missing, which could alter the flows negatively. Furthermore, despite efforts to obtain accurate and up-to-date official data, discrepancies, and errors might persist due to data collection or reporting issues.

The validation of the regional load distribution is generally positive, but it reveals some possible deficiencies in how the model aggregates generator and load units. The observed discrepancies in load distribution between regions suggest that the model does not fully capture the nuances of electricity demand within the regions of the Nordic power system. However, as mentioned in Section 4.4.2, the comparison of the load distribution in the model to official numbers is not optimal. The load distribution in the model is influenced by industrial activities and seasonal variations, among other things. Hence it is reasonable that it does not match up completely with the yearly load distribution. Furthermore, the data sample is too low to draw conclusions from since only 4 of the total 8 760 hours in a year have been modeled. It can be established that more data is needed, either from the model or more specific official load distribution data, to use this validation method efficiently.

7.2 Load and Generation Matching the 2045 Scenarios and Cases

To be able to discuss how well the generation and consumption match, the reasoning behind the choices made for these cases needs to be discussed first. There are endless possibilities on how to combine import and export, generation from different sources, and the distribution and size of loads for all scenarios. High and low wind cases were chosen because the availability of wind in the future will be crucial for the different scenarios.

It is important to consider that by assuming solar to produce at 20 % of capacity, the highs and lows of solar are not taken into account. If the power generated from solar would be zero, additional power would need to be produced or imported to supply the same load. Furthermore, in high wind scenarios, additional solar could increase the excess in power.

In considering future scenarios for the import and export of electricity, it has been assumed that neighboring countries can accommodate imports and provide export as needed. However, it is important to acknowledge certain issues with this assumption. For instance, it is important to recognize that if wind speeds are low in the Nordics, they are also likely to be low in neighboring countries. As a result, these countries may not have an excess of power available for export, and the opposite can be true in high wind cases. To address these complexities, different approaches have been used, aiming to achieve a reasonable equilibrium between wind generation, import and export, load sizing, and the flexibility of hydropower generation.

In situations of high wind, the Nordic region faces a surplus of electricity production, exceeding what can be consumed during normal load conditions. To address this, specific adjustments were made in the different cases. In Case 3b, the electrolysis loads were doubled, and industrial loads were increased by a factor of 1.2, in Case 1 the electrolysis loads set to 1.5 of the average load, and in Case 2b, the electrolysis load was only increased by a factor of 1.2, and an additional 7 GW load was introduced in Finland. Between the different scenarios, Scenario 3 was the scenario which needed the most flexibility from the electrolysis loads.

These modifications revealed important insights. In Cases 1 and 3b, where the electrolysis loads were significantly increased, the need for export was limited as these increased loads largely consumed the excess electricity. On the other hand, in Case 2b, where the increase in electrolysis load was comparatively smaller, the demand for export was much higher. Consequently, the interconnections with neighboring countries operated at close to maximum capacity to balance the system.

When comparing the scenarios with low wind conditions, Case 2a demonstrates that by operating hydro and nuclear power plants close to their maximum capacity, there is no necessity for power imports to meet the load requirements. Furthermore, electrolysis loads are not entirely removed in this scenario, implying that following a similar approach as in the other cases would even result in a surplus of power. However, it should be noted that this scenario heavily relies on nuclear and thermal power generation operating at high capacity, which leaves limited flexibility in the event of cloudy conditions, as hydropower is also operating at a high level of its capacity. On the other hand, in Case 3b, where hydropower is underutilized and thermal power is set at a relatively low level, there is a need for power imports. Nevertheless, leveraging the available hydropower could offset this import requirement, as it is not being fully utilized in this scenario.

Considering flexible loads, the assumption is that electrolysis loads are completely flexible between 0 - 200 % of the yearly average. No considerations have been made with regard to start-up time and duration of load operation in order to make it cost-efficient. For example, solar power is limited to certain hours, so if large loads are to be shifted to compensate for peak solar generation, it must be profitable to align with its intermittent pattern. The implications of load participation in flexibility markets are also worth considering, although beyond the scope of this report.

Overall, assuming that the electrolysis loads can be either reduced to zero or doubled, the matching of the generation and load works well in both high and low-wind scenarios. However, this requires high and low household and industry load scenarios to coincide with high and low wind scenarios, respectively, which may not be the case. For instance, on a cold calm winter day in the middle of the week, industry and household loads will likely not be at 80 % of the yearly average. More studies are needed to find out if the power available is enough to supply the demand. These studies find that there is some margin in the cases described in this report but do not investigate the worst-case scenarios.

By comparing the approaches in Scenario 2, where load reduction and adaptation of generated power were implemented, to those in Scenarios 1 and 3, where load reduction was the primary method of adaptation, it becomes evident that there is no single solution for balancing the system. However, the significance of having weather-independent power generation or large flexible loads is apparent across all cases. If electrolysis is considered a load that can be adjusted based on available power, it becomes a crucial source of load flexibility. For example, in Scenario 3, where the yearly energy requirement for electrolysis is estimated to be 253 TWh, assuming it operates 50 % of the time, the total installed capacity of electrolysis loads amounts to 58 GW. This is a substantial capacity, equivalent to the total installed hydropower capacity in the Nordics. This observation underscores the importance of incorporating such flexible loads into the system, as they can be turned on or off as needed to balance power supply and demand, contributing to a more resilient and adaptable energy system.

7.3 Grid Sufficiency in 2045

To start with, the 2045 model has a reduced need for reactive power transmission compared to actual conditions, which means that the lines are less loaded in the model than they would be in reality. The analysis reveals that overloads occur within the bidding zones where buses with few connections to the rest of the system are burdened with large loads or generation units. This becomes very apparent in SE1, around the Hybrit loads distributed over buses there. Furthermore, the lines from Porjus to Harspånget are almost always overloaded, and other lines in that area are too. Moreover, two areas that also suffer from overloads in most cases are the NO1-SE3 cross-border connection and the FI-SE1 cross-border connection.

The Nordic grid has limits on transfer capacity between bidding zones, as shown in Figure 2.1 in Section 2.1.1. However, in this report, the permitted inter-area flow is solely based on the thermal limits of the lines between bidding zones. Since the thermal limits of the lines between bidding zones are higher than the capacities displayed in Figure 2.1, these capacity limits are violated in several cases and scenarios, as can be seen in Section 5.5.1 through 5.5.5. This indicates that the grid's capacity can still be exceeded even though thermal limits are not exceeded. The studies have found an increasing need for transfer capacity over some bidding zones, even in terms of thermal capacity, which means that more reinforcements are likely needed due to reasons not investigated in this report.

One cause of the overloads in the NO1-SE3 area is likely due to Norway's extensive use for regulation purposes. The interconnectors and high hydro capacity mean that in situations where there is a power deficit, it is easy to increase the power from Norway. This power is primarily transmitted through the NO1-SE3 connection causing the lines in this area to overload. The same issue was found in the SE1-FI area. This indicates a need for further reinforcements in these two areas. Alternatively, the need for inter-area flow could be mitigated by further regulating the load and

generation within the bidding zones. Additional inter-area connections experiencing increasing flows have not been observed.

Svk's grid plans reveal few new lines planned in SE1, except for the Aurora line, which is a third transmission line between FI-SE1. Instead, multiple lines are planned between SE2-SE3. An interesting observation is that power flowing from SE2 to SE3 does not exceed 6 000 MW in any scenario. This raises questions about the necessity of additional lines, given that the current transmission capacity is 7 000 MW. If more loads are added in the north, potentially reducing the power surplus there, the need to transmit power from the north to the south could decrease. In the scenario with the SE2-SE3 flow, none of the twelve lines from SE2-SE3 are loaded more than 50 % during N-0 conditions.

Examining the variation in loading on lines surrounding the Hybrit and H2 Green Steel loads in Sweden and the increased loads in Finland is intriguing. In Finland, all load added in the 2045 scenarios was scaled, which means it was distributed over already existing loads. Additionally, the grid in Finland, particularly in the southern regions, is meshed and well interconnected, unlike the grid in SE1. Due to this, Finland experiences few instances of overloads, while in SE1, the lines connecting mining industry loads to the rest of the grid were frequently overloaded. It is worth mentioning that the mining industry loads were not added in optimal parts of the grid in SE1. Instead, they were placed near existing mines. It is reasonable to believe that in Finland and elsewhere, electrolysis loads will be placed in beneficial locations seen from a grid perspective. The same is most likely not possible for the Hybrit loads since they need to be situated close to the mines.

The simulation results identify certain areas as more sensitive than others, including the NO1-SE3 and FI-SE1 cross-border connections, as well as large loads in SE1. Generally, within bidding zones and countries, the grid appears well-equipped in terms of thermal capacity, with the exception of SE1, as long as offshore wind is placed near large loads and offshore wind farms are distributed across different buses. This distribution of offshore wind farms was primarily done in Norway, where the installed capacity in certain spots became too high to connect to one bus.

7.4 Changes in the Demand of Reactive Compensation

When constructing the future cases, all generators have been given infinite reactive power capability in order to control the voltage, as described in Section 5.6. This frees up transmission capacity in the transmission lines since all generator buses can maintain 1 p.u voltage without the need for imported reactive power. This increased transmission capacity can lead to lines being misrepresented as lightly loaded. However, the approach provides insight into the change in reactive power demand since the same approach is used in both models.

Similar trends were observed when comparing different scenarios in the 2020 and 2045 models. Both models found that the total demand for absorbed reactive power was relatively consistent across the cases, but comparing the 2020 cases to the 2045 cases, the 2045 cases had a slightly increased demand for absorbed reactive power. On the other hand, more significant variations were noted in the total injected reactive power among the different cases.

However, a contrasting pattern emerged when examining the total reactive power as a percentage of the total generated power. In this analysis, the injected power showed similarity between the scenarios, whereas considerable fluctuations were observed in the absorbed reactive power. Even though the total need for reactive power increases in the 2045 cases, the injected reactive power as a percentage of generated power does not increase significantly. A conclusion from this is that if future generators have the same reactive capability as today, about the same level of reactive power compensation in the grid today would be needed in the future as well.

What was found in Section 5.6.2 was that in many cases, more reactive compensation than what is available is needed at each bus. In normal operation, the need can, to some extent, be transferred from surrounding buses. Suppose it is a bus with little generation connected to it in an area with high generation. In that case, this need can most likely be compensated for if there is transmission capacity to transfer the reactive power. However, as can be seen in Tables 5.20 and 5.21, the exceeding need is quite high, sometimes in areas with little generation and heavily loaded lines. In these areas, it is reasonable to believe that reactive power compensators are needed in the future. An example of such an area is the NO1-SE3 area, whereas SE2 is an area with much generation, and it is reasonable to believe that the generators could be able to compensate for a lot of the exceeding reactive power needed at some buses there. Important to notice as well is that the grid code requirement on reactive power compensation capability is a minimum. It could be that the generators can compensate more than what is required, but since it cannot be demanded, it cannot be assumed.

Furthermore, in this report, the voltage has always been assumed to be 400 kV, but often the grid is run at a somewhat higher voltage, especially in the north. If this is possible to do in the future as well, this could make it possible to transmit more power with less current, reducing the voltage drop in heavily loaded areas. As this is not investigated in this report, no further conclusion can be drawn about this configuration. However, it would be interesting to compare the change in the need for reactive power if the voltage was increased.

7.5 The ACCC and Sensitivity Analysis

As previously mentioned, determining the accuracy of specific line loadings is challenging, and in future scenarios, assumptions were made regarding the distribution of loads and generators. However, this section will discuss the patterns observed in the findings. The results obtained from the ACCC analysis indicate that, in

most cases where the grid is not overloaded under normal conditions (N-0), there are fewer occurrences of overloads during contingencies (N-1). Initially, the decision was made to set the line rating in N-0 to 70 % of the maximum thermal capacity, allowing for contingencies and enabling the lines to operate at full capacity in N-1 conditions. It is difficult to determine whether this approach was effective or not, but it demonstrated that despite some overloads, the majority of lines did not experience overloading during contingencies. The lines that did become overloaded were primarily heavily loaded parallel lines. To avoid overloads during contingencies, 50 % of their capacity would need to be available in N-0 conditions, if they should be able to withstand the increased loading from the other parallel line during a contingency. Achieving a balance between redundancy and cost in these cases necessitates careful consideration.

An important difference between the ACCC results in 2020 and 2045 is the increased occurrence of overloads in the 2045 grid. Additionally, in the heavily loaded scenarios in 2020 the winter line ratings were used, while the summer line ratings were used throughout all 2045 cases.

In summary, the analysis indicates that maintaining a balance between line redundancy and cost is crucial, considering the occurrence of overloads in parallel lines during contingencies. The comparison between the 2020 and 2045 ACCC results highlights the higher frequency of overloads in the 2045 grid and the lower line ratings in the heavily loaded scenarios compared to 2020.

The presence of increased overloads in the 2045 grid had significant implications for the results obtained from the sensitivity analysis. In comparison to the 2020 grid, there was a significant reduction in the size of loads and generators that could fit in the grid in the 2045 cases, as shown in Figures 6.1-6.3. Considering the knowledge we have about the congested nature of the 2020 grid, where both generation and load connection requests are denied, the discovery of good locations to add 2.5 GW loads and generators in the 2020 cases suggests that the limiting factor for load connections is not solely the thermal limits. This suggests that other issues related to power system stability come into play, such as voltage stability and system stability under dynamic conditions. Alternatively, it indicates that the thermal ratings used in the model are overestimated.

These results indicate that despite the perception of the 2045 grid being well-equipped, additional capacity is likely required to accommodate all the stability requirements in the grid. Therefore, the 2045 grid, despite its apparent adequacy in this report, likely faces challenges in meeting stability demands, highlighting the need for further measures to ensure a robust and stable power system.

Lastly, one can assume bottlenecks by comparing the suitable locations presented in Figures 6.1 to 6.3. These are consistent with the results from the ACCC analysis. Moreover, a clear alignment is visible when comparing the suitable locations for generation in the 2020 model with the chosen location of new onshore and offshore

wind and solar plants. This, at least to some degree, validates the chosen process for placement of new generation in the 2045 model.

7.6 Ethics

While the method of the project itself does not give rise to immediate ethical concerns, it is important to address ethical considerations about the project's objectives. The confidentiality of the grid models held by the TSOs is crucial due to the critical nature of the grid infrastructure. Creating a model that identifies potential weaknesses in the grid could expose security risks for the Nordic countries. However, it is worth noting that the project relies on open sources, often published by the TSOs themselves. Because of this, it is reasonable to assume that a security assessment has been conducted before the publication of this information. Consequently, utilizing such publicly available information should not raise significant ethical concerns.

7.7 Sustainability

Through modeling the current and future Nordic transmission grid, this report evaluates the integration of renewable energy sources on a large scale. By gaining insights into this transition, renewable energy can be integrated into the Nordic grid in a smooth and efficient way, and, as a consequence, the reliance on fossil fuels can be reduced. Furthermore, this report has aimed to identify potential inefficiencies and vulnerabilities within the Nordic grid. By using this information, energy losses can be reduced, resulting in improved system efficiency. Additionally, by strengthening the resilience of the grid, the reliability of energy transmission can be increased and the risk of disruptions can be reduced.

8
Conclusions

This report presents the creation and projection of a model of the Nordic transmission grid for the years 2020 and 2045. The 2020 model underwent verification through various methods and demonstrated accuracy regarding power flow at the bidding zone level. Although, due to a lack of data to input and validate against on a regional level, these results were interpreted with caution. The limitations on the model's accuracy primarily stem from generalizations used in the model due to a lack of open-source data. Despite this, the model is a good representation of the general conditions in the 2020 grid. Hence, it was a good foundation when developing the 2045 grid model. It also served as a benchmark when comparing the results between the two grid models.

In the 2045 model, the 2020 model was updated based on the ten-year development plans published by the TSOs. It was also the TSOs' own generation and load projections for 2045 that were used to create the simulated scenarios in this report. Due to the nature of long-term projections, the 2045 model relied heavily on assumptions. Overall, the updated grid in the 2045 model demonstrated effective handling of load and generation scenarios after adding some limited reinforcements. Two bottlenecks were observed in several scenarios, the first being the interconnection between NO1-SE3 and the second SE1-FI.

Furthermore, it was found that a high level of load flexibility is required in the future due to the intermittent nature of the power generation mix in 2045. This flexibility is essential to avoid the overloading of lines and to ensure that the load matches the demand rather than the other way around, which is the common practice today. Important to take into consideration is that these findings are related to the thermal capacity. Combing these results with the results of the sensitivity analysis, and knowledge of the state of the grid today, the grid plans may not be as sufficient as they seem when only considering thermal limits.

The cross-border flows of the future cases and scenarios provided interesting information when compared to the 2020 scenarios. In the 2020 scenarios, the absence of heavy loads in the north, together with the significant hydro capacity in SE1 and SE2, prompted a substantial north-to-south power flow within Sweden. However, in 2045, heavy industrial loads in SE1 alter the general flow patterns, and an active power flow from SE2 to SE1 occurs in some instances.

Finally, the reactive compensation required in the future exhibits similar patterns

to the 2020 conditions. However, there are notable changes in the locations where the highest demand for injected reactive power is observed, with a comparatively greater need at specific bus locations.

8.1 Future Work

This thesis primarily examines the balance between generation and load in future scenarios and its impact on line loading. However, due to limited data on grid configuration, several assumptions and generalizations were necessary for the analysis.

To determine whether the 2045 grid is adequately prepared for the various scenarios, additional factors must be considered beyond the scope of this thesis. This includes conducting dynamic simulations to investigate the stability of voltage, frequency, and rotor angles. Additionally, further investigation could be undertaken to analyze the technical characteristics of the loads and generators that will be integrated into the future grid, along with their impact on the overall grid performance. Running the model using a higher voltage, for instance, 420 kV, and studying the loading of the lines and the reactive power need could also be interesting in order to investigate other solutions than more equipment in the grid to mitigate overload and voltage issues. Furthermore, performing cost benefit analyses on the planned grid reinforcements with the future scenarios would also be interesting.

Moreover, in this report matching generation and load was done purely based on installed capacity and active power input and output. Therefore, the economic aspects and dispatch management have yet to be investigated or discussed but are essential to consider. It would also be beneficial to study what is needed and what is possible when installing electrolysis loads. How can they be run in a way that is both profitable for the owner and beneficial from a grid perspective? What level of flexibility is needed from this type of load, what is technically possible, and how can this be combined in the best way? What are the longest continuous period industries and electrolysis loads can be either working on low or full capacity?

Regarding the 2020 model, it was only tested for four different time stamps. It would be intriguing to assess the model's accuracy by conducting a time series simulation to evaluate its performance over an extended duration. Improvements on the 2020 model could also be performed with a less standardized approach and using local sources instead of the sources that the PyPSA-eur model uses, better accuracy in the model could be achieved.

References

[1] Energimyndigheten, *Det klimatpolitiska ramverket — energimyndigheten.se*, https://www.energimyndigheten.se/klimat--miljo/sveriges-energi--och-klimatmal/det-klimatpolitiska-ramverket/, [Accessed 24-1-2023], 2022.

[2] Svenska kraftnät, *Systemutvecklingsplan 2022-2031*, https://www.svk.se/siteassets/om-oss/rapporter/2021/svk_systemutvecklingsplan_2022-2031.pdf, [Accessed: 24-1-2023], 2021.

[3] Statnett, *Long-term market analysis 2020-2050*, https://www.statnett.no/globalassets/for-aktorer-i-kraftsystemet/planer-og-analyser/lma/lma-update-2021.pdf, [Accessed: 27-1-2023], 2021.

[4] Fingrid, *Fingrid's electricity system vision 2022 - draft scenarios for the future electricity system*, https://www.fingrid.fi/globalassets/dokumentit/en/news/fingrid_electricity_system_draft_scenarios.pdf, [Accessed: 27-1-2023], 2022.

[5] Energinet, *Energinets lanfsigtitede udviklinsplan 2022*, https://energinet.dk/media/jjil5e23/energinets-langsigtede-udviklingsplan-2022-8423930_1_1.pdf, [Accessed 27-Jan-2023], 2022.

[6] Svenska kraftnät, *Kraftbalansen på den svenska elmarknaden - rapport 2022*, https://www.svk.se/siteassets/om-oss/rapporter/2022/kraftbalansen-pa-den-svenska-elmarknaden-rapport-2022.pdf, [Accessed: 19-5-2023].

[7] Statnett, *Long-term Market Analysis 2020-2050 - Update Spring 2021*, 2021. [Online]. Available: https://www.statnett.no/globalassets/for-aktorer-i-kraftsystemet/planer-og-analyser/lma/lma-update-2021.pdf.

[8] ENTSO-E, *Entso-e transparency platform*, https://transparency.entsoe.eu/dashboard/show, [Accessed: 17-3-2023].

[9] Svenska kraftnät, *Kraftbalansen på den svenska elmarknaden - rapport 2022*, https://www.svk.se/siteassets/om-oss/rapporter/2022/kraftbalansen-pa-den-svenska-elmarknaden-rapport-2022.pdf, [Accessed: 17-3-2023].

[10] Svenska kraftnät, *Kraftbalansen på den svenska elmarknaden - rapport 2020*, https://www.svk.se/siteassets/om-oss/rapporter/2020/kraftbalansen-pa-den-svenska-elmarknaden-rapport-2020.pdf, [Accessed: 17-3-2023].

[11] Nordenergi, *Study on opportunities and barriers to electrification in the Nordic region*, Accessed Feb. 7, 2023. [Online]. Available: https://www.energiforetagen.se/globalassets/dokument/nordenergi/electrification-in-the-nordics---nordenergi_19_05_2021.pdf.

[12] Energinet, *Langsiktet netstruktur for eltranmissonsnettet*, https://energinet.dk/media/cpmdxbuv/langsigtet-netstruktur-for-eltransmissionsnettet-2021.pdf, [Accessed: 19-4-2023].

[13] Statnett, *Nettutviklinsplan 2021*, https://www.statnett.no/for-aktorer-i-kraftbransjen/planer-og-analyser/nettutviklings-og-investeringsplan/, [Accessed: 14-3-2023], 2021.

[14] Svenska kraftnät, *Långsiktig marknadsanalys 2021*, Svk2019/3305 Verison 1.0. [Online]. Available: https://www.svk.se/siteassets/om-oss/rapporter/2021/langsiktig-marknadsanalys-2021.pdf.

[15] SR, *Grafik: Så länge håller de svenska kärnkraftverken*, https://sverigesradio.se/artikel/6080442, [Accessed: 10-5-2023].

[16] Nordpool, *Principles for determining the transfer capacity in the nordic power market*, https://www.nordpoolgroup.com/4aad73/globalassets/download-center/tso/principles-for-determining-the-transfer-capacities_2020-09-22.pdf, [Accessed: 22-5-2023].

[17] EU, *Kommissionens förordning (eu) 2017/1485: Artikel 35: Hantering av oförutsatta händelser*, https://eur-lex.europa.eu/legal-content/SV/TXT/HTML/?uri=CELEX:02017R1485-20210315&from=EN#tocId107, [Accessed: 10-5-2023].

[18] M. Ovaere **and** S. Proost, "Optimal electricity transmission reliability: Going beyond the n-1 criterion," *The Energy Journal*, **jourvol** 39, **october** 2018. DOI: 10.5547/01956574.39.4.mova.

[19] Svenska kraftnät, *Om elmrknaden*, https://www.svk.se/om-kraftsystemet/om-elmarknaden/, [Accessed: 9-5-2023].

[20] Svenska kraftnät, *Stödtjänster och avhjälpande åtgärder i ett energisystem under förändring*, https://www.svk.se/siteassets/om-oss/rapporter/2021/rapport-regeringsuppdrag-avseende-stodtjanster_211018_.pdf, [Accessed: 24-3-2023].

[21] J. Hörsch, F. Hofmann, D. Schlachtberger **and** T. Brown, "PyPSA-eur: An open optimisation model of the european transmission system," *Energy Strategy Reviews*, **jourvol** 22, **pages** 207–215, **november** 2018. DOI: 10.1016/j.esr.2018.08.012. [Online]. Available: https://doi.org/10.1016%2Fj.esr.2018.08.012.

[22] N. Brekelmans, *Nordic transmission grid model based on open sources*, 2023.

[23] Zenodo, *Gridkit extract of entso-e interactive map*, https://doi.org/10.5281/zenodo.55853, [Accessed: 22-5-2023].

[24] F. Gotzens, H. Heinrichs, J. Hörsch **and** F. Hofmann, "Performing energy modelling exercises in a transparent way - the issue of data quality in power plant databases," *Energy Strategy Reviews*, **jourvol** 23, **pages** 1–12, 2019, ISSN: 2211-467X. DOI: https://doi.org/10.1016/j.esr.2018.11.004. [Online]. Available: https://www.sciencedirect.com/science/article/pii/S2211467X18301056.

[25] O. P. S. Data, *Data platform - time series*. DOI: https://doi.org/10.25832/time_series/2020-10-06.

[26] F. Aurenhammer, R. Klein **and** D.-T. Lee, *Voronoi Diagrams and Delaunay Triangulations*, 1st. USA: World Scientific Publishing Co., Inc., 2013, ISBN: 9789814447638.

[27] Wikipedia, the free encyclopedia, *Voronoi diagram*, [Online; accessed March 8, 2023], 2023. [Online]. Available: https://en.wikipedia.org/wiki/Voronoi_diagram#/media/File:Euclidean_Voronoi_diagram.svg.

[28] ENTSO-E, *Interconnected network of northern europe*, https://eepublicdownloads.entsoe.eu/clean-documents/Publications/maps/2019/Map_Northern-Europe-3.000.000.pdf, [Accessed: 5-4-2023].

[29] Jul. 2021. [Online]. Available: https://www.svk.se/utveckling-av-kraftsystemet/transmissionsnatet/avslutade-transmissionsnatsprojekt/sydvastlanken/byggnation/sydvastlankens-likstromsforbindelse-ar-nu-i-drift-och-en-del-av-transmissionsnatet/.

[30] *Openinfra*, https://openinframap.org/#4.69/59.99/21.79/L,P,S, [Accessed: 20-4-2023].

[31] Statnett, *Her er våre prosjekter*, https://www.statnett.no/vare-prosjekter/, [Accessed: 14-3-2023].

[32] Svenska kraftnät, *Overhead transmission lines, technical guideline*, [Accessed: 14-3-2023], 2020.

[33] amokabel, *Characteristics of aluminium conductors steel reinforced used in norway - type al1/st1a according to en50182*, https://www.onninen.no/amokabel-feral-380-grackle-amo-kraft/p/GCS456, [Accessed: 14-3-2023].

[34] Statnett, *High voltage installations - guide for work in electromagnetic fields*, [Accessed: 14-3-2023].

[35] H. Saadat, *Power system analysis.* PSA Publishing, 2010, ISBN: 9780984543861. [Online]. Available: https://search.ebscohost.com/login.aspx?direct=true&db=cat09075a&AN=clpc.oai.edge.chalmers.folio.ebsco.com.fs00001000.3b1235ca.cd7e.48b8.901e.b6842113772a&site=eds-live&scope=site&authtype=guest&custid=s3911979&groupid=main&profile=eds.

[36] "Ieee standard for calculating the current-temperature relationship of bare overhead conductors," *IEEE Std 738-2012 (Revision of IEEE Std 738-2006 - Incorporates IEEE Std 738-2012 Cor 1-2013)*, **pages** 1–72, 2013. DOI: 10.1109/IEEESTD.2013.6692858.

[37] S. Arnborg, *Reaktivt effektutbyte.* https://www.svk.se/siteassets/om-oss/organisation/vara-rad/planeringsradet/arkiverat/bilaga-1-reaktivt-effektutbyte.pdf, [Accessed 10-Mar-2023], 2014.

[38] Mimer, Svenska krafnät, *Produktionsstatistik*, [Online; accessed March 8, 2023]. [Online]. Available: https://mimer.svk.se/ProductionConsumption/ProductionIndex.

[39] A. V. Nilsson **and** H. B. Robles, "Energimarknadsinspektionens föreskrifter om fastställande av generellt tillämpliga krav för nätanslutning av generatorer," **page** 9, 2018.

[40] L. Kuhlin, *Info om svensk vattenkraft.* [Online]. Available: https://vattenkraft.info/.

[41] Energimyndigheten, *Vindbrukskollens karttjänst*, https://www.energimyndigheten.se/fornybart/vindkraft/vindlov/vindbrukskollen/, [Accessed: 15-5-2023].

[42] NVE, *Finn vindkraftverk i kart*, https://www.nve.no/energi/energisystem/vindkraft/kart/, [Accessed: 15-5-2023].

[43] Wikipedia, the free encyclopedia, *Kategori:varmekraftverk i danmark*, [Accessed: 15-4-2023]. [Online]. Available: https://no.wikipedia.org/wiki/Kategori:Varmekraftverk_i_Danmark.

[44] Wikipedia, the free encyclopedia, *Kategori:varmekraftverk i danmark*, [Accessed: 15-4-2023]. [Online]. Available: https://sv.wikipedia.org/wiki/Kategori:Kraftv%5C%C3%5C%A4rmeverk_i_Sverige.

[45] Energimarknadsinspektionen, *Standardkostnader regionnätet*, [Accessed: 6-Mar-2023], 2009. [Online]. Available: https://www.ei.se/download/18.4306b017176842faf913a9
1610530575721/Standardkostnader-Regionn%C3%A4tet.pdf.

[46] H. Energy, *Seriekompensering. sätter turbo på kraftledningen*, https://www.hitachienergy.com/se/sv/about-us/pioneering-technologies/sa-funkar-det/seriekompensering, [Accessed: 17-4-2023].

[47] Nordpool, *Exchange no4-ru*, https://www.nordpoolgroup.com/en/Market-data1/Power-system-data/Exchange1/NO/Hourly1/?dd=NO%20-%20RU&view=table, [Accessed: 20-4-2023].

[48] Statnett, *Data from the power system*, https://www.statnett.no/en/for-stakeholders-in-the-power-industry/data-from-the-power-system/import-and-export, [Accessed: 14-3-2023].

[49] Svenska kraftnät, *Map of the national grid*, https://www.svk.se/en/national-grid/map-of-the-national-grid/, [Accessed: 15-3-2023].

[50] Energifaktanorge, *The electricity grid*, https://energifaktanorge.no/en/norsk-energiforsyning/kraftnett/#:~:text=In%20Norway%2C%20Statnett%20is%20the%20designated%20transmission%20system,the%20transmission%20grid%20is%20about%2011%20000%20km., [Accessed: 15-3-2023].

[51] FINGRID, *Electricty system of finland*, https://www.fingrid.fi/en/grid/power-transmission/electricity-system-of-finland/, [Accessed: 15-3-2023].

[52] *Öppna geodata för regionala statistikområden (regso)*. [Online]. Available: https://www.scb.se/vara-tjanster/oppna-data/oppna-geodata/regso/.

[53] *Administrative enheter fylker*. [Online]. Available: https://kartkatalog.geonorge.no/metadata/administrative-units-counties/6093c8a8-fa80-11e6-bc64-92361f002671.

[54] *The regions of finland 2021 with the 2018 regional codes - esri shapefile*. [Online]. Available: https://www.avoindata.fi/data/en_GB/dataset/suomen-maakunnat-2021-vuoden-2018-maakuntakoodeilla/resource/3c2a8036-e774-458a-810a-2c1fc0f80d5f.

[55] *Slutanvändning (mwh), efter län och kommun, förbrukarkategori samt bränsletyp. år 2009 - 2021.* [Online]. Available: https://www.statistikdatabasen.scb.se/pxweb/sv/ssd/START__EN__EN0203__EN0203A/SlutAnvSektor/.

[56] *10314: Net consumption of electricity, by consumer group (gwh) (m) 2010 - 2021. statbank norway*, Jun. 2022. [Online]. Available: https://www.ssb.no/en/statbank/table/10314/.

[57] *Sähkönkäyttö maakunnittain 2007-2021.* [Online]. Available: https://energia.fi/uutishuone/materiaalipankki/sahkonkaytto_maakunnittain_2007-2021.html#material-view.

[58] NUCS, *Unavailable capacity*, https://www.nucs.net/outage-domain/unavailability-messages/show, [Accessed: 15-3-2023].

[59] Statnett, *Forbrukningsutvikling i norge 2022-2050 - delrapport till lma 2022-2050*, https://www.statnett.no/for-aktorer-i-kraftbransjen/planer-og-analyser/langsiktig-markedsanalyse/, [Accessed: 20-3-2023].

[60] Statnett, *Forbruk, havvind og nett på sør og østlandet*, , [Accessed: 20-3-2023].

[61] Equinor, *Equinor and partners consider 1 gw offshore wind farm off the coast of western norway*, https://www.equinor.com/news/20220617-considering-1gw-offshore-wind-farm-off-western-norway, [Accessed: 22-3-2023].

[62] Energistyrelsen, *Analyseforudsætninger til energinet 2022 - datasaet*, https://ens.dk/service/fremskrivninger-analyser-modeller/analyseforudsaetninger-til-energinet, [Accessed: 17-4-2023].

[63] Energinet, *Muligt-net-2040*, https://energinet.dk/media/0tlmje3a/muligt-net-2040.pdf, [Accessed: 19-4-2023].

[64] Fingrid, *Main grid development plan 2022-2031*, https://www.fingrid.fi/globalassets/dokumentit/en/customers/grid-connection/fingrid-main-grid-development-plan-2022-2031.pdf, [Accessed: 19-4-2023].

[65] Fingrid, *Electricity system vision 2023*, https://www.fingrid.fi/globalassets/dokumentit/en/news/electricity-market/2023/fingrid_electricity_system_vision_2023.pdf, [Accessed: 20-4-2023].

[66] Svenska Kraftnät, *Investeringspaketet nordsyd*, https://www.svk.se/contentassets/c174001439e04e6eb8485f1f16471e9f/svenska-kraftnats-investeringspaket-nordsyd.pdf?_t_id=qWowEhUA1rBRRNtzXdqH-w%3d%3d&_t_uuid=DGLSPCJfT7ia9P7-QapvJw&_t_q=nordsyd&_t_tags=siteid%3a40c776fe-7e5c-4838-841c-63d91e5a03c9%2clanguage%3asv%2candquerymatch&_t_hit.id=SVK_

WebUI_Models_Media_OfficeDocument/_a4f64553-3739-4195-90bf-af3797f9ff5f&_t_hit.pos=2, [Accessed: 20-4-2023].

[67] Finnish Wind Power Association, *Wind power projects in finland*, https://tuulivoimayhdistys.fi/en/wind-power-in-finland/map, [Accessed: 15-5-2023].

[68] J. Wickström, "Så påverkas boden av det gröna stålet," *Tidningen Energi*, **april** 2021. [Online]. Available: https://www.energi.se/artiklar/2021/april-2021/sa-paverkas-boden-av-det-grona-stalet/#:~:text=H2%5C%20Green%5C%20Steel%5C%20ska%5C%20bygga%5C%20en%5C%20v%5C%C3%5C%A4tgasfabrik%5C%20med,%5C%28motsvarande%5C%20knappt%5C%20tio%5C%20procent%5C%20av%5C%20dagens%5C%20svenska%5C%20elanv%5C%C3%5C%A4ndning%5C%29..

[69] Northvolt, *Europe's first homegrown gigafactory*, https://northvolt.com/manufacturing/ett/, [Accessed: 15-5-2023].

[70] Hybrit, *Lkab and vattenfall building unique pilot project in luleå for large-scale hydrogen storage investing a quarter of a billion swedish kronor*, https://www.hybritdevelopment.se/en/april-7-2021-hybrit-ssab-lkab-and-vattenfall-building-unique-pilot-project-in-lulea-for-large-scale-hydrogen-storage-investing-a-quarter-of-a-billion-swedish-kronor/#:~:text=Fossil-free%20iron%20and%20steel%20production%20using%20HYBRIT%20technology%2C,per%20year%20%28including%20the%20majority%20of%20SSAB%E2%80%99s%20needs%29., [Accessed: 15-5-2023].

[71] M. Törnwall, "Nya batterifabriken kan driva upp svenskt elpris," *Svenska Dagbladet*, **april** 2022, [Accessed: 15-5-2023]. [Online]. Available: https://esvd.svd.se/p/naringsliv/2022-02-05/a/nya-batterifabriken-kan-driva-upp-svenskt-elpris/1003/494259/26100005.

[72] I. E. Haukeli, A. Stavseng, D. Spilde *et al.* NVE, 2020. [Online]. Available: https://publikasjoner.nve.no/rapport/2020/rapport2020_36.pdf.

[73] NVE, *Vannkrafdatabase*, https://www.nve.no/energi/energisystem/vannkraft/vannkraftdatabase/, [Accessed: 20-4-2023].

A

Appendix A - Calculations of the Current Ratings of the Transmission Lines

The convection heat loss rate per unit length is calculated in Equation A.1. The quantity is calculated in two different ways, q_{c1} and q_{c2}. They are both valid, but according to IEEE [36] it is recommended to set the largest of the two equal to q_c.

$$\begin{aligned} q_{c1} &= K_{angle} \cdot (1.01 + 1.35 \cdot N_{Re}^{0.52}) \cdot k_f \cdot (T_s - T_a) \\ q_{c2} &= K_{angle} \cdot 0.754 \cdot N_{Re}^{0.6} \cdot k_f \cdot (T_s - T_a) \end{aligned} \tag{A.1}$$

The magnitude of convective heat loss is a function of the Reynolds number, which is dimensionless. This quantity is shown in Equation A.2, where D_0, ρ_f, V_w, and μ_f corresponds to the outside diameter of the conductor, the density of air, the speed of the air stream at the conductor, and the absolute viscosity of air respectively.

$$N_{Re} = \frac{D_0 \cdot \rho_f \cdot V_w}{\mu_f} \tag{A.2}$$

In Equation A.3, the wind direction factor is calculated, where ϕ is the angle between the wind direction and the conductor axis. In this project, this angle has been approximated as 90°, which makes the wind correction factor equal to 1.

$$K_{angle} = 1.194 - \cos(\phi) + 0.194 \cdot \cos(2\phi) + 0.368 \cdot \sin(2\phi) \tag{A.3}$$

Equation A.4 presents the equation for determining the rate of radiated heat loss per unit length. In this equation, the variables ϵ, T_s, and T_a represent the emission coefficient, construction temperature, and ambient temperature of the cable, respectively.

$$q_r = 17.8 \cdot D_0 \cdot \epsilon \cdot ((\frac{T_s + 273}{100})^4) - (\frac{T_a + 273}{100})^4) \tag{A.4}$$

The heat gain rate from the sun per unit length is calculated using Equation A.5, where α, Q_{se}, θ, and A' correspond to the absorption coefficient of the cable, the total solar and sky radiated heat intensity corrected for elevation, the effective angle of incidence of the sun's rays, and the area of the conductor, respectively.

$$q_s = \alpha \cdot Q_{se} \cdot \sin(\theta) \cdot A' \tag{A.5}$$

To calculate θ, the Equation shown in A.6 was used. In this equation, H_c represents the solar altitude of the sun, Z_c represents the solar azimuth, and Z_1 represents the line azimuth.

$$\theta = \arccos\left(\cos\left(H_c\right) \cdot \cos\left(Z_c - Z_1\right)\right) \tag{A.6}$$

The solar altitude of the sun is calculated in Equation A.7, where Lat is the latitude of the line, δ is the solar declination, and ω is hour angle relative to noon.

$$H_c = \arcsin\left(\cos\left(Lat\right) \cdot \cos\left(\delta\right) \cdot \cos\left(\omega\right) + \sin\left(Lat\right) \cdot \sin\left(\delta\right)\right) \tag{A.7}$$

The solar declination δ is calculated in Equation A.8, where N is the day of the year (June 10 = Day 161 etc.).

$$\delta = 23.46 \sin\left(\frac{284 + N}{365} \cdot 360\right) \tag{A.8}$$

The solar azimuth is calculated in Equation A.9, C is 180 in degrees or π in radians depending on the unit of χ, which is the solar azimuth variable.

$$Z_c = C + \arctan\left(\chi\right) \tag{A.9}$$

The solar azimuth variable is calculated in Equation A.10.

$$\chi = \frac{\sin\left(\omega\right)}{\sin\left(Lat\right) \cdot \cos\left(\omega\right) - \cos\left(Lat\right) \cdot \tan\left(\delta\right)} \tag{A.10}$$

In Table A.1, the constants used in the calculation of the current-temperature relationship are displayed, these were used to obtain the relationships displayed in Figure 3.2.

Table A.1: Constants used in the calculation of current ratings of lines.

Symbol	**Value used**	**Unit**
K_{angle}	1	-
N	161	-
Lat	60	Degrees
Q_{se}	950	W/m^2
T_s	50	°C
T_a	20	°C
V_w	0.6	m/s
Z_1	90	Degrees
α	0.5	-
ϵ	0.5	-
ρ_f	1.2046	kg/m^3
μ_f	$2.043{\cdot}10^{-5}$	kg/m-s
ω	-15	Degrees

B

Appendix B - Injected and Absorbed Reactive Power per Bidding Zone

Table B.1: Induced and consumed reactive power, as well as the generated and consumed active power in each bidding zone in the high load - high wind case in 2020.

hl_hw	DK2	FI	NO1	NO2	NO3	NO4	NO5	SE1	SE2	SE3	SE4	Total	% of P_gen
$Q_{absorbed}$ [Mvar]	-324.8	-1 962.5	-761.9	-761.9	-557.3	-709.1	-491.1	-985.3	-2 355.6	-1 638.5	-52	-10 600	-19.9
Q induced [Mvar]	78	269.8	412.1	412.1	52.7	46.7	273.1	40.3	703.4	654.8	574.8	3 517.8	6.6
P_gen [MW]	1 664	9 050.8	2 120.2	7 423.4	2 950	2 672.1	2 922.6	3 045.3	8 412.6	11 021.1	1 913.1	53 195.2	
Load [MW]	1 896	10 536	5 187	4 697	3 719	2 723	2 237	1 312	2 004	11 341	3 300	48 952	

Table B.2: Induced and consumed reactive power, as well as the generated and consumed active power in each bidding zone in the high load - low wind case in 2020.

hl_hw	DK2	FI	NO1	NO2	NO3	NO4	NO5	SE1	SE2	SE3	SE4	Total	% of P_gen
$Q_{absorbed}$ [Mvar]	-283.1	-2 518.1	-464.8	-464.8	-438.5	-670.3	-288.2	-900.8	-1 143.9	-733.6	-75.2	-7 981.3	-13.9
Q induced [Mvar]	86.5	160.2	746.5	746.5	185	58.2	697.2	24.6	1 043.3	2 336.7	491.2	6 575.9	11.5
P_gen [MW]	1 099	10 235.7	2 513.1	8 598.9	3 919.4	4 399.9	4 118.8	4 053.7	7 407.7	10 086.9	799.1	57 232.2	
Load [MW]	2 003	11 524	6 143	5 475	3 991	2 774	2 219	1 377	1 818	13 335	3 755	54 414	

Table B.3: Induced and consumed reactive power, as well as the generated and consumed active power in each bidding zone in the low load - high wind case in 2020.

ll_hw	DK2	FI	NO1	NO2	NO3	NO4	NO5	SE1	SE2	SE3	SE4	Total	% of P_gen
$Q_{absorbed}$ [Mvar]	-282.5	-3 110.7	-528.6	-528.6	-626.4	-762.8	-352.1	-991.4	-1 881.6	-2 177.7	-259.8	-11 502.2	-32.8
Q induced [Mvar]	43.2	79.2	608.3	608.3	66.1	24.5	376.9	20.1	3.2	169.6	128.6	2128	6.1
P_gen [MW]	824.1	5 899.3	946	4 250.4	2 393.7	2 308	3 641.6	2 200.9	4 007.3	7 692	892.6	35 055.9	
Load [MW]	1 035	7 178	2 614	3 398	2 470	1 744	1 513	927	1 129	7 202	1 704	30 914	

Table B.4: Induced and consumed reactive power, as well as the generated and consumed active power in each bidding zone in the low load - low wind case in 2020.

ll_lw	DK2	FI	NO1	NO2	NO3	NO4	NO5	SE1	SE2	SE3	SE4	Total	% of P_gen
$Q_{absorbed}$ [Mvar]	-235.1	-2 314.8	-679.2	-679.2	-684.2	-806.9	-450	-787.9	-1 262.5	-1 182.8	-120.4	-9 203	-27.3
Q induced [Mvar]	51.9	154.8	373.1	373.1	33.7	7.0	266.4	55.6	640.4	390.1	297.4	2 643.5	7.8
P_gen [MW]	296.2	5 407.9	2 185	4 060.8	2 734.3	2 764	2 700.8	2 857.4	4 923.7	5 535.0	292.4	33 757.5	
Load [MW]	1 142	6 947	2 064	3 048	2 209	1 743	1 422	863	1 068	5 961	1 606	28 073	

Table B.5: Induced and consumed reactive power, as well as the generated and consumed active power in each bidding zone in the fossil free low wind case in 2045

FF_LW	DK2	FI	NO1	NO2	NO3	NO4	NO5	SE1	SE2	SE3	SE4	Total	% of P_gen
Q absorbed [Mvar]	-286.4	-3 523.9	-309.5	-1 497.1	-676.3	-960.5	-951.3	-805	-2 953.4	-4 507.1	-285	-16 755.5	-22.7
Q induced [Mvar]	286.2	398.5	1 563.1	688.2	507.5	101.3	611.3	533.3	1 173.6	2 149.8	390.6	8 403.4	11.4
P_gen [MW]	1 429.9	17 349.5	2 820.3	11 010.2	4 289.9	3 869.8	8 100.4	4 304.9	6 989.9	12 123	1 517.4	73 805.2	
Load [MW]	3 320	17 943	4 309	7 135	4 671	3 540	3 011	6 430	3 020	14 200	3 691	72 271	

Table B.6: Induced and consumed reactive power, as well as the generated and consumed active power in each bidding zone in the fossil free high wind case in 2045

FF_HW	DK2	FI	NO1	NO2	NO3	NO4	NO5	SE1	SE2	SE3	SE4	Total	% of P_gen
Q absorbed [Mvar]	-447.7	-2 397.9	-304.9	-1 684.2	-719.9	-1 385.3	-866.5	-373.4	-3 227.7	-3 939	-275.3	-15 621.8	-12.0
Q induced [Mvar]	1 032.4	3 873.5	933	1 050.3	524.1	105.7	543.4	1 600.1	1 796.8	2 409.2	239.8	14 108.3	10.8
P_gen [MW]	5 189.8	52 859.7	2 244.3	13 392.4	6 988.1	5 424.3	5 700.5	7 384.0	8 836.2	17 685.1	4 828	130 532.4	
Load [MW]	4 192	45 156	8 654	11 130	6 860	4 740	4 130	11 000	4 647	14 435	6 733	72 271	

Table B.7: Induced and consumed reactive power, as well as the generated and consumed active power in each bidding zone in the renewable high wind case in 2045

ren_HW	DK2	FI	NO1	NO2	NO3	NO4	NO5	SE1	SE2	SE3	SE4	Total	% of P_gen
Q absorbed [Mvar]	-360.3	-1 922.8	-272.2	-1 661.5	-792.6	-1 496.5	-858	-511.5	-2 890	-2 919.2	-686.9	-14 371.5	-9.1
Q induced [Mvar]	881.7	6 939.5	1 301.9	1 955.2	1 098.8	232.1	1 449.8	1 056.2	1 983.4	2 848.1	366.1	20 112.8	12.8
P gen	5 196.7	58 909.7	3 074	18 995.3	7 840.4	7 196.6	9 814.1	10 832.8	13 541.7	12 854.3	9 241.0	157 496.6	
Load	5 453	54 960	8 386	13 735	8 828	6 569	5 641	10 436	7 314	20 618	7 597	149 537	

Table B.8: Induced and consumed reactive power, as well as the generated and consumed active power in each bidding zone in the renewable low wind case in 2045

ren_LW	DK2	FI	NO1	NO2	NO3	NO4	NO5	SE1	SE2	SE3	SE4	Total	% of P_gen
Q absorbed [Mvar]	-427.1	-2 599.2	-295.6	-1 540.4	-634.7	-1 117.6	-977	-587.1	-3 504.5	-4 737.6	-552.1	-16 972.9	-31.4
Q induced [Mvar]	205	542.1	885.6	705	509.3	46.1	300.7	1 048.7	628.3	516	13	5 399.8	10.0
P gen [MW]	1 165.7	12 111.2	2 955.5	9 359.5	3 234.7	3 250.0	6 790.5	3 700.0	5 104.5	4 546.7	1 892.2	54 110.5	
Load [MW]	2 192	7 876	4 480	5 146	4 695	3 484	3 142	7 221	4 401	8 399	4 468	55 504	

C

Appendix C - Sources Used for the Grid Models and Load and Generation Scenarios

The sources used for the 2020 grid model (topology):

- **ENTSO-E grid map**: A map of the Northern European grid [28].
- **Svk transmission grid map from the 10 year system development plan [2]**
- **Statnett transmission grid map from the 10 year system development plan [13]**.
- **OpenInfraMap:** An open source grid map which was used when higher resolution was needed [30].

The sources used for the installed capacities (actual values) in the 2020 model:

- **ENTSO-E transparency platform**: Presented values used for Denmark's, Norway's and Finland's installed capacities per type, per bidding zone [8].
- **Svk, Kraftbalansen på den svenska elmarknaden - rapport 2020:** Presented values for Sweden's installed capacities per type, per bidding zone [6].

The sources used to include new generators in the model:

- **vattenkraft.info**: A private initiative to document the hydro power units in Sweden [40].
- **Vindbrukskollen**: A map of installed wind power, and wind power under consideration in Sweden, provided by Länstyrelsen and Energimyndigheten [41].
- **NVE - Vannkraftdatabase**: Provides information on hydro power units in Norway, run by a the oil and energy department in the Norwegian government [73].
- **NVE - Vindkraft kart**: A map over installed wind power and wind power under consideration [42].
- **Wikipedia**: Information on thermal power plats in Denmark [43] and Sweden [44].

The sources used for the generated power and load in the 2020 cases:

- **ENTSO-E transparency platform**: This was the source for the data on

load per region and generation per type, per bidding zone for Denmark, Finland and Norway, and load per bidding zone in Sweden [8].
- **Mimer**: This source was used for the generation per type per bidding zone in Sweden, due to unavailability on ENTSO-E transparency platform [38].

The sources used for the grid reinforcements in the 2045 model:
- **DK2**
  - Energinet's long-term grid structure analysis was used for inframtion on future grid reinforcement plans[12].
  - Energinet's map over the possible 2040 grid was also used [63].
- **Finland**
  - Fingrid's Main grid development plan 2022-2031 was used to find planned changes to the grid [64].
- **Norway**
  - Statnett's System Development Plan 2021 was used to find the grid reinforcement plans in Norway [13].
- **Sweden**
  - Svk's System Development Plan 2022-2031 was used to find the planned grid reinforcements in Sweden [2].
  - The investment project NordSyd report was also studied to find more information on how this project would affect the grid [66].

The sources used to find the installed generation capacity for the different scenarios:
- **DK2**
  - Energistyrelsens analyseforudsaetninger till Energinet was used to find one installed generation capacity scenario, used for all scenarios [5].
- **Finland**
  - Offshore wind location and size were extracted from Finnish Wind Power Association Map [67].
  - Fingrid's electricity system vision was used to find the future installed generation capacities for the different scenarios [4].
- **Norway**
  - Offshore wind location and size were extracted from NVE Wind Power Map [42].
  - Statnett's Long Term Market Analysis was used to find the total installed capacity in Norway [59], however some assumptions were made with regards to the distribution of the new installed capacity over the different bidding zones. These assumptions are described in Section 5.2.
- **Sweden**
  - Offshore wind location and size were extracted from Vindbrukskollen [41].
  - Svk's Long Term Market Analysis was used to find the installed capacities per type and per bidding zone for the different scenarios[14].

The sources used to find different loads and load scenarios in 2045:
- **DK2**

  - Energistyrelsens analyseforudsaetninger till Energinet was used to find one load scenario, used for all scenarios [5].
- **Finland**
  - Fingrid's electricity system vision was used to find the future yearly loads for the different scenarios [4].
- **Norway**
  - Statnett's Forbrukningsutvikling i Norge 2022 - 2050 was used to find the different loads for the different scenarios [59].
  - Manually added loads and their respective reference are displayed in Table 5.7.
- **Sweden**
  - Svk's Long Term Market Analysis was used for the different load scenarios [14].
  - Manually added loads and their respective reference are displayed in Table 5.7.

D

Appendix D - additional line reinforcements needed in the different cases in 2045

Table D.1: Added lines in Case 1: Small scale - high wind high load

From bus	To bus	Length [km]
Djuptjärn (SE1)	Viitalajärvi (FI)	81
Harspånget (SE1)	Porjus (SE1)	14
Porjus (SE1)	Vitas (SE1)	96

Table D.2: Added lines in Case 2a: Fossil free low wind low load

From bus	To bus	Length [km]
Borgvik (NO1)	Hasle (NO1)	103
Hasle (NO1)	Halden (NO1)	23
Halden (NO1)	Loviseholm (SE3)	43
Loviseholm (SE3)	Trollhättan (SE3)	67
Flesåker (NO1)	Tegneby (NO1)	54
Tegneby (NO1)	Hasle (NO1)	36
Tegneby (NO1)	Halse (NO1)	36
Tegneby (301 kV) (NO1)	Hasle (301 kV) (NO1)	32
Horred (SE3)	Uddebo (SE3)	49

Table D.3: Added lines in Case 2b: Fossil free high wind high load

From bus	To bus	Length [km]
Borgvik (SE3)	Hasle (NO1)	103
Djuptjärn (SE1)	Viitalajärvi (FI)	81
Hallsjö (SE2)	Vaple (SE2)	21
Porjus (SE1)	Harspånget (SE1)	15
Tuovila (FI)	Seinäjoki (FI)	46

Table D.4: Added lines in Case 3a: Electrification renewable - low wind low load

From bus	To bus	Length [km]
Borgvik (SE3)	Hasle (NO1)	103
Hasle (NO1)	Halden (NO1)	23
Halden (NO1)	Loviseholm (SE3)	43
Djuptjärn (SE1)	Viitalajärvi (FI)	81
Porjus (SE1)	Harspånget (SE1)	14
Viitalajärvi (FI)	Pikkarala (FI)	130
Djuptjärn (SE1)	Svartbyn (SE1)	66
Djuptjärn (SE1)	Viitalajärvi (FI)	81
Viitalajärvi (FI)	Pikkarala (FI)	130

Table D.5: Added lines in Case 3b: Electrification renewable - high wind high load

From bus	To bus	Length [km]
Saurdal (NO2)	Kvilldal (NO2)	23
Flesåker (NO1)	Sylling (NO1)	29
Sylling (NO1)	Oslo (NO1)	32
Eldfjord (NO5)	Dagali (NO5)	79
Porjus (SE1)	Harspånget (SE1)	14
Glentegard (DK2)	Hovegard (DK2)	10
Pikkarala (FI)	Pyhänsel (FI)	12
Pyhänsel (FI)	Isokangas (FI)	40
Ligga (SE1)	Messaure (SE1)	19

E

Appendix E - Table of Offshore Wind Farms

Table E.1: List of all implemented offshore wind farms along with their respective bidding zone, bus and capacity.

Name	Bidding zone	Bus	Capacity [MW]
Bothnia offshore omega	SE1	9409	2 450
Bores krona	SE1	9409	2 050
Bothnia offshore lambda	SE2	6808	2 800
Långegrund 1 & 2	SE3	6346	5 700
Baltic offshore alpha	SE3	6607	4 000
Najaderna	SE3	6584	1 960
Arkona vindkraftspark	SE4	5673	2 430
Krigers flak	SE4	5673	1 150
Sydkustens vind	SE4	5673	900
Baltic offshore beta	SE4	6351	6 160
Utsira North 1	NO2	6689	2 000
Utsira North 2	NO2	6750	2 000
Southern North sea 1 & 2	NO2	6362	5 000
Southern North sea 3 & 4	NO2	6373	5 000
Ferya grounds	NO3	6648	1 000
The old wall	NO3	6648	1 000
Stadt sea	NO3	6648	1 000
Freyabanken	NO3	6864	1 000
North Island - Outer vikna	NO3	6863	1 000
Traena West	NO4	7007	1 000
Traenafjorden - Selvaer	NO4	7007	1 000
Auvaer	NO4	7019	1 000
Vannoya Northeast	NO4	7020	1 000
Sandskallen - South island	NO4	7017	1 000
Additional offshore	NO5	6748	1 000
Korsnäs sea breeze	FI	6810	1 300
Reimari	FI	6810	3 600
Laine	FI	6811	2 500
Halla	FI	6911	2 600
Hesselö	DK2	5642	2 000
Kriegers flak II	DK2	5676	1 000
Energiö Bornholm	DK2	5646	3 000

DEPARTMENT OF ELECTRICAL ENGINEERING
CHALMERS UNIVERSITY OF TECHNOLOGY
Gothenburg, Sweden
www.chalmers.se

CHALMERS
UNIVERSITY OF TECHNOLOGY